UCID- 19743

OPTIONS TO UPGRADE THE MIRROR FUSION TEST FACILITY

K. I. Thomassen and J. N. Doggett,
Editors

April 1983

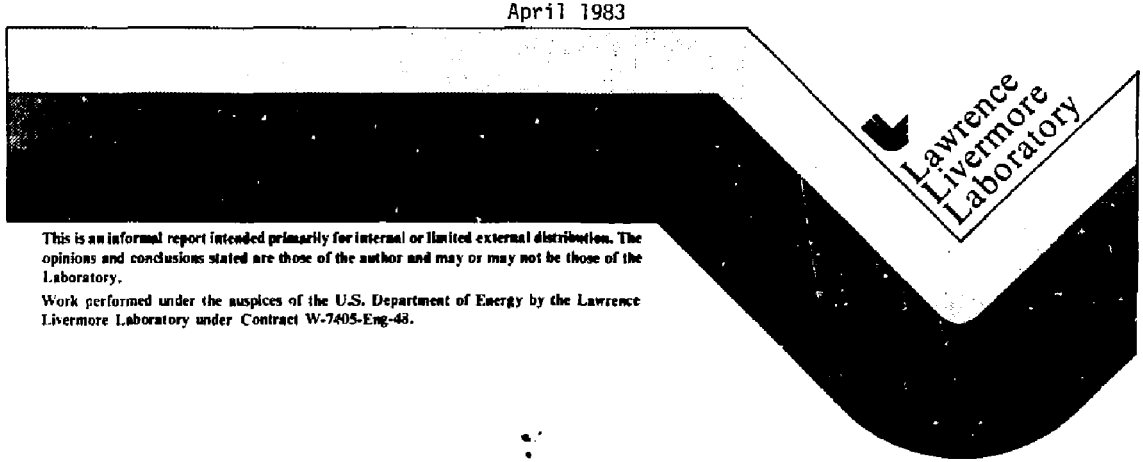

UCID--19743

DE83 009696

CONTENTS

Preface vii
Addendum on Availability and Run Time x
1. Summary 1
1.1 Scope and Objectives 2
1.2 Benefits to the Program 8
1.3 Project Schedule 9
1.4 Project Cost 11

2. Upgrade Options 19
2.1 The MFTF-α+T Upgrade 20
2.1.1 Introduction 20
2.1.2 Physics Description 22
2.1.2.1 The High Q Mode 26
2.1.2.2 The High Γ Mode 38
2.1.3 Engineering Description 48
2.1.3.1 Overview 49
2.1.3.2 Machine Description 54
2.1.3.3 Tritium Systems 73
2.1.3.4 Maintenance 79
2.1.3.5 Facilities 81
2.1.3.6 Testing Program 84
2.1.3.7 Siting and Safety 85
2.2 The MFTF-B+T Upgrade 90
2.2.1 Introduction 90
2.2.2 Physics Description 92
2.2.3 Engineering Description 102
2.3 The MFTF-α Upgrade 103
2.3.1 Introduction 103
2.3.2 Physics Description 104
2.3.3 Engineering Description 104

3. Role of the Upgrade 111
3.1 Objectives for MFTF-B Upgrade 111
3.1.1 Power and Fuel Cycle Technology 111
3.1.2 Systems Integration 114
3.1.3 Operations, Maintenance, and Safety 114
3.2 Benefits to the Mirror Program 115
3.2.1 Physics Improvements 116
3.2.2 New Technologies 116
3.2.3 Relation to FPD 117
3.3 Benefits to the Fusion Program 117
3.3.1 Steps Toward Engineering Feasibility 118
3.3.2 Contribution to ETR 119

4. Relation to the Mirror Program Plan 121
4.1 Introduction 121
4.2 The Experimental Program Plan 121
4.2.1 Physics Issues to be Addressed 121
4.2.2 Plasma Technology Development 124
4.2.3 Alternative Geometries 125
4.2.3.1 TARA, Alternative Magnetic Geometry 126
4.2.3.2 GAMMA 10, Alternate Magnet Geometry 126
4.2.3.3 The Negative Tandem, Alternative Potential Geometry 126
4.2.4 Experimental Program Plan 127
4.3 Technology Development for Mirrors 132
4.3.1 Needs 132
4.3.2 Plan for Development 132

5. Cost and Schedule 137
5.1 The LLNL Preferred Option (α+T) 137
5.1.1 Work Breakdown Structure (WBS) 137
5.1.2 Unescalated Cost 137
5.1.3 Schedule and Cost Profile 142
5.1.4 Impact of Delay Start 142

5.2 The MFTF-B+T Upgrade 145
5.2.1 Work Breakdown Structure 145
5.2.2 Unescalated Cost 145
5.2.3 Schedule and Cost Profile 145
5.3 The MFTF-α Upgrade 145
5.3.1 Work Breakdown Structure 145
5.3.2 Unescalated Cost 154
5.3.3 Schedule and Cost Profile 154
5.4 Overall Program Budget Requirements 154
5.4.1 Program Elements 154
5.4.2 MFAC Budget Guidance 154

6. Industrial Role in MFTF-Upgrade 159

Appendix A. Report of the US-Japan Bilateral Discussions (Q9) 161

LIST OF CONTRIBUTORS

FEDC

Project Manager

W. D. Nelson (GE)

Configuration

J. A. O'Toole (GAC)

Magnet Systems

B. L. Hunter (GE)
J. H. Schultz (MIT)
V. C. Srivastava (GE)

Vacuum Vessel/Shielding/Supports

J. Kirchner (MDAC)

First Wall/Dumps

B. A. Cramer (MDAC)
J. R. Haines (MDAC)
J. G. Murray (PPPL)

LLNL

Mirror Program

W. L. Barr
R. R. Borchers
R. H. Bulmer
R. B. Campbell
F. H. Coensgen
C. C. Damm
J. N. Doggett
D. W. Dorn
J. H. Fink (NEGION)
T. K. Fowler
G. W. Hamilton
C. D. Henning
J. D. Lee
G. W. Leppelmeir
B. G. Logan
J. E. Osher
G. D. Porter
T. C. Simonen
K. I. Thomassen

LIST OF CONTRIBUTORS (continued)

Maintenance

P. T. Spampinato (GAC)

Neutronics

B. A. Engholm (GA)
M. Y. Gohar (ANL)

Facilities

S. K. Ghose (Bechtel)

Tritium Systems

P. A. Finn (ANL)

Heating and Fueling

G. E. Gorker (GE)
D. H. Metzler (GE)

Testing

R. F. Mattas (ANL)

Design

P. J. Fogarty (ORNL)
M. H. Kunselman (CRNL)
H. G. Willey (MIT)

MFTF Project

C. A. Armellino
W. L. Burden
J. A. Day
J. W. Gerich
V. N. Karpenko
T. A. Kozman
K. H. Krause
S. A. Muelder
R. L. Peterson
R. M. Settle
D. W. Shimer
W. H. Sterbentz
R. R. Stone
S. Szybalski
A. L. Throop
L. E. Valby

PREFACE

In this document we describe three options for upgrading MFTF-B, and the nomenclature used for these options is shown on the chart, "MFTF-B Upgrade Options." We propose to add a 4-m-long "reactor-like" insert to the central cell, or to change the end plugs to the new MARS-type configuration, or both. LLNL prefers the third option, labeled MFTF-α+T in the chart, in which both the central cell insert is added and the end plugs are modified. All options are long-pulse or steady-state DT burning experiments.

Those upgrades with the insert would be constructed beginning in FY 86, with operation beginning in mid-FY 92. Confirmation of our intent to modify the end plugs would be sought in FY 88 based on positive results from MFTF-B experiments. The upgrade with only the end plug modification would not start until MFTF-B data are available. The timeline for constructing and operating the MFTF-B Upgrade included at the end of this preface is for reference while reading the text. The various modes of operation shown on the chart are described later.

	No insert	With insert
Old plugs	MFTF-B	MFTF-B + T
New plugs	MFTF-α	MFTF-α + T

MFTF-B Upgrade options

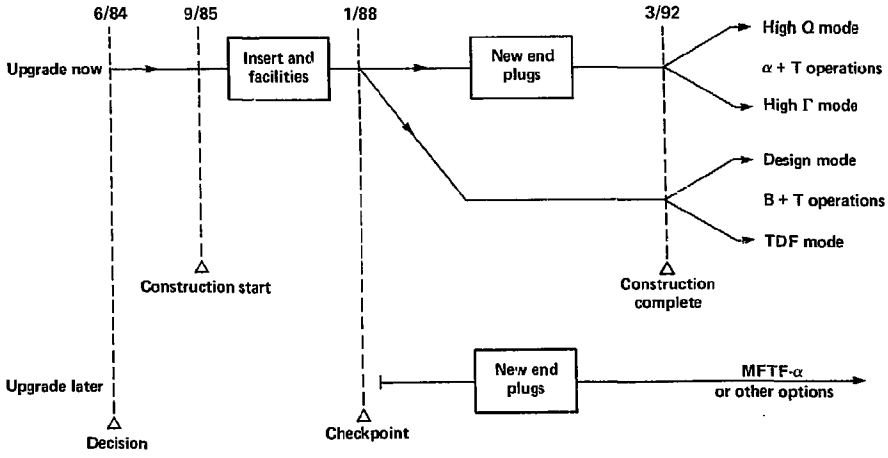

Timeline for construction and operation of MFTF-B Upgrades

ADDENDUM ON AVAILABILITY AND RUN TIME

In this document we arbitrarily chose the uninterrupted running time and availability of 10 hr and 1%, respectively. This choice was first made nine months ago when the only upgrade option considered by LLNL was to insert a reactor-like section in the central cell of MFTF-B (called MFTF-B+T). About three months ago the other two options (described here) were conceived, both requiring the same new end regions in the machine. The first (MFTF-α) does not incorporate the central cell insert but the second (MFTF-α+T), provides the insert and also new end plugs.

After this document was prepared in draft form and discussed among ourselves and in the community, it was clear that longer run times and higher availability were both possible and desirable in the MFTF-α+T option, possibly with little cost impact. The central cell is modular, and maintainability is more easily incorporated there. In contrast, the existing end region of MFTF-B presents many maintenance problems should there be a component failure after the machine is activated and, for that reason, our initial choices of run time and availability were modest. With new plugs those parts of the vessel outside the central cell must be rebuilt, and this affords the opportunity to design these less accessible regions for ease of maintenance.

All systems in MFTF-α+T are designed for CW operation, and end region shielding allows access to the vault area for contact maintenance after 24 hr, even for runs much longer than 10 hr. After considering these matters, we believe that run times up to 100 hr and an ultimate availability of 10% in the later years of operation is an achievable design goal. Consequently, we are adopting this goal in our ongoing studies of MFTF-α+T.

1. SUMMARY

Previous MFAC documents[1] have described the MARS tandem mirror reactor concept, which has a thermal barrier and axisymmetric throttle coils; the remaining physics and technology issues for this concept have been identified, and a program to resolve these issues is in place. Assuming a positive outcome, this research program, culminating in the demonstration of plasma confinement times approaching 1 s in the MFTF-B, will verify the physics design for a tandem mirror reactor by FY 87-88. In this report, we propose upgrading the MFTF for further experiments in the early 1990's.

With MFTF-Upgrade, program emphasis will begin to shift away from resolving specific issues toward systems integration of all subsystems of a tandem mirror reactor. This will also serve to advance plasma confinement parameters and other measures of program progress on a broad front. In this report we describe three upgrade options, all of which call for DT-burning plasmas and, hence, systems integration in the nuclear environment of a reactor. It is our intention in MFTF-Upgrade to go as far towards addressing nuclear systems issues as possible, consistent with technical readiness and budgetary constraints. We do intend that the MFTF-Upgrade be an affordable option, and, as is discussed below, our present cost estimates are consistent with this objective.

The precise role of the MFTF-Upgrade in the tandem mirror program will depend on overall funding levels. In an aggressive funding climate we propose that, in parallel with upgrading the MFTF, we also proceed directly to the construction of the Fusion Power Demonstration (FPD) that would evolve through two phases to become the tandem mirror Engineering Test Reactor (ETR) and finally a demonstration reactor. In such an aggressive program, the main purpose of the MFTF-Upgrade would be to permit the boldest possible step by reducing the risk. It would do this by providing earlier operating experience on a facility having all of the elements of the FPD but on a more modest scale. This is similar to the role that the TMX-Upgrade now serves relative to the MFTF-B. On the other hand, if the FPD were delayed, the MFTF-Upgrade itself would greatly advance the tandem mirror data base and thereby strengthen the case for the FPD when the funding picture improves. Moreover, as we shall see, the MFTF-Upgrade would provide the entire fusion community with a unique capability for complete nuclear systems tests (blankets, tritium, heat

transfer) at power densities and neutron wall loadings close to reactor parameters.

In short, in a constrained budget the MFTF-Upgrade would be the most advanced fusion engineering test facility available in the world in the early 1990's, while in an aggressive funding climate it would enable the tandem mirror program to push ahead with an Experimental Test Reactor at the earliest opportunity.

1.1 SCOPE AND OBJECTIVES

Three options (described in detail in Sec. 2) have been proposed for upgrading MFTF. They include MFTF-α+T, which is our preferred option. It would upgrade both the end plugs and the central cell of MFTF, and would permit two modes of operation, one emphasizing better confinement and higher Q, and the other a high fusion power production in the central cell. The second option, MFTF-α, would upgrade only the end plugs. The third, MFTF-B+T, would upgrade only the central cell.

The MFTF-α+T upgrade has three main objectives:

1. To extend physics performance to Q~2 in a DT plasma, at which point about a third of the central cell heating comes from the alpha particles;
2. To gain experience in integrating tandem mirror systems in a nuclear environment; and
3. To provide a unique capability for operating a power-producing section of a fusion reactor at reactor-like parameters (hours per shot at a neutron wall loading of 2 MW/m^2).

The other two options, although somewhat less expensive, can meet one or another of the above objectives but not all. MFTF-α can meet the first objective but not the third; MFTF-B+T cannot address the first objective, and the neutron wall loading in the central cell would be less because the upgraded end plugs are needed to maintain MHD stability at the higher central cell density specified for MFTF-α+T.

A sketch of MFTF-α+T is shown in Fig. 1-1, and parameters for this option are compared to the FPD and the MARS reactor in Tables 1-1 and 1-2. As the tables indicate, the MFTF-Upgrade is impressively close to reactor conditions, both in physics parameters such as particle confinement time

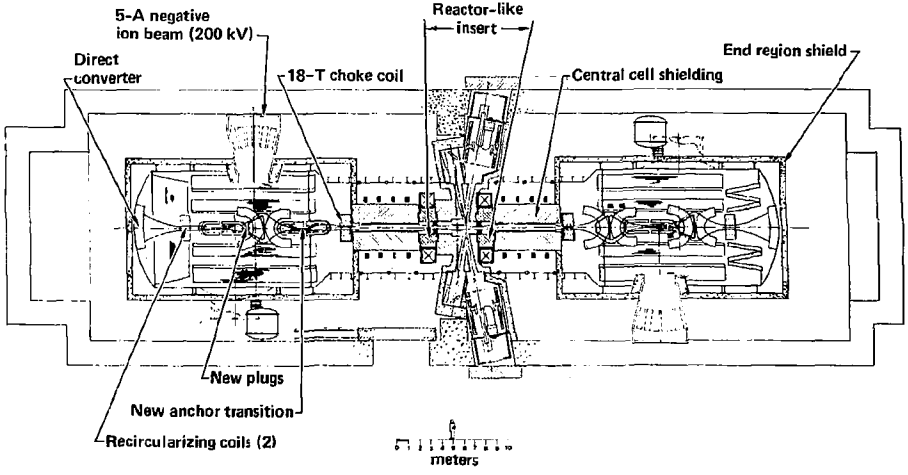

Fig. 1-1. MFTF-α+T Upgrade shown in cross section in the existing MFTF-B vault.

Table 1-1. Physics parameters for tandem mirror facilities.

Parameter	MFTF-B[b]	MFTF-α+T High Γ	High Q	FPD-II[a]	FPD-III[a] demo	MARS[a]
Central cell length (m)	15.8[c]	4.0[c]	20[c]	75[c]	75[c]	130[c]
Central cell plasma radius (m)	0.30	0.15	0.15	0.54	0.6	0.49
Central cell field (T)	1.0[d]	4.5[d]	1.6[d]	2.5[d]	3.5[d]	4.7[d]
Central cell density(10^{14}cm^{-3})	0.39	4.75	1.9	1.5	2.85	3.26
Average ion temperature (keV)	15	27	25(with (axicell)	28.5	30.2	28.6
Electron temperature (keV)	9	7	12	24.3	24.8	24.0
Central cell average β (%)	20	31 (axicell)	40 (central)	47	47	28
Ion ($n\tau$) (particle) (cm^{-3}s)	2.2x10^{13} e	4.7x10^{13} e	1x10^{14} e	4.8x10^{14} e	4.9x10^{14} e	5.15x10^{14} e
Ion lifetime (particle) (s)	0.57[e]	0.26[e]	1.06[e]	3.2[e]	1.72[e]	1.6[e]
Ion confining potential (kV)	30	72	62	153	160	156
Total plug potential (kV)	66	69	141	322	335	329
Central cell Q_c	0.62[f]	1.0[f]	1.7[f]	4.73[f]	4.95[f]	5.08[f]
Effective central cell $(Q_c)_{eff}$	0.62[g]	1.29	2.49	←	gnited (∞)[g]	→
Overall	0.23[h]	1.1[h]	1.5[h]	7.14[h]	18.2[h]	25.6[h]

[a]The MARS and FPD designs have evolved since last described in the MFAC panel I report and these parameters are different. The FPD will continue to evolve since it is in a definition phase, but the MARS design is nearing completion. FPD-I, II, and III refer to different phases of operation of the same facility, succeeding phases requiring upgrade funds.

[b]Parameters for the axicell MFTF-B are taken from K. I. Thomassen and R. A. Jong, "MFTF-B Performance Calculations," UCID-19621, Dec. 1982.

[c]Distance between first mirror peaks at ends of central cell, except for MFTF-α+T. In the high Γ mode we use the 4-m insert length whereas in the high Q mode we use the length between 18 T choke coils.

[d] Axicell field in the high Γ mode, central cell field in the high Q mode. FPD is designed for 3.5 T, MFTF-B is designed for 1.6 T.

[e]The particle $n\tau$ values include radial and axial losses, and average over hot and warm species. Similar treatment of particles gives the lifetime.

[f]The value Q_c is a ratio of fusion power and power losses from the central cell, except that in MFTF-B we give the equivalent value if DT were used. No credit is taken for the α-power makeup of the losses.

[g]The effective value of Q_c uses the full α-power heat to reduce the central cell power losses.

[h]The overall Q is a ratio of fusion power and total plasma power losses.

Table 1-2. Power producing region parameters per meter of length.

	MARS	FPD-III (Demo)	FPD-II	MFTF-Upgrades α+T (High Γ)	MFTF-Upgrades α+T (High Q)[a]
Plasma radius (m)	0.49	0.6	0.54	0.15	0.25
Plasma density x 10^{14}	3.26	2.85	1.5	4.75	1.1
Fusion power density (W/cc)	26.5	20.6	5.8	55.2	1.93
P_{fusion}/unit length (MW/M)	20.0	23.3	5.3	3.9	0.38
Γ (MW/m^2)	4.24	3.57	0.96	2.0	0.11
First wall radius (m)	0.6	0.83	0.7	0.25	0.45
Blanket thickness (m)	0.41	0.41	0.41	0.5 avail.	0.5
Reflector thickness (m)	0.42	0.42	0.42	0.5 avail.	0.5
B_0 (T)	4.7	3.5	2.5	4.5	1.6
Mean coil diam. (m)	5.6	5.6	5.6	5.0	5.0
Coil spacing (m)	3.2	3.2	3.2	5.3	1.25
T_2 production g/day	3.0	3.5	0.8	0.6	0.06

[a]For this option we use the central cell parameters since the axicell is not the primary power producing region in this mode.

(Table 1-1) and in nuclear engineering parameters such as neutron wall loading (Table 1-2).

Note especially the upgraded central cell. This shielded cylindrical region, approximately 4 m long (mirror-to-mirror) and 5 m in diameter, is in all respects a complete working section of a tandem mirror reactor, at full magnetic field and full fusion power density. A complete reactor merely consists of many such cylindrical sections lined up end-to-end. The main compromise in MFTF-Upgrade relative to a full power system is the smaller plasma radius, which reflects lower field strength and smaller magnets in the end plugs of MFTF. To compensate for the smaller plasma radius and still obtain reactor-level power densities in the inner blanket region, the first wall radius is also reduced accordingly. Nonetheless, the overall diameter is about the same, as can be seen in Fig. 1-2, which compares cross sections of the MARS reactor and the MFTF-Upgrade central cell on the same scale. A second compromise is a low operating duty cycle (~1%) to reduce the maintenance expense (see Addendum at front of this report). However, with superconducting coils and essentially dc power systems, any one "shot" in MFTF-Upgrade can be extended to many hours to achieve steady state conditions in the blanket and auxiliary systems. We shall return to this point later.

The possibility of inserting a complete power-producing reactor section in the MFTF-Upgrade is a unique feature of the linear geometry of the tandem mirror, made possible by the use of mirror coils to isolate a short section of central cell from the rest of the machine. Because of its small volume, this isolated section can be maintained at an elevated plasma density and temperature by intensive auxiliary heating. In the MFTF-Upgrade, this heating is supplied by the existing MFTF 80-kV neutral beam system, upgraded for dc operation with tritium, which also fuels the central cell.

As is discussed in Sec. 2, the upgraded end plugs also play an important role in obtaining high fusion power density, by "anchoring" the high-β central-cell plasma to provide MHD stability. In addition, the improved end-plugs permit us to increase the electrostatic potential from ~70 kV (relative to ground) in MFTF to approximately 140 kV in the upgrade (in the High Q mode). This is about half of the potential required to reach ignition in the central cell. In a tandem mirror, ignition means that the alphas heat the central cell so that the only power input is that required to sustain the end plugs; then, Q is directly proportional to the length of the central

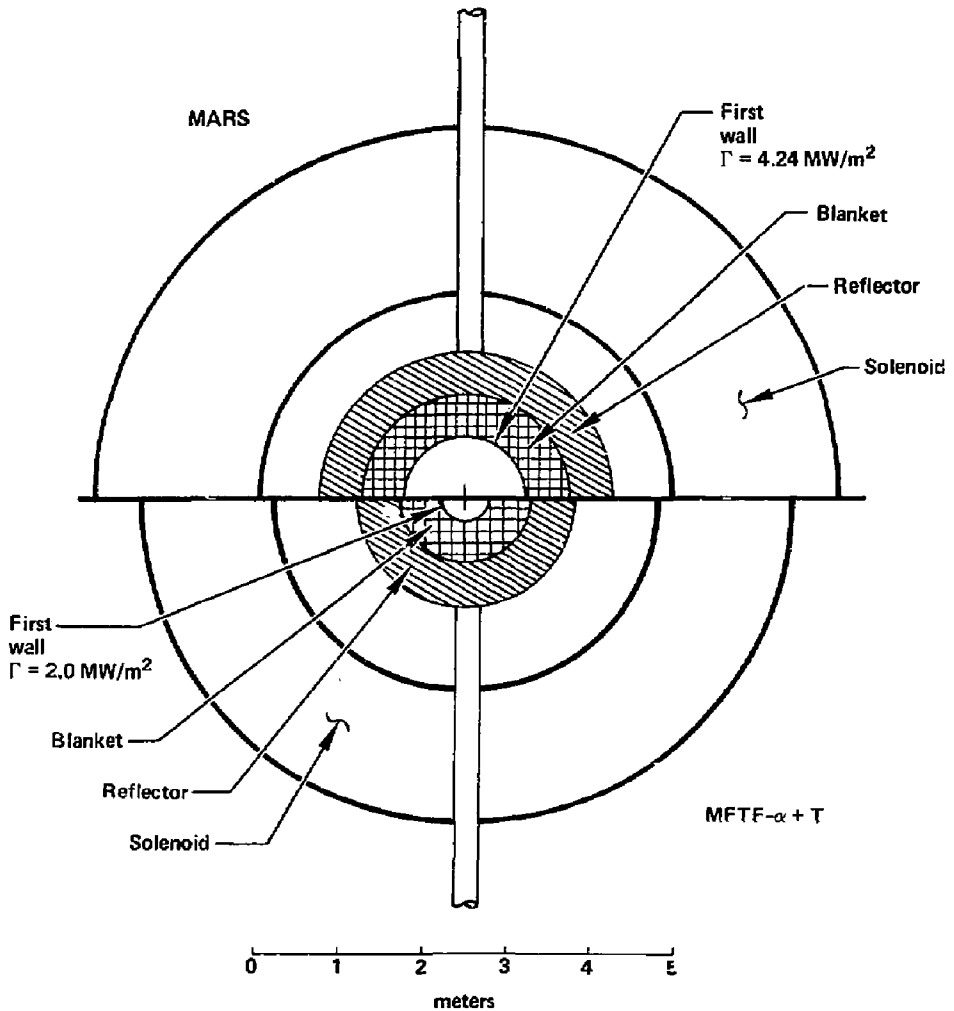

Fig. 1-2. Comparison of power producing regions in the MARS reactor and the MFTF-α+T Upgrade.

cell. In MFTF-α+T, the alphas would supply about 30% of the central cell heating ($Q \sim 2$).

While it would be desirable to demonstrate ignition in the MFTF-Upgrade, we conclude that this is not possible within our cost objectives and, therefore, this task must be deferred to the FPD phase of the program. As is discussed in Sec. 2, the main limitations are the field strength and plasma radius in the end-plug region (the yin-yang anchors, transition coils, and axicell or choke coils), which set the upper limit on adiabatic confinement and hence, the upper limit on ion energies (sloshing ions and passing ions), which in turn set limits on the potential levels. This is an issue of cost, not technical readiness. For example, a full MARS yin-yang anchor is only 30% larger in linear dimension than the existing MFTF yin-yang that has been built and tested, and it could use a NbTi conductor. The differences impacting cost lie in the use of He II (at 1.8 K) to achieve 10-T fields in the conductor, and the larger number of ampere-meter of conductor in the MARS coils.

1.2 BENEFITS TO THE PROGRAM

As noted above, besides advancing tandem mirror physics and technology parameters to near-reactor conditions, the MFTF-Upgrade will provide the first experience in integrating all subsystems of a tandem mirror reactor in a nuclear environment.

Every component of the current MARS reactor design is included in the preferred MFTF-Upgrade option, without exception. In the central cell, in addition to the magnet, vessel, blanket, shield, and other elements of the reactor core, this includes all of the auxiliary systems necessary to recover the tritium and process the heat. In the end plugs, this includes negative ion beams, a direct converter, advanced means of removing trapped ions in the transition region (drift pump), high-power gyrotrons, and a magnet set of the MARS design. These features are described at length in Sec. 2 of this report, and the kinds of information that can be obtained from the facility are discussed in Sec. 3. Finally, although we have based the MFTF-Upgrade on the present reactor design, the project schedule retains the flexibility to incorporate various end-plug design improvements currently being investigated in the research program. We shall return to this point later and again in Sec. 4.

Although the MFTF-Upgrade is aimed specifically at tandem mirror requirements, tandem mirrors and tokamaks (and other concepts) have much technology in common, especially in the power-producing reactor regions, so that information from the MFTF-Upgrade would be valuable during the design, construction, and operation of a tokamak ETR and for the tandem mirror FPD (see Sec. 3). Moreover, even with a limited duty cycle the MFTF-Upgrade can over a period of time test and provide operating experience on several reactor core designs. As is shown in Sec. 2, the design permits the blanket region to be removed and replaced with other designs from time to time.

We believe that the advanced engineering capability of the MFTF-Upgrade will make it especially attractive to industry. It is LLNL's policy to become partners with industry in the construction and operation of the MFTF-Upgrade to the fullest extent possible. A recent step in that direction is a cost-sharing contract, now in negotiation, whereby an industry will assume responsibility for specific subsystems of the MFTF-B now under construction, from design through operational testing on the facility. These and other measures that will involve industry in the tandem mirror program are discussed briefly in Sec. 6.

Finally, with its limited duty cycle, MFTF-Upgrade cannot perform engineering tasks related to failure modes that require many months (see Addendum at front of this report) or years of running time. For these tasks, the MFTF-Upgrade can, however, provide a calibration for other techniques attempting to simulate the fusion reactor environment in various ways.

1.3 PROJECT SCHEDULE

If construction of MFTF-α+T is initiated in FY 86 in parallel with the initial operation of MFTF-B, operation could begin in FY 92, as shown in Fig. 1-3. In this plan, authorization of the entire project would be sought in FY 86 on the basis of positive results from TMX-U and a consensus on the value of the unique reactor systems testing capability of the facility. However, the actual freezing of the end plug design and fabrication of end plug components would be delayed until after MFTF-B data were in hand. The prior work on central cell components and associated nuclear systems not affected by this decision would speed up the completion date by 2 years or more and would provide a continuous transition for the LLNL and industrial construction teams from MFTF-B to the Upgrade.

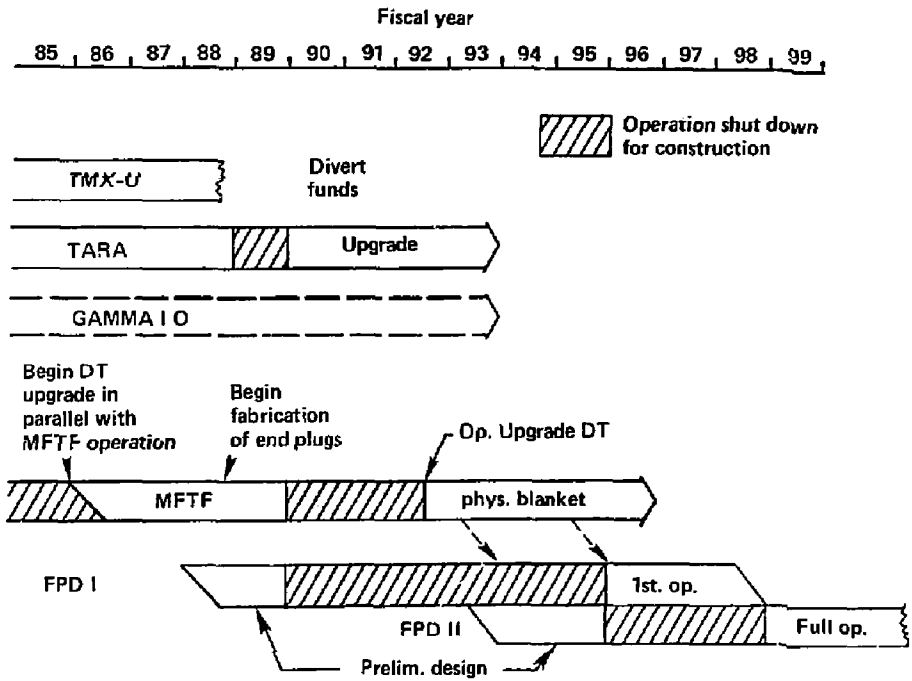

Fig. 1-3. Mirror facilities operation plan. (The start date of FPD has been slipped one year from that given in the National Mirror Program Plan.)

The above plan calls for an initial go-ahead decision in mid-FY 84 in order to initiate project funding in FY 86. A second checkpoint decision to proceed with upgrading the end-plugs would come early in FY 88 (simultaneously with a decision to proceed with the FPD in an aggressive program). The technical readiness of the program at these crucial decision dates is discussed in detail in Sec. 4 of this report.

Briefly, considering first the central cell upgrade, we are confident that a high fusion power output could be obtained in the upgrade, at least to the level of 1 MW/m^2 neutron wall loading, whether or not thermal barriers perform in MFTF-B as well as expected. By FY 84, the TMX-U will further confirm this in experiments with "choke coils" that isolate the central cell as the mirror coils would do in the upgraded central cell of MFTF. Moreover, as is discussed in Sec. 4, by that time the TMX-U is expected to provide substantial verification regarding most of the critical physics issues for the tandem mirror, though not at the performance level of MFTF-B.

If, at the checkpoint decision in FY 88, it were decided for any reason not to proceed with upgrading the end plugs, one could still elect to continue upgrading the central cell, as in the MFTF-B+T option described in Sec. 2. As can be seen from Table 1-3, the physics performance for such critical parameters as the hot ion lifetime is similar for this mode of operation and for TMX-U, while the reactor system test capability remains substantial.

Finally, as noted earlier, the project retains the flexibility to incorporate improved, more axisymmetric end plug magnets and other improvements being investigated in the research program. This information should be available at the time of the end-plug design decision in early FY 88, as discussed in Sec. 4.

1.4 PROJECT COST

1.4.1 The Preferred Option (MFTF-α+T)

As is discussed in Sec. 5, the total estimated cost (TEC) of the preferred MFTF-Upgrade option is approximately $400 M in present dollars.

In Table 1-4, we present an approximate cost profile for the project, with a project completion date in mid-FY 92, and also a plan to fit the project within the overall mirror program. By taking advantage of cost

Table 1-3. Parameter comparison for TMX-U and MFTF-B+T.

Plasma parameters[b]	TMX-U With choke coils[a] and central cell injection	MFTF-B+T TDF mode	MFTF-B+T Design mode
n_c (cm^{-3})	4×10^{13}	3.9×10^{14}	4.2×10^{14}
B_c (T)	0.4	4.5	4.5
$\langle \beta_c \rangle$ (%)	25	15	20
ϕ_c (kV)	2.2	2.0	10.8
$\phi_c + \phi_e$	5.3	15	48
$(n\tau_p)(cm^{-3})$	8.6×10^{11} [c]	2.5×10^{12} [c]	1×10^{13} [c]
(τ_p)(ms)	23[c]	6.5[c]	25[c]
E_{ic} (keV)	5.5	33	49
E_{oc} (keV)	0.7	2.3	6.2
r_p (cm)	17	15	15
Reactor parameters			
Wall flux (MW/m^2)		1.0	1.3
Fusion power (MW)		5.5	7.3
Fusion power line density (MW/m)		2.0[d]	2.6[d]
Fusion power density (W/cm^3)		28.3	36.8

[a]See D. L. Correll et al., Throttle Coil Operation of TMX-U, Lawrence Livermore National Laboratory Report, UCID-19650 (1983).

[b]Subscript c refers to central cell, ϕ_c is the confining potential, and $\phi_c+\phi_e$ is the total potential.

[c]The $(n\tau)$ and τ values average over radial and axial losses and over hot, warm, and (for TDF mode) pellet-supplied warm ion populations.

[d]The effective central cell length, 2.8 m, is used here.

Table 1-4. Tandem mirror budget (B/A) in $M (constant FY 84).

	Fiscal year							
	85	86	87	88	89	90	91	92
Mirror base, with MFTF-α+T Upgrade								
MFTF								
Exp. ops.	5	17	61	61	61	20	20	65
MFTF-B const.	67	44	--	--	--	--	--	--
Upgrade const.	--	*15*	*20*	*50*	*60*	*100*	*100*	*55*
Upgrade pre. design	10	--	--	--	--	--	--	--
Other LLNL[1]	30	30	30	20	10	11	11	11
Non-LLNL[1]	17	17	17	17	17	17	17	17
	129	123	128	148	148	148	148	148
Mirror base, MFAC report[1]	108	108	108	108	108	108	.....	
Increment	21	15	20	40	40	40	.....	

savings in FY 90-91 from reduced experimental operations during a 2-yr shutdown to install upgrade components in the MFTF facility, the incremental cost to carry out the upgrade project is $15 M in the first project construction year (FY 96), increasing to $40 M in later years. A longer shutdown would reduce the out-year cost increment. This cost increase over that of a level base program must be judged against the unique value of the MFTF-Upgrade to the tandem mirror program and the fusion program in general.

The above costs do not include ongoing mirror research funded by Applied Plasma Physics or development of the negative ion beams, magnets and dc neutral beams for the central cell. However, these costs are largely covered by ongoing, funded programs.[1]

Finally, we note that our cost estimate is contingent upon being able to carry out the project at the Livermore site with appropriate modifications of the existing MFTF building as planned. While major nuclear activities are already an integral part of LLNL programs and the Laboratory has filed an Environmental Impact Statement covering the existing activities, it remains to be determined whether the MFTF-Upgrade falls within the scope of that statement. This important topic is discussed briefly in Sec. 2.

1.4.2 Other Options

As we noted at the outset, in this document we concentrate on DT-burning options for upgrading the MFTF, both because of the importance we attach to early experience in systems integration in the DT environment and because the timing and minimal cost impact of other options do not require the attention of MFAC at this time. These other options resemble the MFTF-α option (discussed in Sec. 2) with deuterium plasmas only. Thus, there is no need for extensive shielding and tritium handling facilities. The focus would be on physics and advanced physics technology, such as negative ion beams.

Focusing on the DT options, Table 1-5 compares the cost and main functions of the three MFTF-Upgrade options discussed in Sec. 2. Also listed is the cost if the preferred option were constructed from scratch, showing a savings of $250 M by upgrading the present facility. Finally, we list the present estimated cost of a new facility, the TDF, that would be similar to the MFTF-Upgrade but with a high duty factor to provide high fluence exposure over a period of years.

Table 1-5. Comparison MFTF-α, MFTF-B+T, MFTF-α+T, a new facility, and TDF.

Option	Purpose	TEC FY 84 ($M)	Annual increment to mirror base budget ($M)
MFTF-α (upgrade plug only)	Physics (Q ∿2)	267 (FY 89 start)	20
MFTF-B+T (upgrade central cell only)	Reactor system test ($\Gamma \sim 1$ MW/m^2)	334	20
MFTF-α+T (upgrade plug and central cell)	Physics and reactor system test (Γ = 2 MW/m^2)	401	20 to 40
New facility (like α+T)	Physics and reactor system test (Γ = 2 MW/M^2)	650	
TDF	Reactor system test, high fluence	1000	

Among these choices, we have selected the MFTF-α+T option as the most affordable one that advances both physics and technology objectives for the tandem mirror program.

REFERENCES

1. Report of the Review Panel on Tandem Mirrors and Tokamaks to the Magnetic Fusion Advisory Committee, J.R. Gilleland, Chairman (September 1982).

2. UPGRADE OPTIONS

A unique feature of the tandem mirror is the ability to insert a reactor-like section in the central cell to gain early experience in fusion reactor engineering. At LLNL we have incorporated this insert into MFTF-B in two of three proposed options. The first option uses the MFTF magnet set, adds tritium and the associated facilities (and is therefore called MFTF-B+T), and allows infrequent 10-hr runs of the facility (see Addendum).

A second option concentrates on improved physics through better end plugs, uses DT to produce α particles (so is called MFTF-α), and has a significant role in DT mirror system integration. Run times of 1000 s permit virtual steady-state physics operation at $Q \sim 2$, producing ~6 MW of fusion power in the central cell. The higher Q is achieved by creating a higher confining potential, and to do so requires higher sloshing beam energies and plug magnetic fields (for higher adiabatic energy limits). Drift pumping replaces neutral beam pumping, so that the only neutral beam of consequence in this option is the 1-MW, 200-kV beam in each plug.

The final option, with a reactor insert, combines the above options to accomplish both the mirror physics and system integration tasks and the reactor system engineering demonstrations. In this option, called MFTF-α+T (although it might better be called a Reactor System Engineering Facility), the reactor insert section can be run at a higher wall loading (2 MW/m^2 vs 1.3 MW/m^2) than in the MFTF-B+T option because the better end plugs allow higher β values.

The MFTF-α+T would operate in the $Q \sim 2$ mode by driving the insert with 30 A of deuterium and tritium beams, and each end plug would operate at the full 62-kV confining potential. In the mode where $\Gamma_n = 2$ MW/m^2, the insert would be driven with 190 A of current and the plugging potential would drop to 22 kV to provide a loss channel consistent with the higher particle input. Particle confinement time in the insert depends on the performance of the tandem that surrounds it to provide MHD anchoring and a warm plasma bath for microstability. The higher the potential that can be erected to confine the warm plasma, the higher the bath temperature. Because particle lifetime for the mirror-trapped ions in the insert is determined partially by electron drag on that background plasma, it is indirectly set by the end plug performance. In MFTF-α+T (high Γ mode) and MFTF-B+T, respective confining potentials of

22 and 11 kV lead to ion lifetimes of 260 and 25 ms, respectively. By using pellet injection to inject cold plasma directly into the insert, the electron temperature can be further lowered. So, with 2-kV potential and a 6.5-ms ion lifetime, the objectives of the reactor cell can stil be met; 1-MW/m^2 wall loading can still be produced by modestly increasing the beam injection power.

We describe each of these three options, starting with MFTF-α+T because it is the option we prefer at LLNL. We describe MFTF-α+T in the most detail, and devote less attention to the other two options.

2.1 THE MFTF-α+T UPGRADE

2.1.1 Introduction

Central to the theme of the upgrades is the insertion of an axisymmetric mirror cell in the central cell of MFTF-B. This 4-m cell--its length defined by the 12-T peaks in the mirror field--is beam-fueled and heated from two beamlines, each having four beam injection ports. Two large superconducting coils produce the 4.5-T mirror midplane field, while two copper coils create the peak mirror fields. When driven by six sources (240 A incident), 11 MW of fusion power is generated, giving a 2-MW/m^2 peak wall flux. Figure 2-1 shows these components and the shielding required to minimize nuclear heating in the coil and activation in the area around the machine. Also depicted is a 1-m-long blanket test module that can easily be inserted and removed.

In many respects this insert can be considered a small section of a reactor, although at less than full scale, complete with support systems and technologies of a full-scale operating reactor. This ability to create reactor-like conditions in a small part of the machine is unique and affords the fusion program an early opportunity to gain experience with reactor systems at a relatively modest cost.

Although this insert is the main feature of two of the proposed upgrades, in MFTF-α+T the end plugs would also be new. These end plugs are geometrically similar to those designed for the MARS reactor and would allow $Q \sim 2$ operation in the machine. The improved performance results from the higher potential that can be sustained in the plugs, i.e., a 62-kV confining potential compared to 30 kV in MFTF-B. A 1-MW, a 200-kV sloshing beam is required to generate the end plug potential, and higher fields than those in MFTF-B are needed to raise the adiabatic energy limits in the plug and anchor

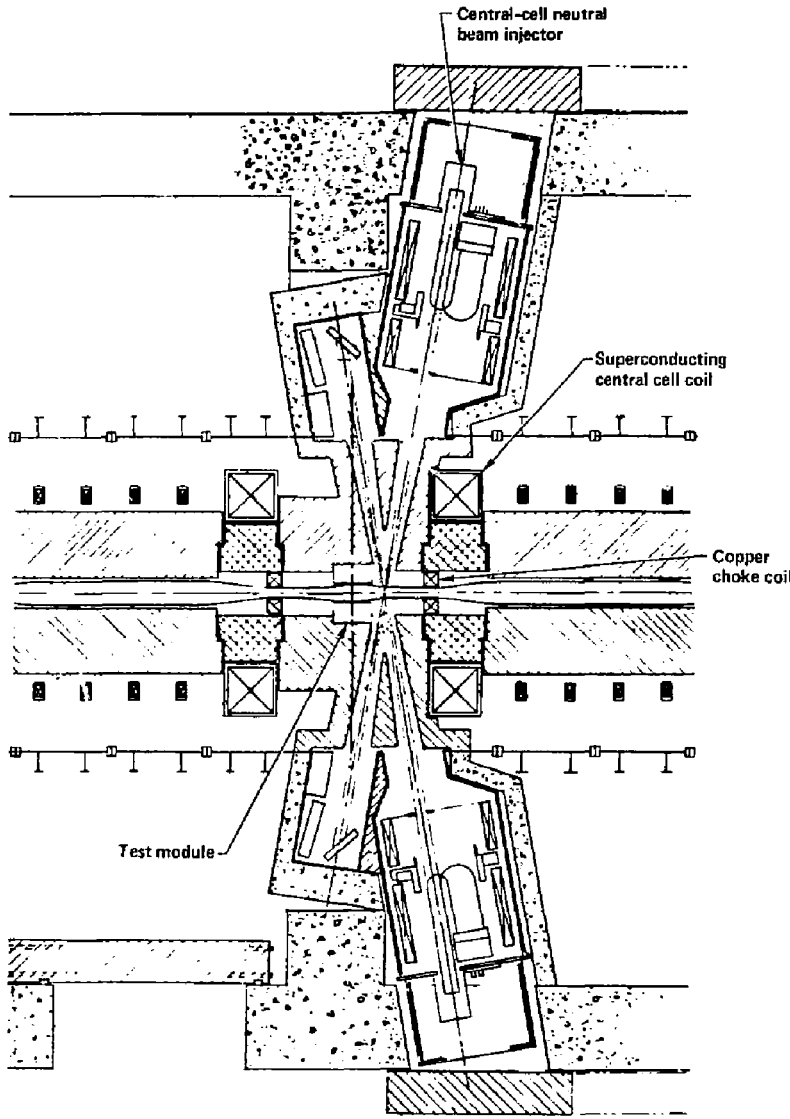

Fig. 2-1. The central cell reactor-like insert in MFTF-α+T.

cells. Figure 2-2 shows the MFTF-B end region magnet set alongside the new magnet set.

In this new set the MFTF-B axicell is replaced by an 18-T choke coil, and the two transition coils are replaced by three coils that create a 2.6-T anchor cell and allow the transition to the choke coil. A 2-T yin-yang plug replaces the 1-T plug of MFTF-B, and two recircularizing coils are added outside of the plug. The last of these recircularizing coils is the axisymmetric 6-T coil from the MFTF-B axicell.

A new feature of the MARS-style end plug is the added anchor cell in the transition region, a feature that is a natural one in the new "double fan" transition design first invented by Baldwin and Bulmer to minimize transport and parallel currents in MFTF-B. This added minimum-B anchor gives extra MHD stability to the tandem mirror by introducing hot ions at an average β of 40%. Not only does this add more pressure-weighted good curvature, but the axial location of the anchor between the two elliptical fans in the transition makes it particularly effective against ballooning instabilities in the transition. As a result of the added stability of the new end plug, the axicell insert in the central cell can hold more pressure, and therefore produce higher wall flux, than it would when anchored by the present MFTF-B end plugs.

2.1.2 Physics Description

For DT operation, MFTF-α+T includes a shielded, high field axicell ($B_{midplane}$ = 4.5 T) with continuous beam injection (> 10 hr, E_{inj} = 60 keV D^0 and T^0) in the central cell; new end plug magnets (see Fig. 2-3) that are geometrically similar to the MARS reactor design; 200-kV sloshing beam injection; ICRH; and drift pumping. Combining these central cell and end plug upgrade elements meets three objectives:

1. Improves confinement of DT plasma to provide significant alpha heating ($Q \sim 2$) in a tandem-mirror central cell.
2. Gives more reactor-relevant experience with mirror systems and tritium in a nuclear environment.
3. Provides economical blanket technology testing (hours per shot at $\Gamma_n \simeq 2$ MW/m^2).

All objectives are to be achieved in the same upgrade, although objectives 1 and 3 would not occur at the same time.

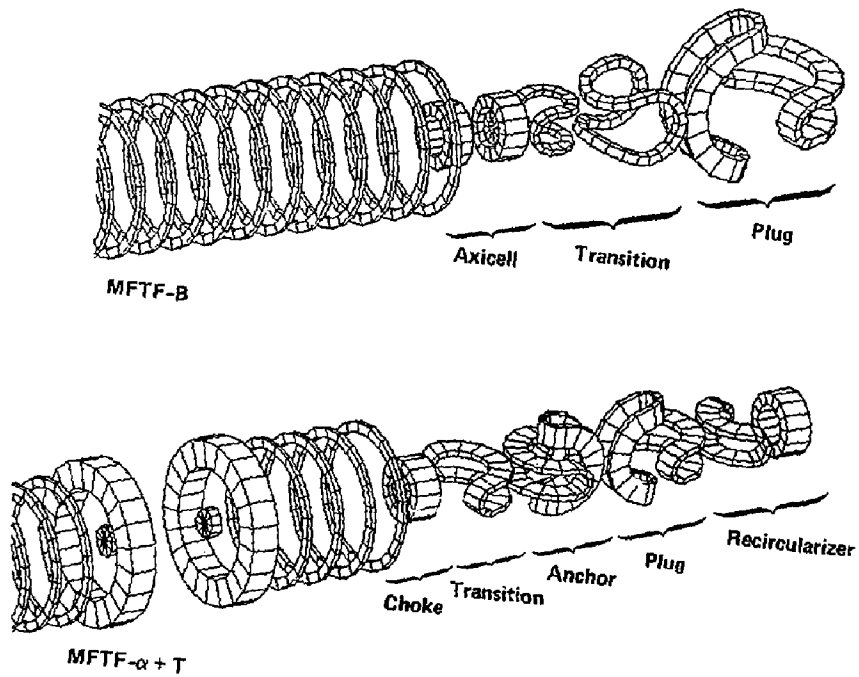

Fig. 2-2 Magnetic configurations for MFTF-B and α+T.

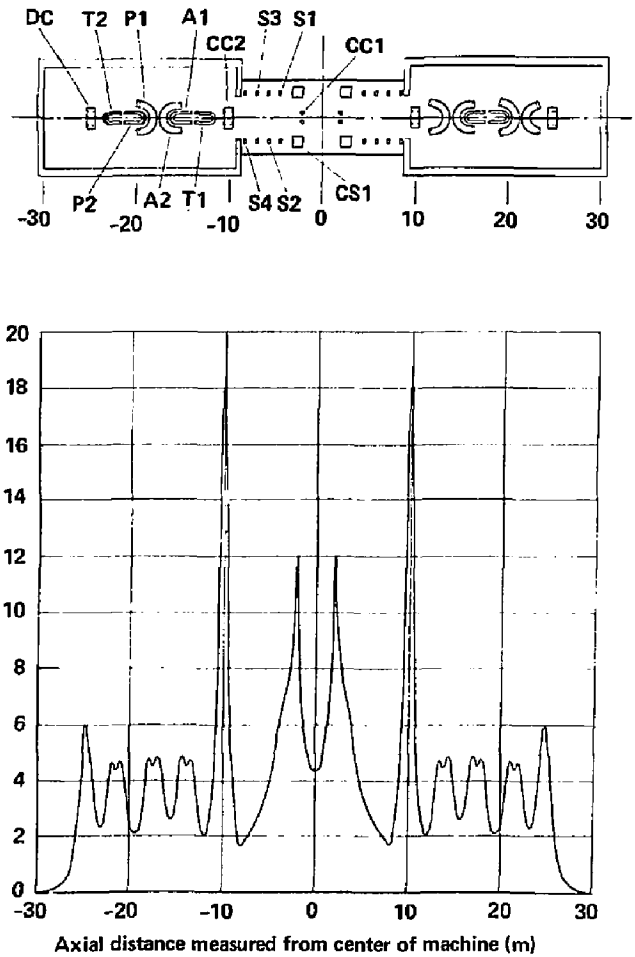

Fig. 2-3. MFTF-α+T magnet configuration, field on axis.

As we found in the TDF study,[2] large end plug confining potentials are not required to create high enough densities in a small-beam-injected mirror cell to produce interesting levels of 14-MeV neutron production. Indeed, 2XIIB (Ref. 3) produced $n > 10^{14}$ cm^{-3}, $T_i > 10$ keV at $\beta \simeq 1$, which would have generated > 1 W/cm^3 fusion power density in a few liters of volume with DT.

Because such plasmas are anisotropic, high densities and neutron fluxes can be generated with manageable beam powers in a small mirror cell volume even with a small $(Q_c)_{eff} \equiv$ fusion power/injection power, where, since injection power = central cell losses minus alpha heating,

$$(Q_c)_{eff} \simeq \frac{1/4\ n_{DT}^2 \langle\sigma v\rangle_{DT}\ 17600\ \text{keV}}{\left[\frac{n_{DT}^2}{(n\tau)_c}(E_{iloss} + \phi_e + T_{ec}) - P_{alpha}\left(\frac{\text{keV}}{\text{cm}^3\,\text{sec}}\right)\right]}\ , \qquad (1)$$

and where

$$(n\tau)_c^{-1} \simeq (n\tau)_{mirror}^{-1} \sim (2n\tau_{90}\ \log_{10}R)^{-1} + \left(n\tau_{drag}\&n\ \frac{E_{inj}}{E_{iloss}}\right)^{-1} \qquad (2)$$

would be a mirror ion confinement parameter limited by ion-ion scattering and electron drag.

Although mirror confinement alone may be adequate for neutron production, much more confinement is needed to ignite the central cell in a tandem mirror reactor, where the alpha heating term [P_{alpha} in Eq. (1)] equals the central cell energy losses $(Q_c)_{eff} \to \infty$. Because the required confinement time for ignition is many ion-ion scattering times, the central cell pressure tends to become isotropic, i.e., mirror throat density approaches the midplane density. In MFTF-B Upgrade the maximum mirror throat density that can be electrostatically plugged with thermal barriers (10^{14} cm^{-3} Maxwellian density, limited in part by ECRH absorption) is less than the peak midplane density supportable with 15 MW of available beam power in the most compactly designed mirror DT axicell. So, we are led to a design in which maximum $(Q_c)_{eff}$ and maximum Γ_n are achieved in two different operating modes--the "high Q" mode and the "high Γ" mode, respectively. However, we can make sure that the entire set of central cell and end plug hardware components for both modes of operation are compatible in the same device so that switching from one mode of operation to the other can be made as quickly

and easily as possible. Moreover, while the maximum plugging potentials in the high Q mode may not be needed in the high Γ mode, combining the end plug upgrade with the central cell upgrade provides a healthy margin in plugging potential generation for the high Γ mode. Aside from plugging potentials, the end plug upgrade provides an extra anchor cell for increased MHD β-limit and improved thermal barrier pumping (drift pumping), allowing the high Γ mode to be extended to 2 MW/m^2, significantly beyond the maximum of 1.3 MW/m^2 possible with the present MFTF-B end plugs.

2.1.2.1 The High Q Mode. Figure 2-4 shows axial profiles of magnetic field, potential, and density along the axis of the MFTF-Upgrade operated in the high Q mode. Table 2-1 lists plasma parameters in the DT axicell, central cell, transitions, anchors, and plugs. Table 2-2 lists heating systems parameters, and Table 2-3 summarizes performance parameters for this case. The coils and fields in Fig. 2-4 are taken as identical to the high Γ mode described in the next section, although future analysis may indicate a more optimum adjustment of coil currents and fields to maximize β and Q.

The potential profiles shown in Fig. 2-4 are plotted with respect to end wall plates biased to a sufficient negative voltage so that, with proper radial tailoring of the pumping ECRH and end wall potentials, the central cell radial electric field is held to a small fraction of T_{ec}/r_c. This minimizes resonant radial ion transport due to ExB drifts, which would otherwise reduce the radial ion confinement to much less than the 10^{14} cm^{-3}/sec required to achieve a Q = 2. Even with E_r = 0 in the central cell, there is still a residual neoclassical radial transport for central cell ions passing to the plugs. However, the geodesic curvature components in the quadrupole transition fields of this upgrade magnet design are smaller than in the present MFTF-B transition coil design by nearly a factor of three, increasing $(n\tau)_{neoclassical}$ by almost an order of magnitude, to an estimated 5×10^{14} cm^{-3} sec.

The dominant radial loss of central cell ions is expected to occur as a result of collisional trapping in the end transition regions, followed by radial loss induced by bounce-resonance drift pumping. This type of central cell loss, required to maintain low density thermal barriers in the ends, scales crudely as

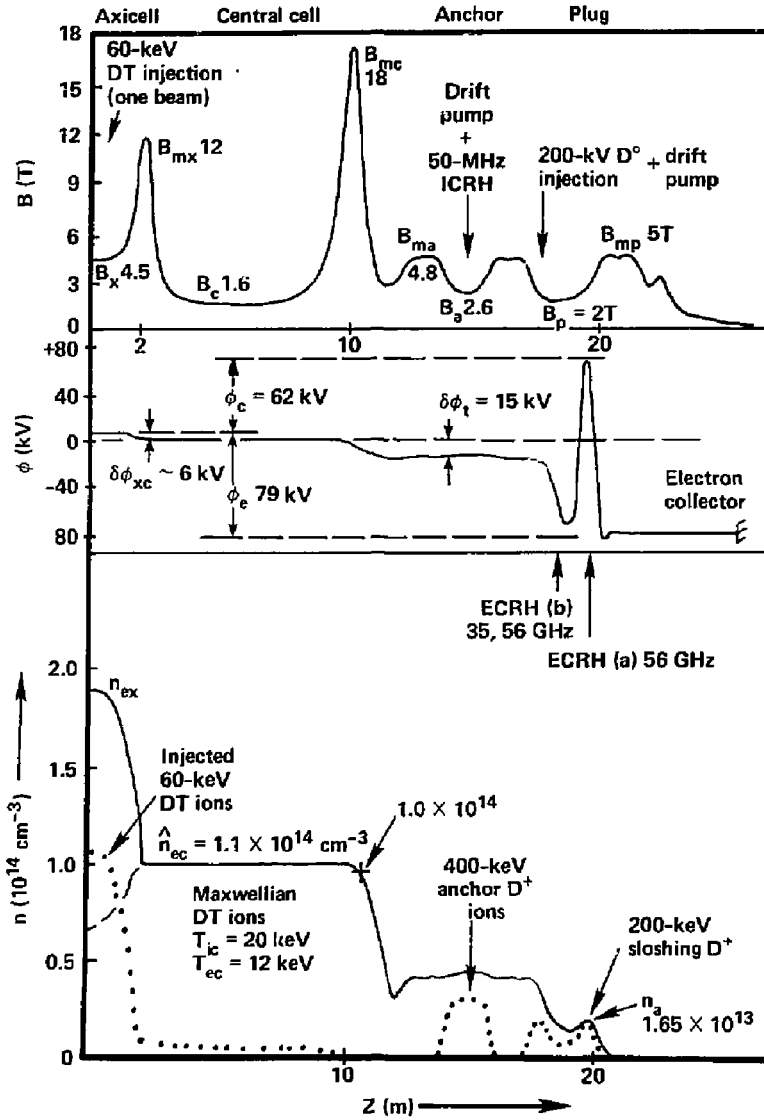

Fig. 2-4. Profiles of field, potential, and density in the high Q mode of MFTF-α+T.

Table 2-1. MFTF-B Upgrade (α+T, high Q_{ceff} = 2.4 mode).

Plasma parameter	Value
DT axicell	
B_x	4.5 T
B_{mx}	12T
$\bar{E}_{ix}$	50 keV
T_{ec}	12 keV
$\hat{n}_x$	1.9×10^{14} cm^{-3}
$\hat{\beta}_x$	0.28 \ quartic
$\langle\beta_x\rangle$	0.19 / radial profile
Φ_e	79 kV
Φ_c	62 kV
$(n\tau)_{\text{local mirror}}$	2.5×10^{13} cm^{-3}/sec
$\langle\sigma v\rangle_{DT}$	6.6×10^{-16} cm^3/sec
P_{fusion} (axicell)	2.25 MW
r_x	15 cm
r_{wall}	25 cm
L_{axicell}	4.0 m
$L_{x,\text{eff}}$	3.5 m
Γ_n (at r = 25 cm)	0.33 MW/m^2

Table 2-1. (Continued.)

Plasma parameter	Value
Central cell	
B_c	1.6 T
B_{mc}	18 T
n_{ec}	1.1×10^{14} cm^{-3}
n_{icw}	1.0×10^{14} cm^{-3}
n_{ich}	1.0×10^{13} cm^{-3}
T_{icw}	20 keV
T_{ichot}	30 keV
T_{ec}	12 keV
$\hat{\beta}_c$ (total)	0.6 (quartic)
$<\beta_c>$	0.4 (profile)
I_c (Pastukhov)	4.4 A
$(n\tau)_{Pastukhov}$	5.5×10^{14} cm^{-3} sec
ϕ_{ic}	68 kV
ϕ_{ec}	73 kV
r_c	25 cm
r_{wall}	45 cm
L_c	20 m
$L_{c,eff}$	12 m
P_{fusion} (central cell region)	4.55 MW
Γ_n (central cell region) at r_w = 45 cm	0.11 MW/m^2

Table 2-1. (Continued).

Plasma parameters	Value
Anchor	
$n_{pass}(B_A)$	5×10^{12} cm^{-3}
$n_H(B_A)$	2.4×10^{13} cm^{-3}
$n_e(B_A)$	3.4×10^{13} cm^{-3}
B_A	2.6 T (vac)
B_{res}	3.3 T (with plasma)
B_{nA}	4.8 T
$\hat{\beta}_A$	0.6 (quartic)
$<\beta_A>$	0.4 (profile)
$\bar{E}_H$	400 keV (D^+)
L_A	2.7 cm
L_{Aeff}	1.3 cm
r_A	20 cm
Transition (choke to $\hat{\phi}$)	
I_{trap}	21 A
I_{neo}	5.6 A
$\overline{\delta\Phi_t}$	15 kV
n_{pass} (3T)	8×10^{12} cm^{-3}
g_b	2.0

Table 2-1. (Continued).

Plasma parameters	Value
	Plug
n_{pass} (point b)	2×10^{12}
n_b (point b)	1.0×10^{13}
g_b	2.0
G_b	5.0
n_a	1.65×10^{13}
B_a	1.65 T (plasma)[a]
B_p (point b)	2.0 T (vac) 1.25 T (plasma)
B_a' (injection point)	2.7 T (plasma)
$\bar{E}_{eh}$	580 keV
T_{ew}	100 keV
$\hat{\beta}_p$	0.6 (quartic)
$<\beta_p>$	0.4 (profile)
$\delta\phi_{a'\rightarrow a}$	78 kV
$\delta\phi_a$	125 kV
$\hat{n}_{slosh}/n_s$(b)	2.75

[a]β-depressed values are denoted (plasma).

Table 2-2. MFTF-B Upgrade heating systems (α+T, high Q_{ceff} = 2.4 mode).

System	Trapped power current	Incident power current	Frequency (voltage)
Axicell beams	1.86 MW 31 A	2.7 MW 45 A	E_{inj} (60 keV) $\theta_{inj} \geq 75^{o}$
Anchor drift pump	15 kW (antenna dissipation) + 50 kW (plasma dissipation) each anchor	0.66 MW reactive (each anchor) $I_{antenna}$ $\sim$ 1.3 kA RMS (each 4 loops)	f_o = 160 kHz $\Delta f_o = \pm$ 32 kHz N = 12 oscillators 5.3 kHz apart
Plug drift pump	1.5 kW (antenna dissipation) + 65 kW (plasma dissipation) each plug	0.2 MW reactive (each plug) $I_{antenna} \sim$ 0.4 kA RMS (each 4 loops)	f_o = 1.2 MHz $\Delta f_o = \pm$ 84 kHz 1 FM oscillator 0.1 sec sweeptime
Anchor ICRH	350 kW absorbed each anchor 67 kW absorbed each anchor	700 kW (antenna) 130 kW (antenna)	25 MHz (ω_o fundamental) 50 MHz (2 ω_o for β control)
Plug ECRH	320 kW each plug at b 300 kW each plug at b 60 kW each plug at a	384 kW 360 kW 72 kW	35 GHz 56 GHz 56 GHz
Plug sloshing beam	125 kW 0.63 A (each plug) at a'	0.84 MW 4.2 A (each plug) at a'	200 keV (D^{o})

Table 2-3. MFTF-B Upgrade (α+T, high Q_{ceff} = 2.4 mode).

Composite confinement parameters (combined axicell, central cell), n^2 x volume-weighted average

$(n\tau)_{DT}$	= 1.0×10^{14} cm^{-3} sec	Radial + axial ion
τ_{DT}	= 1.06 sec	particle containment
$(n\tau)_{energy}$	= 4.2×10^{13} cm^{-3} sec	Radial + axial
τ_{energy}	= 0.42 sec	energy containment

$$Q_c = \frac{P_{fusion}\ (axicell + cc)}{(axicell + cc)\ energy\ losses} = 1.7$$

$$Q_{ceff} = \frac{P_{fusion}\ (axicell\ cell + cc)}{energy\ losses - alpha\ heating} = 2.4$$

$$Global\ Q = \frac{P_{fusion}\ (axicell + cc)}{total\ cc + plug\ injected\ power} = 1.5$$

$$(n\tau)_{pump} \simeq 10 n\tau_{ii} \left(\frac{B_{max}}{B_c}\right) \frac{L_{ceff}}{2 L_t} \simeq (1.8 \times 10^{14}\ cm^{-3}\ s), \qquad (3)$$

where $n\tau_{ii}$ is the 90^0 ion-ion scattering time at temperature T_{ic} (20 keV), and B_{max} (18 T) and L_t (10 m) are the peak mirror field and transition length, respectively, over which pumping is required. The length of a uniform cylinder of radius r_c = 25 cm, having the same volume as the central cell plasma, is $(L_c)_{eff}$ = 12 m. The factor of 10 in Eq. (3) comes from matching Fokker-Planck calculations. With central cell ion plugging potential of ϕ_c = 62 keV (*Fig. 2-2*), *which is sufficient to give an axial confinement* $(n\tau)_{axial} = (n\tau)_{pastukhov} = 5 \times 10^{14}\ cm^{-3}\ s$, the equivalent radial ion losses due to transition drift pumping exceed the axial electrostatic ion losses. So, $(n\tau)_{radial} = [(n\tau)^{-1}_{pump} + (n\tau)^{-1}_{neoclassical}]^{-1} = 1.4 \times 10^{14}\ cm^{-3}\ s$, and $(n\tau)_{total} = [(n\tau)^{-1}_{radial} + (n\tau)^{-1}_{axial}]^{-1} = 1.0 \times 10^{14}\ cm^{-3}\ s$. The scaling for $(n\tau)_{pump}$ by Eq. (3) is what motivates the development of higher field (18-T) choke coils placed a maximum 20 m apart, as shown in Fig. 2-4, to maximize $n\tau$ and Q. The estimated neoclassical electron transport is much smaller than for the ions, so that all electron losses are taken as axial losses to the negative electron collectors at each end. The mainly radial ion loss and the axial electron loss is the same situation as in the MARS reactor, where collection of the electron losses at $-\phi_e$ potential on a biased, gridless plate constitutes a simple and efficient direct conversion. Although end plugging was not sufficient to stem all the axial ion loss in TMX, there was a net electron current collected in the ends, consistent with the predictions of neoclassical theory.[4]

To be confined by the plug mirrors, sloshing ions must be injected with an energy above a cutoff

$$E_{cutoff} > \frac{(\phi_c + \phi_e)}{\frac{B_{mirror}}{B_{inj}} - 1}, \qquad (4)$$

which, for a total potential drop $\phi_c + \phi_e$ = 140 kV, requires approximately 200 keV of negative-ion-based neutral beams. These ion energies are within, but not far from, the adiabatic energy limit for conservation of μ of deuterium ions

$$E_{adiabatic} < 250\ B_p^2(T)\ (1-B_p)\ L_m^2(m)\ keV, \qquad (5)$$

or, $E_{adiabatic} < 320$ keV for $B_p = 2T$, $\beta_p = 0.6$, and magnetic doubling scale length $L_m = 0.9$ m in the plugs. In other words, the potentials shown in Fig. 2-4 are near the maximum consistent with adiabatic sloshing ion energy limits in the end plug magnets. Because the central cell ion temperature, electrostatic potential, and sloshing ion energy tend to scale together, the adiabaticity limit sets an upper limit on the end plugging capability with the upgrade end plug magnets, given a negative ion beam to match the adiabatic limits. This observation, together with the limits on radial confinement set by pumping Eq. (3), which depends on basic machine parameters such as mirror ratios and central-cell-to-end-plug-length ratios, lead to the conclusion that $Q \simeq 2$ may be the maximum that can be achieved in an MFTF-Upgrade device with physical dimensions similar to the present MFTF-B machine.

A particularly significant improvement in the MFTF-Upgrade end plug magnet design, besides the higher fields raising adiabatic energy limits compared to MFTF-B, is the inclusion of an extra yin-yang anchor in the transition region between the choke coil and the plug. This anchor region evolved from the MFTF-B design by replacing the transition-baseball coil in the MFTF-B transition design[1] with a yin-yang pair and raising the local fields and mirror ratio to provide a local mirror cell into which beams or ICRH could be used to add anisotropic ion pressure in a region of good curvature. Present thinking favors the use of ICRH to add the pressure, but energetic negative ion beams might also be used as an alternative. The extra anchors in the MFTF-Upgrade design more than double the MHD β-limit in the central cell because the higher fields (compared to MFTF-B transitions) reduce the magnitude of bad curvature in the connecting flux tube fans and add more good curvature in the anchor wells. (Reduced geodesic curvature also accompanies reduced normal curvature, thus reducing neoclassical transport as we have noted.)

The density profiles in shown Fig. 2-4 represent the maximum value in the central cell region consistent with a calculated MHD β-limit $\langle\beta_c\rangle \simeq 0.4$ (volume average). For a given β-limit, the central cell density could be raised by proportionately lowering all the temperatures, potentials, and beam energies. However, because both central cell and end plug losses are dominated by Coulomb collision processes, $n\tau$ would decrease proportional to $T^{3/2}$. Moreover, the fusion reaction rate $\langle\sigma v\rangle_{DT}$ would decrease, so that $Q \sim n\tau \langle\sigma v\rangle$ would drop on both counts. On the other hand, maintaining

the temperatures specified in Fig. 2-4, while lowering all the densities and betas, would not affect Q much because collision-rate-limited ($n\tau$)'s are independent of density. Thus, only the maximum neutron wall loading depends strongly on the β-limit in this high Q mode, which is limited to 0.33 MW/m^2 in the axicell and 0.11 MW/m^2 in the central cell for the maximum densities and betas assumed in Fig. 2-4. In addition to the β-limits corresponding to $\beta = 0.6$ on axis in the central cell, anchor, and plug mid-planes, the maximum central cell density would be constrained by the maximum plug density for ECRH heating, together with the relationship between plug and central cell densities for pumped thermal barriers

$$n_p \approx n_c \left(\frac{B_p}{B_{max}}\right) \left(\frac{T_{ic}}{\pi(\phi_c - \phi_p)}\right)^{1/2} \left(\frac{n_{trap} + n_{pass}}{n_{pass}}\right)$$

$$\sim n_c B_p/B_{max}, \qquad (6)$$

where n_c is the Maxwellian density at the throat of the $B_{max} = 18$ T choke coil. Here again we see the motivation to increase B_{max} to as high a field as practical in MFTF-Upgrade, either by increasing n_c for a given plug density (increased fusion power), or by reducing n_p and plug ECRH power $\propto n_p^2$ for a given n_c. For $B_p \approx 2$ T ($f_{ce} = 56$ GHz), the maximum useful density for ECRH heating would be four times that of the TMX-Upgrade ($B_p \sim 1$T, 28 GHz, $n = 5 \times 10^{12}$ cm^{-3}), or $n_p(max) \approx 2 \times 10^{13}$. This would produce $n_c(max) \approx 1.8 \times 10^{14}$ in Eq. (6), not much higher than the 1.1×10^{14} cm^{-3} limited by β.

By providing the fueling (30 A equivalent DT) and auxiliary heating (1.8 MW) required to sustain the central cell losses in the high Q mode with one neutral beam of 30 A, 60 keV (trapped) injected into the DT axicell, Fokker-Planck calculations indicate that the local peaking of injected ion density in the axicell would be less than a factor of two over the Maxwellian density in the central cell. Substituting an alternative combination of 30 A equivalent of pellet injection with an equal power (1.8 MW) of ICRH, Fokker-Planck models indicate the local density peak would be even smaller than with a beam. From the foregoing considerations, we conclude that for this maximized Q mode, the maximum neutron wall loading would probably be limited below 0.1 MW/m^2.

The primary purpose of the high Q mode is to approach as close as possible to conditions in an ignited tandem mirror reactor such as MARS or FPD. In terms of the relative importance of alpha heating to the central cell energy balance, the high Q mode is about a factor of 3.5 away from ignition; i.e., the central-cell energy losses consist of (21 A pump radial ion loss + 5.6 A neoclassical ion radial loss) x 3/2 T_{ic} = 0.8 MW; (4.4 A axial ion loss) x (ϕ_c + T_{ic}) = 0.4 MW; (31 A of axial electron loss) x (ϕ_e + T_{ec}) = 2.8 MW, giving a total power loss of 4.0 MW. The fusion power in the central cell is 4.55 MW and the fusion in the axicell (the source of central cell heating and fueling) is 2.25 MW, or 6.8 MW total fusion power. The alpha power generated is thus 6.8 (0.2) = 1.36 MW, of which Fokker-Planck calculations give 85% (1.16 MW) as mirror-trapped and transferred to the central cell ions and electrons. Thus, fusion alpha heating constitutes 1.16/4.0 = 29% of the central cell energy losses. These effects of alpha heating on central cell energy balance are certainly enough to be measurable, and experimental determination of the fractional energy transfer of the alpha energy to the plasma (to compare with Fokker-Planck), would be an important goal of MFTF-Upgrade in the high Q mode.

In terms of $n\tau$, the high Q mode is about a factor of 5 away from central cell ignition; $(n\tau)_{DT} \approx 10^{14}$ cm^{-3} sec in MFTF-Upgrade vs 5×10^{14} cm^{-3} sec needed for ignition in MARS and FPD. The reason ignition $n\tau$ is more than $(0.29)^{-1}$ times 10^{14} cm^{-3}, where alpha heating is 29%, is because the energy losses per ion-electron pair ($E_{i\ loss}$ + ϕ_c + T_{ec} + ϕ_e) in Eq. (1) must increase as $n\tau$ increases, since both ion and electron confining potentials increase as $\ell n\ (n\tau/n\tau_{cat})$. In spite of the "ignition gap" in $n\tau$, the high Q mode can operate in the same physics confinement regime as in MARS and FPD, where the relative importance of pumping and neoclassical radial ion losses would be nearly the same.

Another important alpha physics issue which the high Q mode of MFTF-α+T can address is the accumulation of thermal alphas and the efficiency of their removal by neoclassical radial transport and bounce-resonance drift pumping. Without such radial loss mechanisms, Fokker-Planck calculations show that equilibrium thermal alpha fractions could build up to very high levels in a tandem mirror:

$$\frac{n_\alpha(\text{thermal})}{n_{DT}} \simeq f_{\text{thermal}}\, f_{\text{burnup}} \left(\frac{\exp \phi_c/T_{ic}}{z_\alpha^2}\right) , \qquad (7)$$

where $f_{\text{thermal}} \simeq 0.7$ is the fraction of alphas thermalized to the DT temperature, and $f_{\text{burnup}} \simeq 1/2(n\tau)_{DT} \langle\sigma v\rangle_{DT}$ is the DT burnup fraction. For MARS and FPD with $f_{\text{burnup}} \simeq 0.15$ and $\phi_c/T_{ic} \simeq 5$, Eq. (7) predicts a disastrous $n_\alpha = 4\ n_{DT}$, but even for MFTF-Upgrade with $f_{\text{burnup}} = 0.02$ and a lower $\phi_c/T_{ic} = 3.4$, Eq. (7) still give a significant concentration level $n_\alpha = 0.1$. Consequently, n_{DT} is 20% higher than n_e and there is a 40% increase in the DT ion collision rate. Therefore, determination of radial loss rates of thermal alphas in MFTF-Upgrade is both possible--because the consequences of factors of 2 in the radial loss rates would have significant effects on n_e/n_i and on scattering rates--and valuable in pinpointing ignition conditions for FPD. We could, of course, inject helium into the central cell to simulate part of the thermal alpha physics, but only DT operation would confirm the actual thermalization fraction f_{thermal} originating from 3.5-MeV alphas, and produce the correct radial profiles upon which the transport rates depend.

2.1.2.2 The High Γ Mode. Figure 2-5 shows axial profiles of magnetic field, potential, and density along the axis of the MFTF-Upgrade operated in the high Γ mode. Table 2-4 lists plasma parameters in the DT axicell, central cell, transitions, anchors and plugs. Table 2-5 lists heating systems parameters for this mode, and Table 2-6 summarizes performance parameters. The coils, magnetic fields, and end plug heating equipment used in this mode of operation are the same as those used in the high Q mode described in the previous section. Essentially, only the amount of beam power injected into the DT axicell and the amount of plug ECRH are changed significantly (1 axicell beam in the high Q mode → 6 axicell beams in the high Γ mode, 1.36 MW total absorbed ECRH power in the high Q mode → 2.0 MW ECRH in the high Γ mode).

Neutral beam injection into the central DT axicell (the blanket test cell) is increased sixfold in the high Γ mode for the sole purpose of increasing the peak density of mirror-trapped DT ions in the test cell to the maximum set by MHD β-limits, thereby maximizing the local 14-MeV neutron flux ($\Gamma_n = 2\ \text{MW/m}^2$) for blanket testing purposes. The maximum axicell

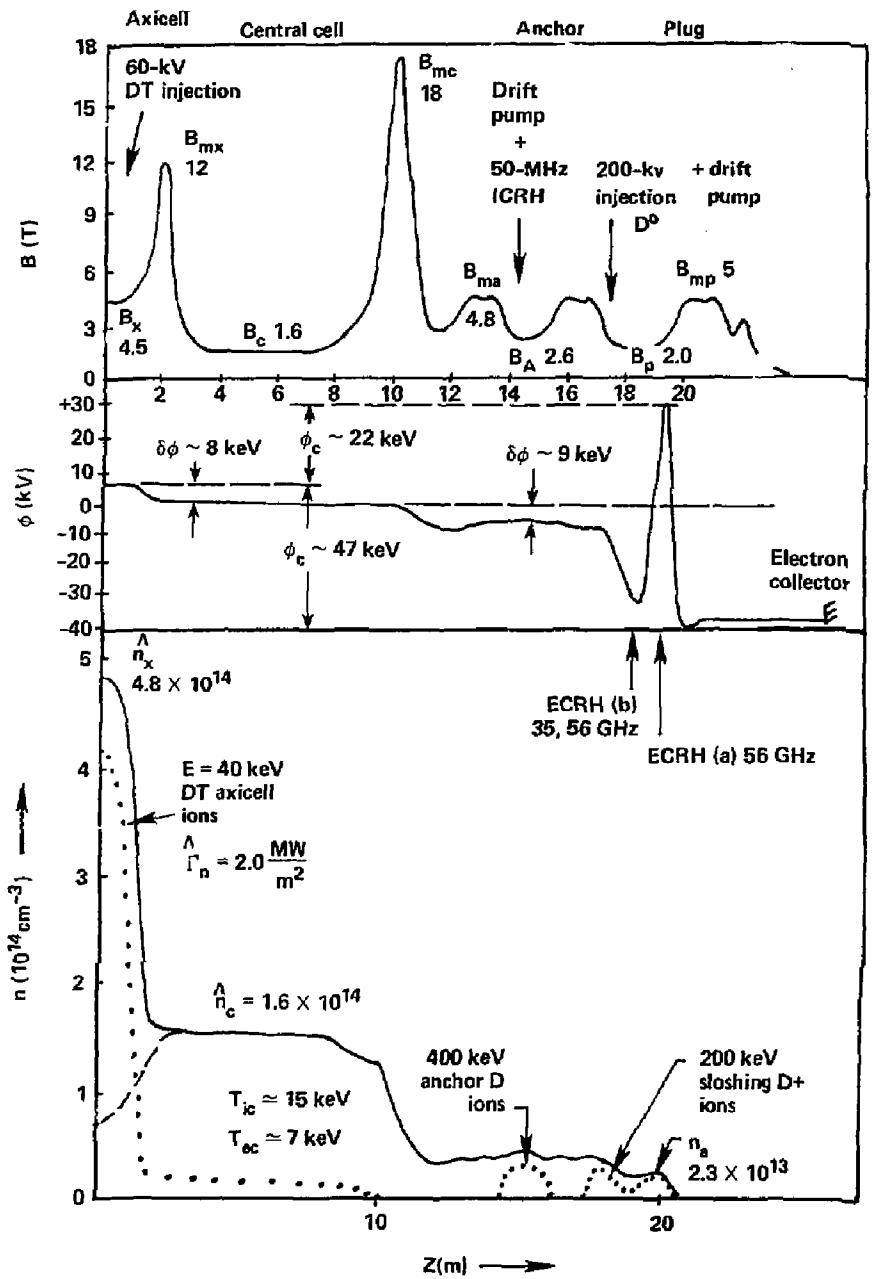

Fig. 2-5. Profiles of field, potential, and density in the high Γ mode of MFTF-α+T.

Table 2-4. MFTF-B Upgrade (α+T, high Γ_n = 2 MW/m^2 mode).

Plasma parameter	Value
DT axicell	
B_x	4.5 T
B_{mx}	12T
$\bar{E}_{ix}$	40 keV
T_{ec}	7 keV
$\hat{n}_x$	4.75×10^{14} cm^{-3}
$\hat{\beta}_x$	0.46 (quartic)
$\langle\beta_x\rangle$	0.31 (radial profile)
ϕ_e	47 keV
ϕ_c	22 keV
$(n\tau)_{\text{local mirror}}$	2.0×10^{13} cm^{-3}/sec
$\langle\sigma v\rangle_{DT}$	6.6×10^{-16} cm^3/sec
P_{fusion} (axicell)	11.0 MW
r_x	15 cm
r_{wall}	25 cm
L_{axicell}	4.0 m
$L_{x,\text{eff}}$	2.8 m
Γ_n (at r = 25 cm)	2.0 MW/m^2

Table 2-4. (Continued.)

Plasma parameter	Value
Central cell	
B_c	1.6 T
B_{mc}	18 T
n_{ec}	1.6×10^{14} cm^{-3}
n_{icw}	1.3×10^{14} cm^{-3}
n_{ich}	3×10^{13} cm^{-3}
T_{icw}	15 keV
T_{ichot}	20 keV
T_{ec}	7 keV
$\hat{\beta}_c$ (total)	0.6 (quartic)
$<\beta_c>$	0.4 (profile)
I_c (Pastukhov)	90 A
$(n\tau)_{Pastukhov}$	4.7×10^{13} cm^{-3} sec
ϕ_{ic}	30 kV
ϕ_{ec}	39 kV
r_c	25 cm
r_{wall}	45 cm
L_c	20 m
$L_{c,eff}$	12 m
P_{fusion} (central cell region)	5.9 MW
Γ_n (central cell region) at r_w = 45 cm	0.14 MW/m^2

Table 2-4. (Continued.)

Plasma parameters	Value
Anchor	
$n_{pass}(B_A)$	7.75×10^{12} cm^{-3}
n_H (B_A)	2.4×10^{13} cm^{-3}
n_e (B_A)	3.7×10^{13} cm^{-3}
B_A	2.6 T (vac)
B_{res}	3.3 T (with plasma)
B_{nA}	4.8 T
$\hat{\beta}_A$	0.5 (quartic)
$\langle\beta_A\rangle$	0.4 (profile)
$\overline{E}_H$	400 keV (D^+)
L_A	70 cm
L_{Aeff}	130 cm
r_A	20 cm
Transition (choke to ϕ)	
I_{trap}	97 A
I_{neo}	3 A
$\overline{\delta\phi}_t$	10 kV
n_{pass} (3T)	1.2×10^{13} cm^{-3}
g_b	1.7

Table 2-4. (Continued.)

Plasma Parameters	Value
Plug	
n_{pass} (point b)	3×10^{12}
n_b (point b)	1.2×10^{13}
g_b	1.7
G_b	4
n_a	2.3×10^{13}
B_a	2.2 T (plasma)
B_p (point b)	2.0 T (vac) 1.25 T (plasma)
$B_{a'}$ (injection point)	2.7 T (plasma)
$\bar{E}_{eh}$	475 keV
T_{ew}	60 keV
$\hat{\beta}_p$	0.6 (quartic)
$\langle\beta_p\rangle$	0.4 (profile)
$\delta\phi_{a'\to a}$	37 kV
$\delta\phi_a$	60 kV
$\hat{n}_{slosh}/n_s(b)$	3.3

Table 2-5. MFTF-B Upgrade heating systems (α+T, high Γ_n mode).

System	Trapped power current	Incident power current	Frequency (voltage)
Axicell beams	11.4 MW 190 A	14.4 MW 240 A	E_{inj} (60 keV) $\theta_{inj} \geq 75^{o}$
Anchor drift pump	80 kW antenna dissipation + 150 kW plasma dissipation (each anchor)	3 MW reactive (each anchor) $I_{antenna}$ $\sim$ 3 kA RMS (each 4 loops)	f_o = 140 kHz $\Delta f_o = \pm$ 28 kHz N = 10 oscillators 5.6 kHz apart
Plug drift pump	1.5 kW antenna dissipation + 24 kW plasma dissipation (each plug)	0.2 MW reactive (each plug) $I_{antenna} \sim$ 0.4 kA RMS (each 4 loops)	f_o = 1.2 MHz $\Delta f_o = \pm$ 84 kHz 1 FM oscillator 0.1 sec sweeptime
Anchor ICRH	400 kW absorbed each anchor 170 kW absorbed each anchor	800 kW (antenna) 340 kW (antenna)	25 MHz (ω_D, fundamental) 50 MHz (2 ω_D for β control)
Plug ECRH	500 kW each plug at b 400 kW each plug at b 100 kW each plug at a	600 kW 480 kW 120 kW	35 GHz 56 GHz 56 GHz
Plug sloshing beam	85 kW 0.42 A (each plug) at a'	0.44 MW 2.2 A (each plug) at a'	200 keV (D^o)

Table 2-6. MFTF-B Upgrade (α+T, high Γ_n = 2 mode).

Composite confinement parameters (combined axicell, central cell)

$(n\tau)_{DT}$	$= 4.7 \times 10^{13}$ cm^{-3} sec	Radial + axial ion particle containment[a]
τ_{DT}	= 0.26 sec	
$(n\tau)_{energy}$	$= 2.2 \times 10^{13}$ cm^{-7} sec	Radial + axial energy containment[a]
τ_{energy}	= 0.11 sec	

$$Q_c = \frac{P_{fusion}\ (\text{axicell + cc})}{(\text{axicell + cc})\ \text{energy losses}} = 1.0$$

$$Q_{ceff} = \frac{P_{fusion}\ (\text{axicell cell + cc})}{\text{energy losses - alpha heating}} = 1.2$$

$$\text{Global } Q = \frac{P_{fusion}\ (\text{axicell + cc})}{\text{total cc + plug injected power}} = 1.1$$

[a] $n\tau$ values are (n^2V) weighted, and τ values are (nV) weighted.
V = volume.

β $<\beta_x>$ = 0.31 in the high Γ mode is moderately higher than the β $<\beta_x>$ = 0.19 in the high Q mode because the pressure of Maxwellian plasma in the central cell and passing through the transitions is 11% lower in the high Γ mode than in the high Q mode due to lower T_{ic} and T_{ec} (20 keV and 12 keV in the high Q mode vs 15 keV and 7 keV in the high Γ mode). MHD stability allows pressure in one bad curvature region to be traded off with pressure in another bad curvature, although this is limited to some extent by ballooning. Because some of the bad curvature drive in the central cell regions could, as an option, be reduced by drift-pumping the Maxiwellian component down to the density of passing ions in <u>both</u> the central cell and transition regions, the allowed β in the axicell could be raised beyond $<\beta_x>$ = 0.31 and, correspondingly, Γ_n could be increased beyond 2 MW/m^2, provided enough neutral beams were added (in part to match the increase in n_x^2, and to compensate for a 20 to 30% reduction in $n\tau_{local}$ caused by the central cell pumping). Because six to eight beams are a reasonable match to the space available for beam lines in the compact axicell design that we are considering for the MFTF-Upgrade, we have decided to forgo the option of beam pumping to remove pressure from the central cell regions. So, significant fusion power (5.9 MW) continues to be generated between the 12- and 18-T mirrors of the central cell in the high Γ mode as in the high Q mode. Aside from the benefit of an additional 1 MW of alpha heating to the central cell power balance, keeping a long Maxwellian plasma column in the central cell allows almost as much physics data to be taken in the central cell region during high Γ mode operation as in high Q mode operation. Therefore, operating time for blanket testing need not conflict with time needed to diagnose fusion physics in the central cell.

However, some quantitative reductions in $n\tau_{DT}$ and $Q_{c\ eff}$ are required for high Γ operation compared to high Q operation. Increasing the injected beam current from 30 A in the high Q mode to 190 A in the high Γ mode in the same volume axicell produces about a sixfold increase in n_x^2 in the axicell. This is because in the axicell $n\tau_{local}$ is mostly a mirror-scattering $n\tau$ [see Eq. (2)] and we have held E_{inj} fixed at 60 keV. Because the 18-T mirror field is significantly higher than the 12-T axicell mirror field, most of the injected axicell current will transfer into the Maxwellian central cell plasma. If we held ($n\tau$) in the central cell fixed to the values of the high Q mode (i.e., T_{ic} and ϕ_c held to 20 keV and 62 kV, respectively), then

six axicell beams would cause the central cell density to rise by the same factor ($\sqrt{6}$) as in the axicell. MHD stability allows only a smaller increase in central cell density, to $n_{cwarm} \approx 1.3 \times 10^{14}$ cm^{-3} Maxwellian density--allowed by the decrease in T_{ic} and T_{ec} in the high Γ mode). Therefore, the local $(n\tau)_c$ for the central cell ions must drop by a factor of almost four, from 10^{14} cm^{-3} sec to around 2.5×10^{13} cm^{-3}, to accommodate the sixfold increase in current. This is accomplished in the high Γ mode by a lower $(n\tau)$ pump $\sim 5 \times 10^{13}$ cm^{-3} sec [due to lower T_{ic} and smaller transition $g_b = (n_{trap} + n_{pass})/n_{pass}$, which reduces the coefficient in Eq. (3) below 10], and by a 10x lower $(n\tau)_{pump}$ Pastukhov (axial) $\sim 5 \times 10^{13}$ cm^{-3} sec (due to lowering of ϕ_{ic} from 68 to 30 kV).

Because the same DT ions spend time in both the high and low field portions of the central cell, a composite $(n\tau)_{DT}$ defined by an n^2-weighted average

$$(n\tau)_{DT} = \frac{\frac{16}{30}\,(n_x^2\, V_x + n_c^2\, V_c)}{I/q} \tau \tag{8}$$

and an average time in the system defined as

$$\tau_{DT} = \frac{\frac{2}{3}\,(n_x\, V_x + n_c\, V_c)}{I_{beam}/q} \tag{9}$$

will always be larger than the local $n\tau$'s and τ's obtained by dividing the current into that local cell alone. However, obtaining the τ_{DT} and $(n\tau)_{DT}$ in this way allows us to better judge the sensitivity of the whole system to unknown loss processes other than the ones that have been included in this analysis. In Eqs. (8) and (9), the factors 16/30 and 2/3 are radial profile factors appropriate for the quartic radial profiles

$$n(r) = n\,[1 - (\frac{r}{r_p})^4] \tag{10}$$

assumed in this report. For energy confinement, we similarly define

$$(n\tau)_{Energy} = \frac{\frac{16}{30}\,[n_x^2\, V_x(E_{ix} + \frac{3}{2}\,T_{ec}) + n_c^2\, V_c(\frac{3}{2}\,T_{ic} + \frac{3}{2}\,T_{ec})]}{I_{injected}\,(E_{iloss} + \phi_e + T_{ec})} \tau \tag{11}$$

and

$$\tau_{Energy} = \frac{\frac{2}{3}\left[n_x V_x\left(E_{ix} + \frac{3}{2} T_{ec}\right) + n_c V_c\left(\frac{3}{2} T_{ic} + \frac{3}{2} T_{ec}\right)\right]}{I_{injected}\left(E_{iloss} + \phi_e + T_{ec}\right)} , \tag{12}$$

where

$$E_{iloss} = \frac{I_{radial}\left(\frac{3}{2} T_{ic}\right) + I_{axial}\left(\phi_c + T_{ic}\right)}{I_{injected}} , \tag{13}$$

$$V_x = \pi r_x^2 L_{x,eff} , \tag{14}$$

$$V_c = \pi r_c^2 L_{c,eff} , \tag{15}$$

$$L_{eff} = \int_{mirror}^{mirror} \left(\frac{n(z)}{n}\right)^2 \left(\frac{B_0}{B(z)}\right) dz . \tag{16}$$

When we compare Table 2-3 and Table 2-6 we see that the high Γ mode requires about a factor of 2 less $n\tau$ (both particle and energy) and about a factor of 4 less τ (both particle and energy) compared to the high Q mode. Thus, the high Γ mode is "safer" with respect to unknown losses, to help ensure blanket testing, while the high Q mode pushes confinement against "known" loss processes to their limit, and therefore is better equipped to test the importance of any "unknown" losses.

2.1.3 Engineering Description

The engineering aspects of the MFTF-α+T Upgrade derive from an engineering study that we conducted to establish a credible design concept, to provide a basis for realistic costing, and to schedule the project in accordance with budget profiles consistent with the needs of the overall mirror program. Although the study was not detailed enough to provide a conceptual design, it did accomplish the above goals.

The upgraded device incorporates some totally new systems and modifies some existing components where necessary. In addition, wherever possible, existing hardware has been incorporated to maximize the contribution of the

current device to the upgrade. The present day value of the MFTF-B systems used in the upgrade is ~$270 M (mid-FY 83 dollars).

The most technologically innovative additions are the continuous 80- and 200-keV neutral beams and the introduction of high-field (18-T) unshielded copper coils. These items require an aggressive development program to be available in reliable form in the time frame of the upgrade construction schedule. The most critical new technology to be incorporated in this plasma confinement device is the tritium fuel cycle and cleanup system. The other challenge will be to design a machine that can be operated and maintained with acceptable reliability in the high radiation fields in a DT burning device.

2.1.3.1 Overview. As we have stated, the MFTF-α+T device is made up of various systems and components integrated into a configuration that meets the machine requirements while making maximum use of the existing MFTF-B experimental facility. The machine is built into the existing MFTF facilities in and around Building 431 (Fig. 2-6). The most noticeable facility modifications are in Building 431 where we have added hot cells for maintenance and a tritium processing facility. Significant modifications to power and cooling systems are also required.

Figure 2-7 is a cutaway plan view of the device showing the major systems and components. In this drawing, the components have been rotated into the plane of the drawing for the sake of clarity. All of the components of the end cells in Fig. 2-7 are actually oriented at 45° to the plane of the drawing. Accordingly, the halo plasma outline is also displaced by that angle.

For engineering purposes, the MFTF-α+T device configuration can be divided into three main areas: the DT axicell, the central cell, and the end cells. The end cells are surrounded by a 50-cm-thick concrete shield outside of the vacuum vessel to reduce activation within the vault.

The DT axicell portion of the fusion chamber that provides the vacuum boundary consists of a new structure designed to accommodate the above components. The two DT axicell beamlines are located on opposite sides of the device, with the beams intersecting the axis at an angle of 80°. The beam lines are angled 2° downward from horizontal (see Fig. 2-8a), so that their internal components may be withdrawn into a hot cell located on the first-floor level. Each of the two central-cell beamlines has a companion dump located opposite the beamline in a chamber outside the vacuum vessel

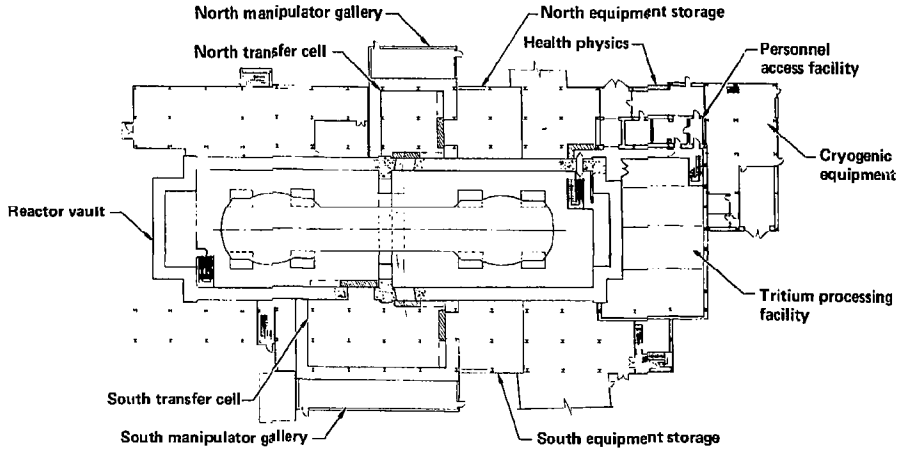

Fig. 2-6. MFTF-α+T facility layout (Building 431, first floor).

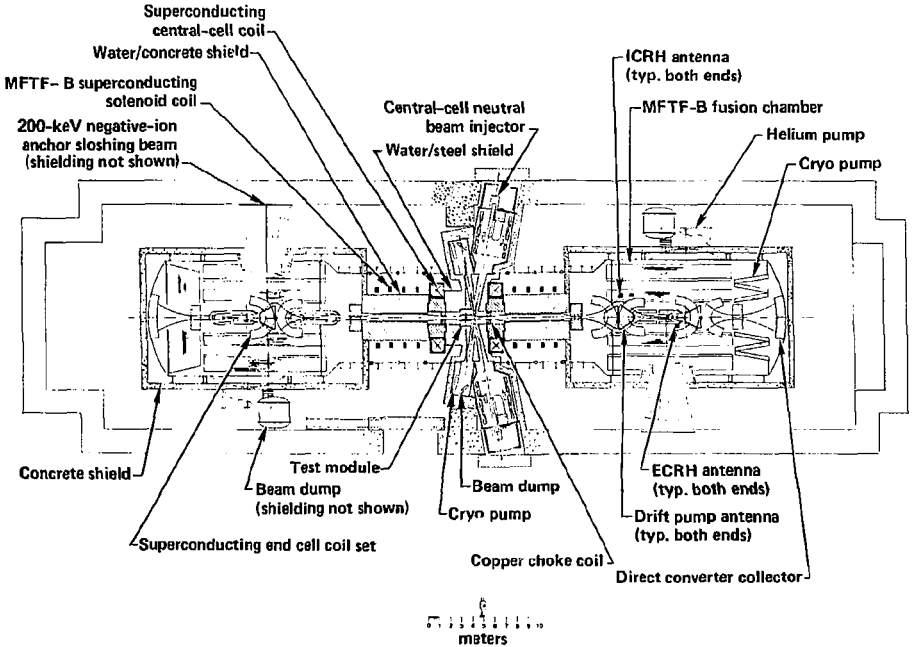

For clarity, components shown rotated into plane of paper

Fig. 2-7. MFTF-α+T Upgrade.

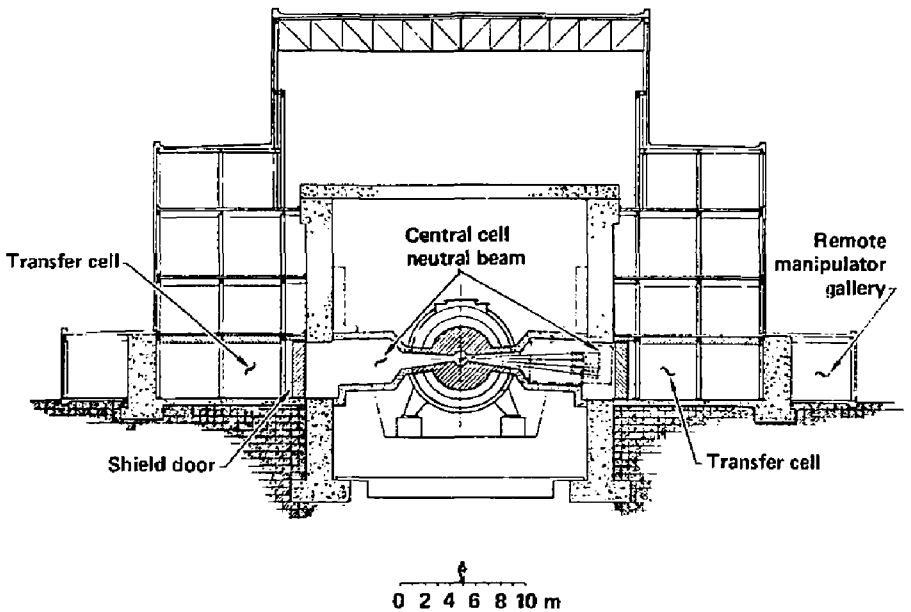

Fig. 2-8a. MFTF-α+T facility elevation through central cell (Building 431).

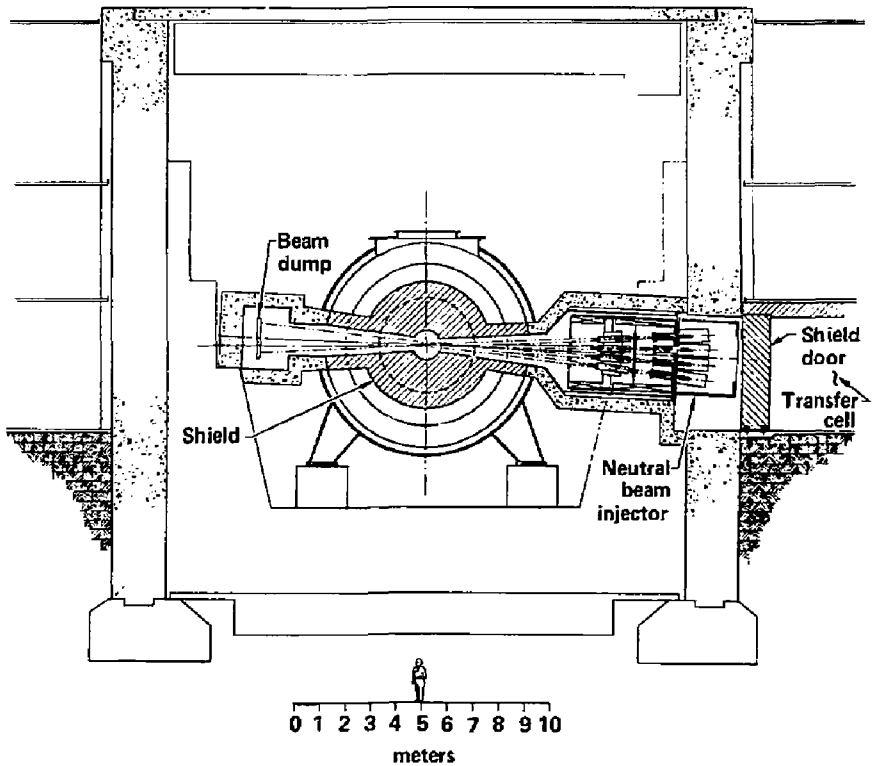

Fig. 2-8b. Elevation through central cell.

(Fig. 2-8b). The dump chamber contains a cryopump to remove the dump gas. The external location provides room for particle pumping and allows maintenance by simple vertical removal of the modular hardware.

The test module, located at the midpoint of the machine, can accommodate complete 360^0 specimens. Figure 2-9 shows the vertical access provided for module maintenance. The test module is located between the two normal conducting choke coils, which are 4 m apart. This distance was selected to provide relatively uniform neutron wall loading over the 1-m-long test module. Additional test volume is available to the side of the test module away from the beamlines.

The central cells are located to each side of the axicell and extend 8 m to the 18-T choke coil. Each portion of the central cell contains nuclear shielding modules within the bore of four MFTF-B solenoid coils. Structural reinforcements are provided to accommodate the nuclear shielding boundary in the anchor and plug coil regions. A 200-keV negative-ion beam is located at the anchor. This anchor sloshing beam is oriented at 45^0 to the vertical, such that the beam passes through the throat of the anchor coil.

A particle dump with its particle pumping cryopanels is located at the extreme end of the coil set. Plasma-streaming guns are provided for startup. The particle-dump design accommodates these guns and provides for their protection from particle bombardment.

2.1.3.2 Machine Description.

Magnets. The MFTF-α+T magnet configuration requires extensive modification of the MFTF-B magnet set. The existing end plugs, including the MFTF-B axicells, must be removed and replaced by the end-plug upgrade. The DT axicell magnets are added to provide the field required for high-flux DT operation. Plasma confinement in the ∿ 8 m between the DT axicell and each end cell is provided by the existing central-cell solenoid coils of MFTF-B. Figure 2-3 shows the MFTF-α+T magnet configuration and the field on axis which results. A listing of pertinent magnet parameters is given in Table 2-7.

The magnet configuration described in Fig. 2-3 and Table 2-7 provides the required field profile on axis. Detailed component design will be required to verify that the winding locations are compatible with structural and shielding design criteria of the components. Access for beams and beam dumps has been

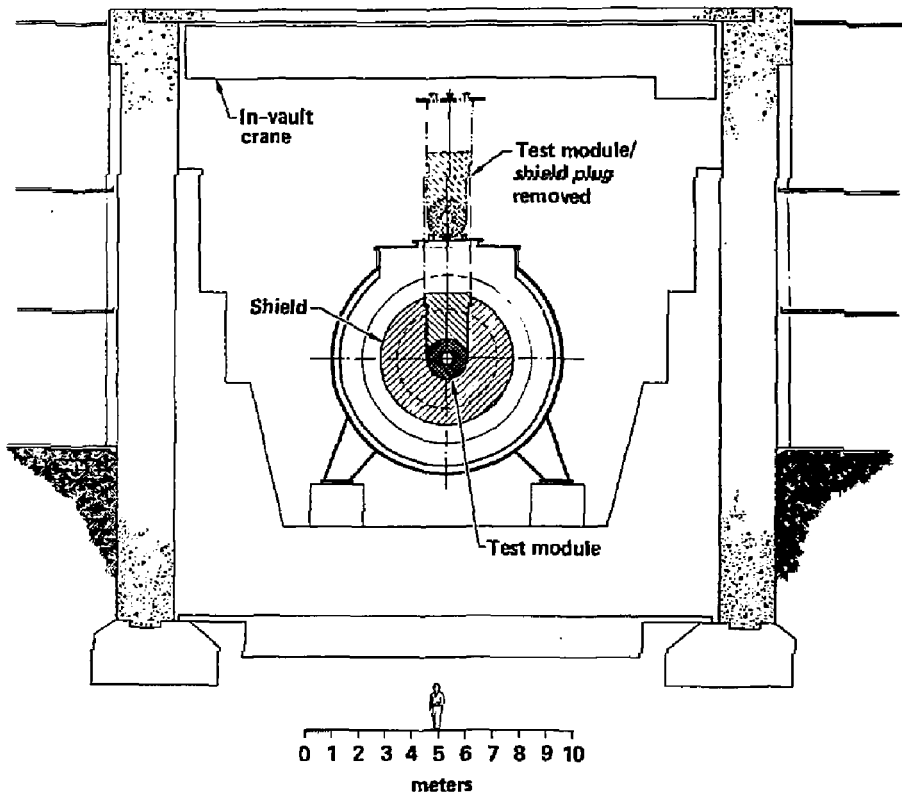

Fig. 2-9. Elevation through test module.

Table 7-7. MFTF-α+T magnet parameters.

Coil	Axial location (m)	Mean diameter[a] or major, minor radii[b] (m)	Sweep angle[b] (deg)	Winding current density (m^2)	MAT	Conductor (SC = Nb-Ti liquid He @ 4.2 K C = water cooled Cu)	Peak field approximate in winding (T)
CC1	±2.0	0.64	NA	2450	28.3	C	12
CS1	±2.65	5.0	NA	2000	25.5	SC	10
S1[c]	±4.375	5.0	NA	3090	1.7		3
S2[c]	±5.625	5.0	NA	3140	1.7		3
S3[c]	±6.875	5.0	NA	3140	1.7	SC	3
S4[c]	±8.125	5.0	NA	3140	1.7	SC	3
CC2	±10.0	1.253	NA	2798	18.9	C	20
T1	±11.811	1.5, 0.5	80	3473	5.6	SC	7
A1	±15.611	1.3, 0.5	90	3473	5.6	SC	7
A2	±15.611	1.3, 0.5	90	3473	5.6	SC	7
P1	±19.411	1.5, 0.5	80	3473	5.6	SC	7
P2	±19.411	1.5, 0.5	80	3473	5.6	SC	7
T2	±23.211	1.3, 0.5	71	3473	5.6	SC	7
DC	±24.711	0.928	NA	2380	9.2	SC	8

[a]Solenoidal coils only.

[b]"C" coils only.

[c]Existing MFTF-B coils, relocated as necessary.

verified in a preliminary fashion. We do not yet know whether the competing requirements for space by the magnets, magnet support structure, shield beams, and beam dumps can all be accommodated using the specific configuration depicted. However, based on previous TDF and MFTF-B+T design studies, we expect that these competing requirements can be successfully satisfied. We do know that shielding will be required in the bore of the end-cell magnets, and preliminary studies show that 15 cm is sufficient and will fit into the present configuration; more detailed calculations may, however, dictate a modest increase in size for some of these magnets.

The superconducting coils to be added are of the same general design as those already built and tested in MFTF and, therefore, will not present any new design or fabrication problems. As indicated, shielding will be required to protect the coils from excessive neutron heating.

The high-field choke coils (12-T and 18-T inserts) do present a new technology for mirror machines. These coils are wound with copper alloy conductors to minimize size while being capable of operating in a high neutron flux. We have proposed the use of internally water-cooled construction in a design based on the TDF study.[2] Here, the duty cycle is relatively low and the coils should last the life of the machine. Because radiation damage will not be an issue, the design will be controlled by heating and magnetically-induced stresses.

Heating. The MFTF-α+T heating system uses both rf and neutral-beam injection. Much of the microwave equipment currently planned for the MFTF-B can be used for the upgrade, either as-is or with modification. The neutral-beam systems are new. A summary of the MFTF-α+T heating system parameters is given in Tables 2-2 and 2-5.

For the axicell, 240 A (total) of 60-keV beams is supplied by two injectors, one using tritium and the other using deuterium, each with four positive ion sources. The source species mix is expected to be 80/15/5, and this source supplies a low-divergence ($\sim 0.5^{o} \times 0.5^{o}$) accelerator. These injectors are similar to those proposed for TDF central-cell injection (see Figs. 2-10 and -11). They are equipped with nuclear and magnetic shielding, the stray magnetic field being about 2 kG. All of these injectors are maintained through the back, where the injector penetrates into the hot cell. The injectors are oriented so that the four beams converge azimuthally at the plasma.

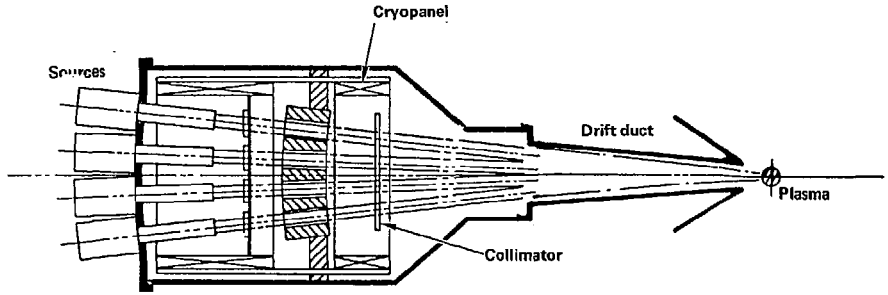

Fig. 2-10. Layout of sources and components in one of the two 80-kV beamlines in the central cell.

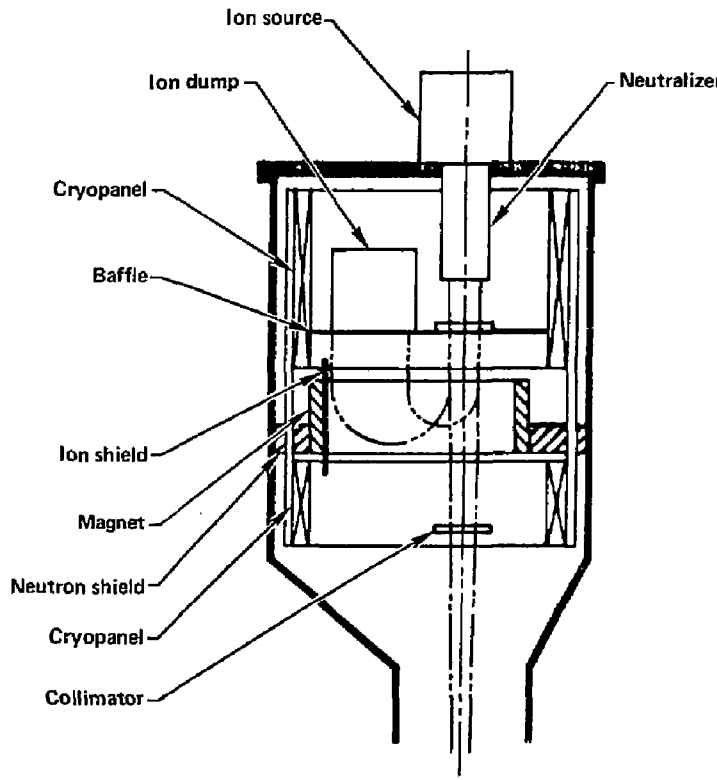

Fig. 2-11. Arrangement of beamline components for each source in the beamline.

The sloshing beam is a 200-keV negative-ion-based beam that supplies 4.2 A of D^0 in the form of 12 sheet beams, each measuring about 50 cm along the axial dimension of the reactor and $\pm 0.4^0$ to the orthogonal plane. Figure 2-12 shows the general placement in the vault, with the beamline penetrating the end cell shield structure. The beams are aimed at the center of the plasma target, 10 cm wide (see Fig. 2-13). This injector will model the sloshing beam injector required in future devices, such as MARS, in that it uses the latest techniques of transverse field focusing (TFF) for transport and acceleration, as shown in Figs. 2-14 and 2-15. Twelve LBL-type sources provide approximately 0.9 A each. Separate gas cells perform the neutralization function. The unneutralized ions are removed from the beam by electrostatic deflection. A relatively low operating efficiency of 30% is expected. This is the result of collumating the beam at the source to obtain low emittance and using a gas neutralizing cell, which provides a neutral fraction of only 60% or so. The nuclear and magnetic shielding requirements are less severe than those of the axicell. A passive magnetic shield will be used.

Electron-cyclotron-resonance-heating (ECRH) is used in the thermal barrier of the end plug. The frequencies required match two of the three presently planned for the MFTF-B (specifically, 35 and 56 GHz). Additional power is required, and assuming a transmission efficiency of at least 80%, eight 200-kW gyrotrons are required for each plug. At point "a," one 56-GHz gyrotron and its transmission system from MFTF-B can be used. At point "b," the three remaining 56-GHz gyrotron systems from MFTF-B are used. Four additional MFTF-B-like equipment strings of 56 GHz each will be required for the other plug. At point "b" there is a requirement for 600 kW of 35 GHz. The two strings of 35 GHz planned for the MFTF-B plus the two 28-GHz equipment strings modified for 35-GHz operation will satisfy the MFTF-α+T upgrade at one plug. Four new strings of the same design will be required for the other plug.

The anchor uses ion cyclotron resonance heating (ICRH) at the fundamental and second harmonic for deuterium. Presently, the MFTF-B plans to use 400 kW at 12 to 20 MHz to heat the central cell. This equipment can be modified to provide ICRH power for the upgrade. The modification will require new resonators and modified or new lauchers. For each anchor, 340 kW incident is required. This is satisfied by one modified MFTF-B ICRH system for one end

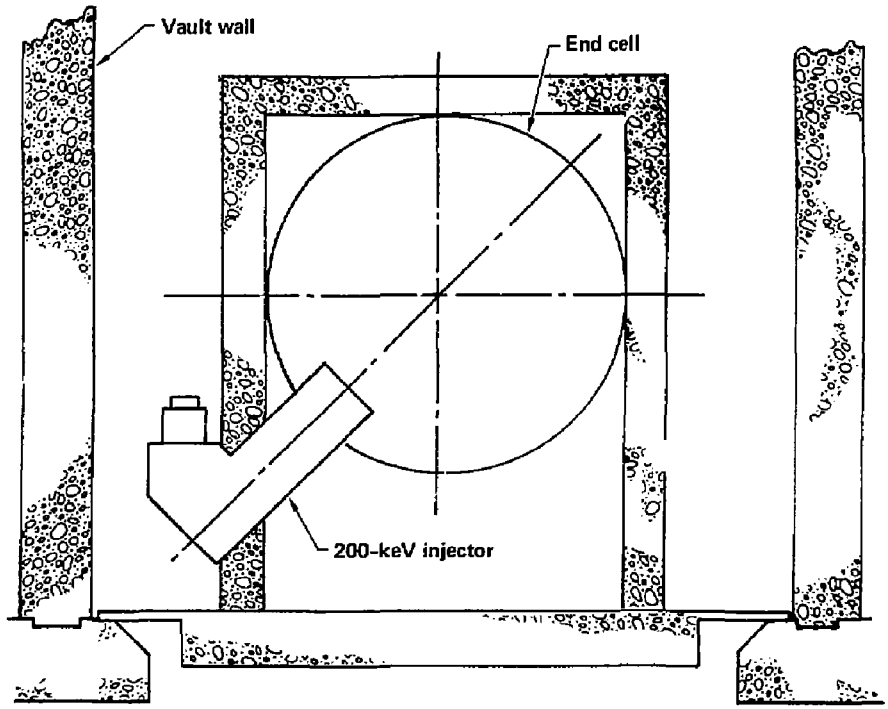

Fig. 2-12. Location of the 200-kV sources and transport section for each anchor sloshing beam. Shown here is the access to the source and penetration of the end region shield.

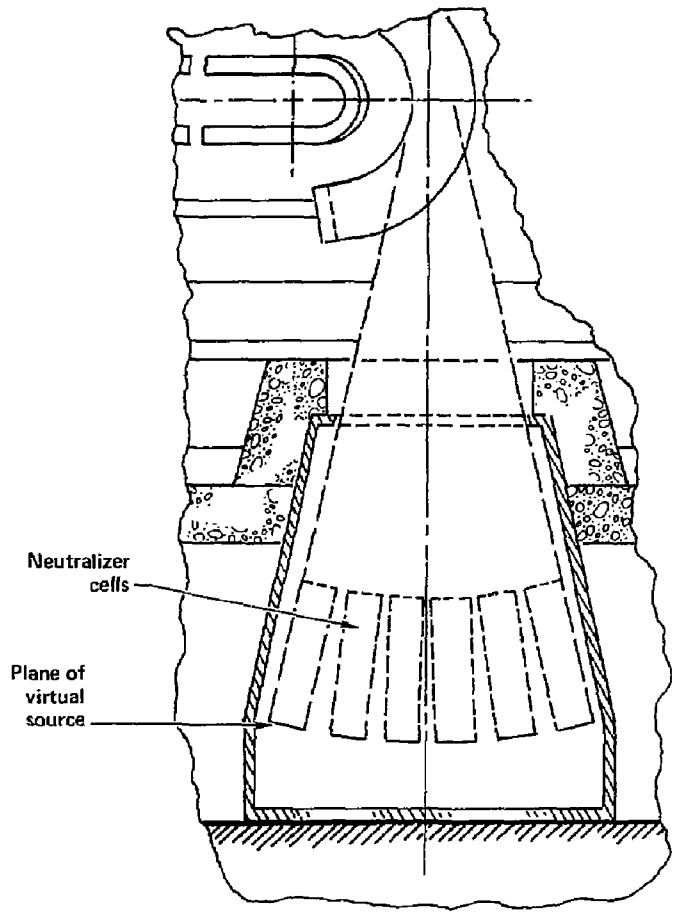

Fig. 2-13. Layout of 200-kV beamline tank showing the focus of each beam from the neutralizer to the plasma target.

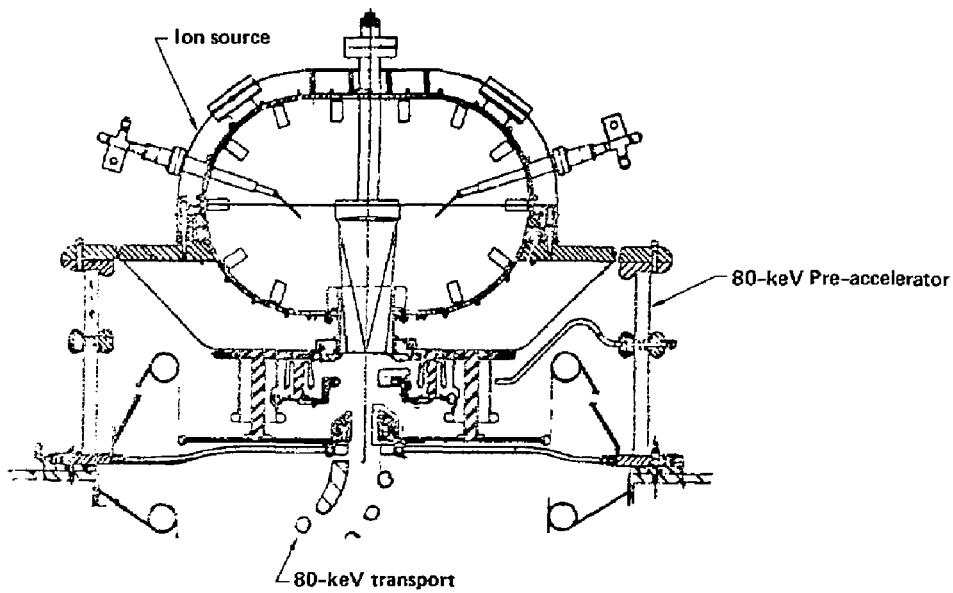

Fig. 2-14. LBL direct extraction source with Transverse Field Focusing (TFF) accelerator.

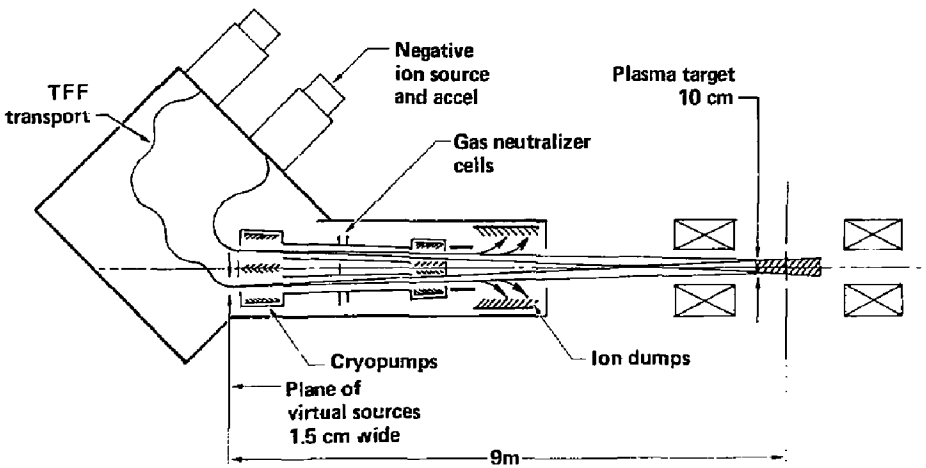

Fig. 2-15. Layout of the two rows of six sources, the TFF section, and the beamline to deliver 4.2 A at 200 kV to the plasma.

and an additional system for the other end. We expect that further savings can be effected by using modified power supplies left over from those required for the NB injectors on MFTF-B. For the 25-MHz ICRH system, two MFTF-B rf generators (or their equivalent) will be used on each anchor to provide 800 kW incident. This approach using developed tested components will be cost effective. These systems will be of the master oscillator-power amplifier (MOPA) type with coaxial transmission lines and tuned loop-type launchers. This technology is currently in use on fusion devices and hence is low risk.

For the drift pump systems, two wide-band frequency modulated sources are required. In the anchor cell, a conventional MOPA chain, operating at 1200 KHz and driving a set of four loop launchers is planned. The rf generator is a broad-band tuned amplifier (Qv7) with a tightly coupled untuned secondary transformer output driving the loop antennas. The master oscillator is a voltage-tuned oscillator controlled by a linear sweep with a periodicity of 0.1 sec. Because the frequency band is much lower for the anchor pump (i.e., 140 kHz), the approach proposed for the generator is different. The generator is a dc-to-ac chopper-type device with the four loops in the device driven from an untuned transformer. A series of low-pass and hi-pass filters is used to limit the spectrum to the 140 kHz $\pm$ 28 kHz. Ten individual choppers, operating 5.6 kHz apart, are required to produce the spectrum.

First Wall and Dumps. First wall surfaces are required to take surface heat loads in the DT axicell and the central cell. Two distinct regions exist in the DT axicell (Fig. 2-16). These are the region in front of the test zone and the region between the test zone and choke coil.

The first wall in front of the test zone is designed for 10% of the sum of the total device input power and one-fifth of the fusion power. This is distributed over a 4-m length at a radius of 25 cm, resulting in a surface flux of 44 W/cm^2. The design for the 1-m-long test zone is a water-cooled stainless-steel cylinder. Construction is double-walled with rib stiffeners. The skins, ribs, and overall wall depth are minimized in this region to provide maximum neutron transparency. Skins are 1-mm thick, so the neutron transparency is 0.90. The wall depth is 7 mm and the water coolant flows radially. The pumping power required is negligible (<100 W).

The region between the test zone and the choke coil makes up the remainder of the DT axicell. The surface heat load in this region is assumed

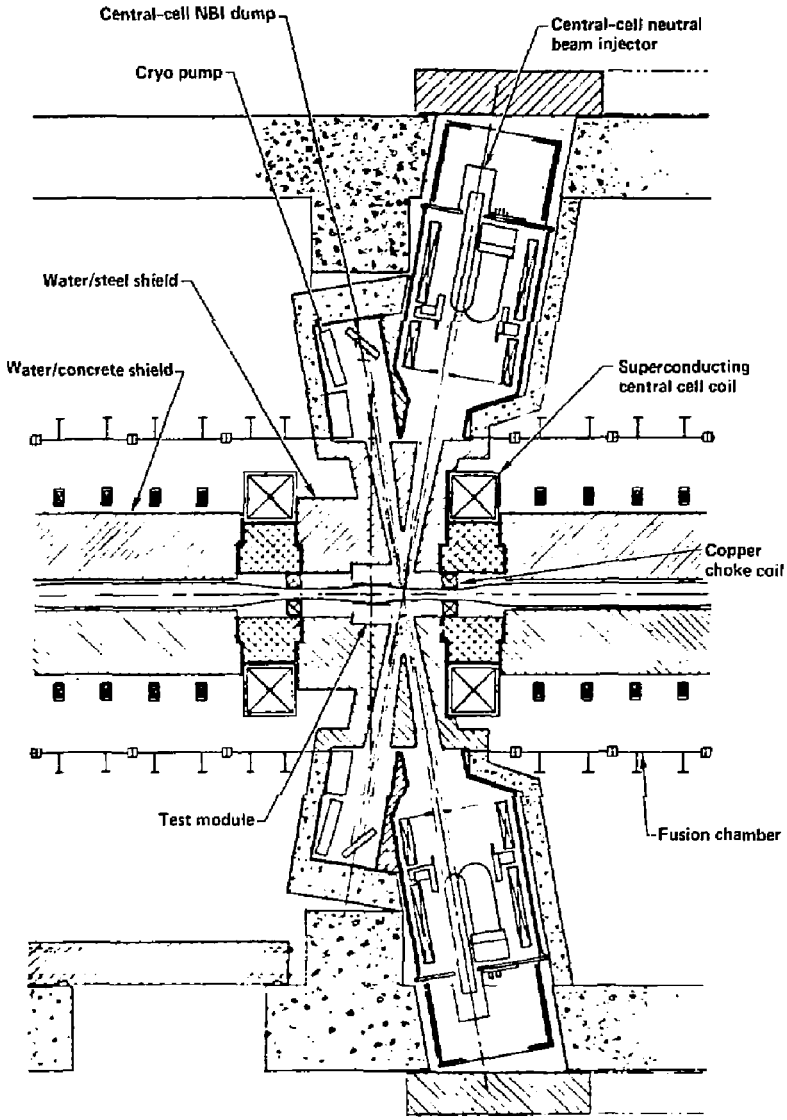

Fig. 2-16. Insert section in MFTF-α+T.

to include 10% of the central-cell beam power (distributed over a 1.2-m length), in addition to the average calculated for the test zone. This total surface heat load is calculated to be 120 W/cm^2. The design for this area consists of water-cooled copper panels. The shape will be complex because of the need for coverage around the choke coils and beam ducts. The total surface area to be protected is approximately 5 m^2.

Beam dumps are required opposite the central-cell beams (Fig. 2-8b) and opposite the plug sloshing beam. These dumps will consist of arrays of 20-x-20-cm water-cooled copper (AMZIRC) panels. Approximately 112 panels are required in the DT axicell and 30 panels are required in each end cell. The heat loads in the DT axicell dumps require that their surfaces be angled to the flow of current to minimize the heat load to 1 kW/cm^2.

The plasma end dumps comprise arrays of water-cooled copper panels. The area to be covered is approximately 15 m^2 at each end and the average heat load is approximately 300 W/cm^2. Some angling of the panels may be required to reduce peak surface heat loads to near the average values. Details of the end-dump design have not yet been addressed but the technology, from a heat transfer standpoint, is well within the state-of-the-art. A major complication is the requirement that these panels be biased to -75 kV to control plasma potential.

Vacuum System. The vacuum system is designed to maintain the required base and operating pressures in the vessel. In addition, the vacuum vessel serves a dual function of superconducting coil dewar and support structure. For α+T, the vacuum vessel will also support all internally located bulk shields. The vacuum vessel is separated into three distinct regions: DT axicell, central cells, and end cells.

The DT axicell vacuum vessel is 8.3 m in diameter and 7.2 m long. This portion of the vacuum vessel will be a completely new component, similar to the existing MFTF-B central cell vacuum vessel (a cylindrical shell of 304 L stainless steel with stiffeners and openings as required). It will support the axicell superconducting coils, the copper choke coils, and the required bulk shielding. Also, interfaces for two neutral-beam injectors and dumps are provided. Support legs will be provided for interface with the modified center structural platform.

The central cell vacuum vessel is the 8-m-long portion on each side of the DT axicell, between the axicell and the end cell. The central cell vacuum vessel is the same as is used on MFTF-B with the addition of required stiffeners for supporting the bulk shield loads. Each half of the central cell vacuum vessel consists of two modified existing central cell segments and a reworked third segment. The three modified segments will be translated outward, toward the end cells, to provide space for the new DT axicell. The support legs will be modified to support the new loads and interface with the modified center structural platform.

The existing end-cell vacuum vessels will be modified to accept the α+T device configuration. This modification will consist of removing the MFTF-B end-cell superconducting coil supports and adding structural support for the α+T superconducting end-cell coils. All unnecessary ports are closed off and new ports will be added as required. Also, supports are added for the bulk shield around and in between the superconducting coils. The MFTF-B fan-shaped end dumps are reworked to support the new circular end dumps. The cone end of the end-cell vacuum vessel is reworked to interface with the relocated central cell. The existing support legs are modified for the new loads. The end-cell vacuum vessel will not support the external bulk shield.

The cryopanel arrangement in MFTF-α+T is the same as the arrangement for MFTF-B+T. It includes 670 m^2 of cryopanel surface area in each end cell. Over half of this area (380 m^2) is in the form of eight 2.2-x-20.8-m axially oriented panels around the periphery of the cylindrical vessel. The remaining area is an accordion array at the end of the end cell. Of the total area, 560 m^2 is continuously pumping. The panel design is the regenerable design developed by Batzer[5] at LLNL. For a gas load per end of the device of 13 Torr-ℓ/s/cm^2, the pressure of the end cell can be maintained below 5 x 10^{-7} Torr.

The present cryopanel arrangement will need to be critically reviewed in view of the shielding needs now being identified for the end cell. Adequate conductance to the cryopanels is the major design consideration.

Neutron Shielding. Neutron shielding from the DT and DD sources will be required throughout the machine. The intensity of the neutron source vs axial position is plotted in Fig. 2-17. These neutrons can cause heating, damage, and activation in various components in the device. Activation of the vault

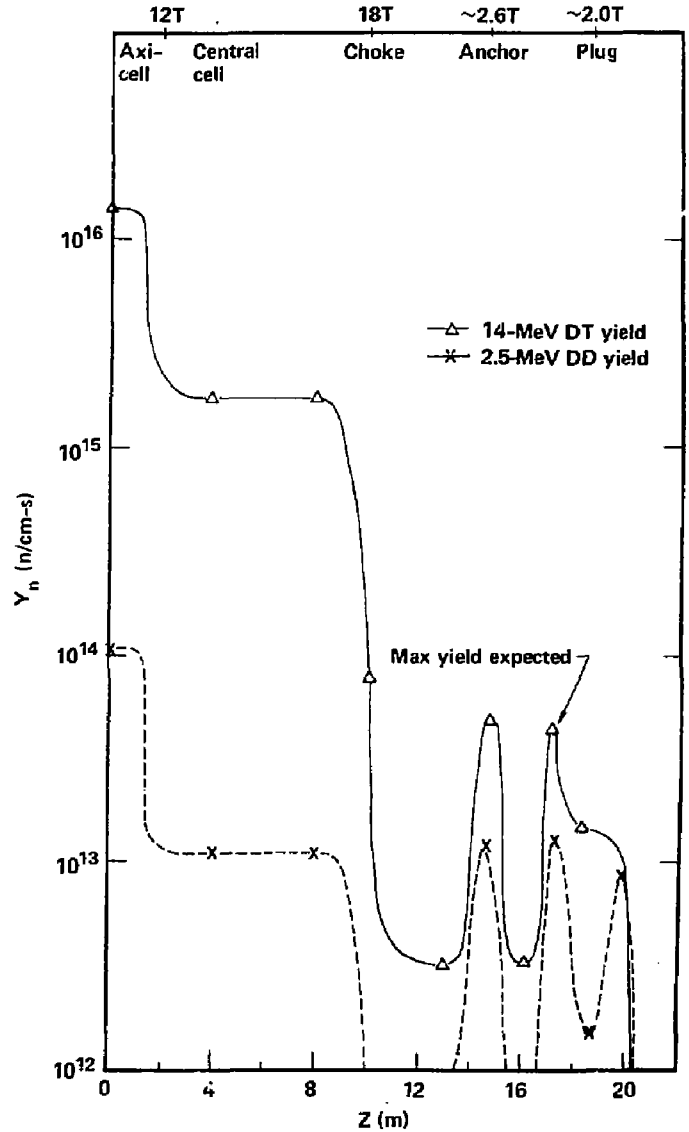

Fig. 2-17. Line density of neutrons generated in MFTF-α+T.

walls must also be considered. Shielding is required to limit some of these effects to acceptable levels. The criteria being used to estimate shield requirements are:

For superconducting coils:

- Maximum local heating — 1.0 to 2.0 mW/cm^3
- Maximum total heating — TBD
- Maximum neutron fluence — 4×10^{18} n/cm^2 (E>0.1 MeV)
- Maximum neutron fluence between anneals — 1×10^{18} n/cm^2 (E>0.1 MeV)
- Maximum gamma dose in insulation — 5×10^{10} rad.

For normal copper coils:

- Maximum, neutron fluence (between anneals/total) — 10^{22} n/cm^2 (E>0.1 MeV)
- Maximum dose in insulation — 10^{13} rad.

An initial appraisal indicates that in most cases the plug coil layout for α-T provides sufficient space (a minimum of 15 cm) for the shielding needed to protect the coils. The most likely exception is that the choke coils will require either a thicker or a more effective shield material than the steel/water proposed. Tungsten is a possible alternative to steel. A trade-study must be done to determine the lowest-cost shield/coil combination. Because of the low duty cycle, local superconducting heating is the limiting criteria in the coils.

Shutdown dose rates in the vault caused by neutrons generated in the end cells are to be kept to an acceptable level by a combination of shields and the coils themselves. The design dose rate 24 hr after shutdown is 0.5 mrem/hr.

The end-cell bulk shield is divided into two major areas: Area 1, inside the vacuum vessel and Area 2, outside the vacuum vessel. Area 1 consists of water-cooled stainless steel, and Area 2 is reinforced concrete.

The shield in Area 1 is further separated into two regions. Region 1 consists of 15-cm-thick water-cooled stainless steel shielding to protect the superconducting anchor coils--the space between the plasma and the coil cases. (The cases themselves are ~10 cm of steel and provide additional coil shielding.) Region 2 is a 50-cm-thick water-cooled stainless steel shield for the spaces not occupied by the superconducting coils. Credit is taken for the shielding effectiveness of the superconducting coils in Region 1 to obtain a similar radiation level as in Region 2. The shielding in both

regions is supported by the end-cell vacuum vessel. Vacuum pumping ducts will likely be required in Region 2.

The Area 2 shield consists of 50-cm-thick reinforced ordinary concrete. The concrete shield will be located far enough away from the vacuum vessel to minimize penetration in the concrete. Equipment protruding beyond the Area 2 shield, such as fueler, neutral beams, dumps, etc., will be individually shielded.

Shielding requirements for the axicell/central cell indicate that there is enough room between the plasma and the superconducting coils for the shielding needed to protect the coils and limit the shutdown dose rate to 0.5 mrem/hr. The DT axicell shield is split into three regions, each with a different shielding composition. Region 1 is the area outside the test module or blanket module. Region 2 is the adjacent area on each side of Region 1 (between the test module and the choke coil). Region 3 is the area under the background superconducting coil and around the choke coil. All the shielding is supported by the vacuum vessel.

The Region 1 shield is 165 cm thick by 120 cm long and consists of discrete layers of H_2O, B_4C, Pb, and ordinary concrete. It is located behind a 50-cm-thick test module, and is designed to allow for test module removal. Region 2 shielding is similar to Region 1 shielding in composition, except that it is located behind a 30-cm-thick test volume. The shield is 195 cm thick (including 30-cm test volume) by 1.33 m long. The Region 3 shield consists basically of water with discrete layers of B_4C and Pb and is 124 cm thick by 1.5 m long.

The central cell shield consists of discrete layers of water-cooled steel, ordinary concrete, B_4C, and Pb. It is built in eight segments and is 165 cm thick and 11.3 m long.

Power Supplies/Conversion. Magnet power supplies from MFTF-B will be used for most of the coils. There are two additional end-cell coils that do not exist in MFTF-B and power supplies are required for these magnets. Power supplies for the axicell and choke coils are also needed.

The two large solenoids have a stored energy of about 1000 MJ each and the coil current is 10 kA. The coil voltage does not exceed 1 kV during a rapid coil discharge. The coils are assumed to be connected in series and driven from a common power source. Coil protection circuitry is similar to that used in MFTF-B.

The electrical power needed for each resistive choke coil is about 10 MW and is designed for a coil current of 100 kA. To decrease the cost of the bussing, large copper pipes will be used to connect the power supply modules with series-connected choke coils. These pipes provide the cooling water to the coils. A large, grounded water-return pipe is electrically isolated and can be made of any noncorrosive material.

The sustaining NB power supplies require continuous power, and existing MFTF-B power supplies can be refurbished for steady-state operation. Two of these MFTF-B power supplies will be connected in series to power the negative-ion NB injector. One of these power supplies must be refurbished with stand-off insulators to operate 200 kV above ground potential.

A common HV power supply will be used for all low-frequency rf generators with separate power conditioning for each generator. The cost estimate is based on providing a new power supply and power conditioners. Similarly, a common HV power supply and separate power conditioning unit will be used for all ICRF generators.

An existing NB power supply will be upgraded to provide all additional ECRH HV power for α+T with separate power conditioners provided as required by design. A new ECRH load station and gyrotron magnet power supplies will be provided for the added ECRH.

Each plasma end cell dump collects electron current and is a direct converter. In the initial stages of α+T, the design concept will provide plasma potential control, but will not be aimed at providing efficient direct conversion. Development and optimization of direct conversion and the interfaces between the halo region and the plasma edge will be considered as a special future development program.

The simple concept for the electron collector plates will be copper disks maintained at the required negative potential. They are water-cooled to remove the thermal energy. The circular, disk-shaped collector plates will be supported by ceramic insulators. The deionized water coolant lines will run through insulator tubes or pipes before the coolant water exits through the vacuum chamber.

To provide for the plasma-gun-beam opening in the center of the collector, a disk will be cut in the collector and rotated so the eye is open during startup and closed during machine operation. This disk, as well as its rotational operating mechanism, will be at the collector potential of 75 kV.

Behind the disk and electron collector plate will be the vacuum tank and neutron shield.

The collectors will have an electrical control system to maintain them at the desired potential (electrical converters could provide ac power). This will be a simple system but one from which we can evaluate the potential power conversion efficiency. There is no planned feedback of the electrical energy into the electrical grid, but it can be accomplished for demonstration purposes.

A negative dip in the plasma potential in front of the plates prevents cold ions, emitted from the electron collector plates, from going back into the hot plasma. Thus, there will be no need for grids in front of the collector plates.

The region between the halo, which is essentially at ground potential, and the plasma at the edge of the electron-collector plate have high potential gradients. This could result in the need for a multiregion electron collector plate (disk and washer construction and antiarc suppressors). This feature, if required, will be provided when the edge effects are better defined.

The currents and power distribution at the end of the machine is as follows:

Ion current to collectors	10.6 A
Electron current to collectors	45.2 A
Electrical power recovery	2.67 MW
Heating power to collectors	2.76 MW
Electrical efficiency	42.0 %
Potential of collector (nominal)	75.0 kV.

2.1.3.3 Tritium Systems. The main function of the tritium system is to process the tritium and deuterium fueled to the plasma, to process the water coolant, and to process the atmosphere in the tritium areas. The units, especially the atmospheric processing units, are designed to function during normal, maintenance, and accident modes of operation.

There is a complete tritium fuel cycle (see Fig. 2-18) capable of processing 600 to 2000 g/d of DT plus impurities. Specifications for many units are found in the Final Safety Analysis Report of the Tritium Systems Test Assembly (SAR-82-1F, Los Alamos National Laboratory, 1982). A complete fuel cycle requires not only the components needed to process and store the

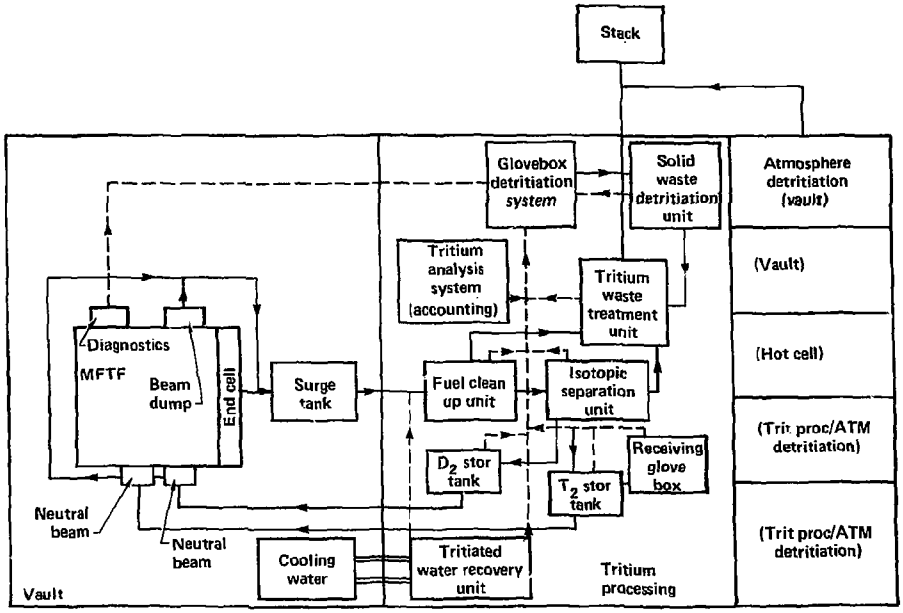

Fig. 2-18. Tritium mass flow paths for MFTF-Upgrades.

fuel (fuel cleanup unit, isotope separation unit, storage beds, receiving glovebox), but also the units required for secondary containment (glovebox detritiation system); waste processing (tritium waste treatment--gasses and tritiated waste processing, solids); tritium analysis (required to detect problems and their solutions in the fuel cycle, and also to maintain accountability records); tritium monitoring (safety consideration); and process control with associated data acquisition (data acquisition system). The basis for each of these units is shown in Table 2-8.

These units will be located in a separate, relatively leak-tight, earthquake-proof space. Earthquake valves will be located on lines between units to minimize any potential releases. An atmospheric processing system will be provided for the area to handle tritium releases. The atmospheric processing units for the vault and the hot cell will also be located in this space. The size of the atmospheric processing units is the most important factor influencing the size of building required. At present the building is estimated to have a volume of approximately 1×10^4 m^3. The specifications for these atmospheric processing units are shown in Table 2-8.

Atmospheric processing systems are needed for each area where tritium is present. The size of these systems is a function of the volume to be processed and the processing rate as determined by the nature of the area (external leak-rate expected under accident conditions, nature of the surfaces, wall, etc., need for quick re-entry, and expected tritium release). The sizes of the potential tritium releases for accident conditions are shown in Table 2-9, where the expected tritium inventories associated with different operating modes are summarized.

In the vault, 10 to 26 g of tritium are present at steady state during each 10-hr run. A sealed vault with an external leak rate of 1 vol%/hr following an accident would require cleanup in ~24 hr to approximately limit the environmental impact.

In the tritium processing area, 200 to 400 g of tritium are present. Due to the large size of a potential release, cleanup in ~24 hr is required with a dedicated system. If the atmospheric processing unit dedicated to the tritium processing area were not functional, or if faster processing rates were required, then the atmospheric processing units dedicated to the vault could be used to address these conditions. Care would have to be used in linking the different units to minimize cross-contamination. The hot cell

Table 2-8. Tritium systems required for MFTF-α+T.

Item	Description	Quantity
1.	Receiving glovebox for tritium; basis is TSTA and TFTR units; upgraded for ~120 g/mo T_2.	1
2.	Uranium beds for storage of tritium and deuterium, ~100 g/bed; basis is TSTA and mount units.	8
3.	Fuel cleanup unit with helium removal; basis is TSTA unit; 600 to 2000 g/d DT.	1
4.	Isotope separation unit with storage beds for accident control; basis is TSTA unit; 600 to 200 g/d DT.	1
5.	Glovebox detritiation system; basis is TFTR/TSDCS; flow capacity 0.3 m^3/min; ~10^{-2} g/d.	1
6.	Tritiated water recovery unit; basis is CECE at mound; flow capacity 100 ℓ/d; no dedicated isotope separation column is provided.	1
7.	Tritium waste treatment unit; basis is TSTA unit; flow capacity 1.5 m^3/min; handles ~10 g T_2/d.	1
8.	Tritiated waste processing unit; basis is solid waste units at TSTA; capacity ~1 kg/d; individual units for atmospheric processing area.	13
9.	Tritium analysis system (accountability); basis is Mound, TFTR, TSTA.	1
10.	Sets of monitors for gaseous tritium (3 areas); basis is TSTA system.	3
11.	Data acquisition system (no software cost); basis is TSTA and mound systems.	1
12.	Atmospheric detritiation system dedicated to tritium processng area; basis is cost of 30-m^3/min systems; each unit 140 m^3/min; flow rate ~1 vol%/min.	1

Table 2-8. (Continued.)

Item	Description	Quantity
13.	Atmospheric detritiation system dedicated to vault; basis is cost of 30-m^3/min systems; each unit 140 m^3/min; flow rate ~1 vol%/min.	2
14.	Atmospheric detritiation system dedicated to the hot cell; basis is cost of 30-m^3/min systems; each unit 140 m^3/min; flow rate ~1 vol%/min.	1

Table 2-9. Summary of tritium inventories[a] for different MFTF-α+T Upgrades, with and without processing during a run.

		Inventory (g)
A.	No processing for 10 hr	
	T_2	208 → 312
	D_2	170 → 260
	Total	380 → 570
B.	Processing during 10-hr run[b]--tritium location at steady state	
	Neutral beams	4 → 10
	End cells	5
	Beam dumps	1
	Surge tank	3 → 5
	Tritium in vault	13 → 21
	Fuel cleanup	50
	Isotope separation	120 → 250
	Storage (1 hr)	21 → 31
	Tritium in processing	191 → 331
	Total	204 → 352

[a] Efficiency of neutral beams: (+) 20-30%; (-) 7-11%.

[b] Regenerable cryopanels used; one-sixth of them processed every 10 min.

also requires a dedicated atmosphere processing unit since it will be used to dismantle test modules and other tritium-contaminated components of the reactor. The size of the unit is dictated by the expected size of the hot cell ($\sim$1 x 10^4 m^3) and the processing rate (1 vol%/min).

The Tritium Systems Test Assembly is wrestling with the question of accountability, which is set at ± 100 Ci. For a tritium inventory of 400 g expected in the MFTF-Upgrades, this requires an accuracy of 25 ppm. This is considered unachievable due to various losses, e.g., permeation into the structure and into the water coolant. In addition, personnel at TSTA have not yet found equipment or methods adequate to deal with this question. It is one of the areas to be investigated in their program.

2.1.3.4 Maintenance. To date, we have considered three aspects of maintenance: the maintenance philosophy, an understanding of the design limitations imposed by this upgrade, and an analysis of component lifetimes.

As with other device concepts, we adopted a maintenance philosophy early to guide the development of the configuration into a viable design. Maintenance requirements have an important influence on the development of a design. For example, the existing vault facility limits component access and handling. The largest-capacity crane system that can be accommodated by the existing vault (with some modifications) is 46 t. Consequently, subsystem components and shield modules are sized to that weight limit. Lifetime estimates for key components were made from data generated from MFTF-B. These extrapolations indicate that scheduled component replacements are infrequent and can be readily accommodated during the device downtime. As an example, sustaining beamline sources have a scheduled replacement approximately every seven calendar months.

The maintenance philosophy for α+T is based on the earlier work done for the Technology Demonstration Facility. It is a fourfold approach which considers operating flexibility for this near-term device along with the opportunity to accomplish numerous maintenance tasks between pulses. The major aspects are listed below:

1. Contact maintenance operations are permitted 24 hr after device shutdown at the shield boundary. This enables personnel to routinely perform hands-on inspection, maintenance equipment setup, and supervision of maintenance activities in the vault before the

device is disassembled. These capabilities are particularly desirable when one considers the amount of time available between pulses.

2. Capability to accomplish scheduled major maintenance and disassembly remotely under normal or emergency conditions is a design requirement. Activation levels within the shield boundary are too high to permit hands-on operations when the device is disassembled; hence, remotely operated equipment is required.
3. Modularized component installations are also a design requirement. Modular components are arranged for independent disassembly and are sized to the lifting limits of crane systems.
4. Utilization of proven remote equipment technology is mandatory for this near-term device. It is not reasonable to assume that major breakthroughs may develop in the next four to five year; hence, maintenance operations are based on presently available handling equipment.

Several considerations related to maintenance operations will be factored into the disassembly scenarios. They are:

- Neither personnel nor maintenance equipment are permitted in the vault during device operation. Personnel are not allowed because personal safety would be compromised in the neutron environment; equipment is not allowed in order to avoid neutron-induced activation that could hinder subsequent maintenance operations.
- Power supplies to the device are shut down, the coils are de-energized, and the tritium is removed during maintenance operations near the device. Clearly, this is a safety requirement for personnel, device systems, and maintenance equipment.
- Superconducting coils may be kept at cryogenic temperatures during maintenance operations that do not affect these magnets.

All of the components that may have scheduled replacements weigh less than 46 t. Following are the major components that fall into this category:

- Choke coils (including shield plug),
- Cryopanel assemblies (six panels plus structure),
- Beamline components,
- Beamdumps (including shield plug),
- Test module (with separate split shield).

The test module and its shield are an example of a component designed around the lift limits within the vault. The total test module/shield weighs 80 t; splitting the shield into two 40-t segments met the lifting requirements and also simplified the module replacement by allowing the lower shield to act as a stationary cradle support for the test module.

Scheduled component replacements will not impact the operation of α+T. This is primarily because there is ample time between pulses to accomplish maintenance and replacements, and because the estimated component lifetimes indicate that replacements will be relatively infrequent. This may also lead to a relatively small inventory of spares.

We used component lifetime-availability data for the MFTF-B machine to make extrapolations for the operation of α+T. By comparing operating hours between these two devices, we can show, at least to first order, that many of the life-limited MFTF-B components may be lifetime components on α+T.

Eighteen replacements of the sustaining sources will be required. This corresponds to a changeout every seven calendar months. Given the operating scenario for α+T, this will not present any availability problems; there are 720 hr in a month, with 10 hr for device operation, leaving 710 hr for maintenance operations and other downtime activities.

The scenario described above is analogous in some ways to the operation of the NASA Space Shuttle. That device operates for one to two weeks, and is refurbished for up to six months.

2.1.3.5 Facilities. The necessity for upgrading the MFTF-B facilities arises from the need to provide: (1) tritium confinement capability; (2) a barrier to the leakage of neutron and gamma radiation through reactor vault roof; (3) on-site tritium and deuterium processing facilities; (4) remote transfer capability of activated reactor components; (5) increased reactor heat removal capability; (6) increased ac power capability; and (7) other miscellaneous capabilities, such as stack ventilation, guaranteed cooling water supply for safety-related equipment, radiation monitoring, and a health-physics program.

The vault must be upgraded to provide for tritium confinement and to add a barrier to prevent neutrons and gamma radiation from leaking through the roof. These are necessary to ensure public and personal protection from release of unacceptable levels of radiation from the plant. The following upgrading of the reactor vault is needed:

Because the vault is the final tritium containment boundary, it is required to withstand a design basis seismic acceleration of 0.5 g. Preliminary analyses indicate that the existing vault is capable of meeting this requirement.

It must also withstand an internal pressure of 136 kPa (≈5 psig) that could result from an accidental release of liquid helium in the vault. Preliminary analyses indicate that the vault is capable of meeting these requirements. However, minor modifications may be needed, which may be determined by detailed analyses.

The vault should be leak-tight (leakage not exceeding 1 vol%/hr at 136 kPa internal pressure) to limit tritium leakage to the environment within acceptable limits. To make the vault leak-tight, all penetrations through the walls and all the cracks between the concrete blocks of the vault wall need to be adequately plugged. To reduce soaking of tritium and to allow decontamination of the internal surfaces, all inside surfaces (walls, floor, and ceiling) are required to be grouted and coated with epoxy paint.

Additional shielding is required to provide a barrier to prevent neutron and gamma radiation from leaking through the roof. This additional shielding may be provided as increased roof thickness or as increased shielding for the reactor.

Two new transfer cells are needed to remotely hanule the activated components of the reactor and its support equipment. The remote maintenance will be performed in existing hot cells. The major components requiring remote maintenance are beamline sources, test modules, beam dumps, and end dumps. The total volume of the transfer cells is estimated to be 3800 m^3. One cell is located on the south side and one is on the north side of the reactor vault.

A new facility is needed to process tritium in the plasma exhaust, and in general to handle deuterium and tritium in the plant. The volume of this facility is estimated to be 10,000 m^3. The existing steel structure to the east side of the vault would be upgraded (to meet DOE safety criteria) to house the tritium system.

The heat removal requirement for α+T is approximately 125 MW continuous during steady-state operation. However, the heat removal capacity of MFTF-B is approximately 10 MW continuous. Thus, to support steady-state operation of α+T, an additional 115-MW heat removal capacity is needed. The heat

transport system is upgraded by providing a parallel heat-removal loop of 115-MW capacity. For ultimate heat rejection, a large nearby heat sink is available (a large water-supply canal); thus, no cooling tower is provided.

The MFTF-α+T needs additional continuous ac power for 10-hr pulse operation. The ac power system will be upgraded to supply this power continuously. The major upgrading needs are:

1. Pulsed-power system upgrade--
   - Provide two new forced-oil, forced-air-cooled cooling systems for existing transformers 230 kV/13.8 kV--60/80/100 MW;
   - Provide ~2000 m of new feeder cables between 13.8-kV substation and the neutral beam power supplies.
2. Facility power upgrade--
   - Replace the T-4000 two-winding transformer (115 kV/4.16 kV, 20 MVA, 115 kV/13.8 kV - MVA);
   - Provide a new 13.8-kV, 2000-A outdoor circuit breaker with associated ducts to the transformer.
   - Provide approximately 2000-m new 15-kV power feeders between the outdoor substation and the rectifier transformers and rf power load centers.
   - Provide approximately 300-m new 5-kV power cable in the tritium building.
3. Tritium facility power--
   - Provide a new 4.16-kV/480-V, 5-MVA double-ended load enter.
   - Provide four new 480-V, 1200-kW diesel generators.
   - Provide approximately 600-m new 480-V feeders from load center to tritium facility loads.
   - Provide new distribution power components suitable for a tritium environment.

The following miscellaneous facilities are also needed to support the safe operation of the MFTF-α+T:

- Radwaste collection system.
- Guaranteed cooling-water supply system.
- Ventilation stack.
- Radiation monitoring and health physics equipment.

2.1.3.6 Testing Program. A program of testing in MFTF-α+T, and the part it will play both in the mirror program and the broader fusion program, can only be developed by an extensive examination of needs and of the capabilities of other facilities. Nevertheless, we have conducted an initial assessment of testing to identify the outstanding questions and to outline the types of tests that can be conducted with the present operating scenario.

The testing assessment has focused only on identifying those tests that can be performed with the present design of MFTF-α+T. The burn time is assumed to be 3.4×10^4 sec (10 hr), the availability is assumed to be 1%, the total burn time in the DT mode is assumed to be $2\text{-}3 \times 10^6$ sec, and the neutron wall loading in the central cell is assumed to be 2 MW/m^2 at 25-cm radius. The impact of increasing these parameters and prioritizing tests will be addressed at a later date.

Previous studies of devices with high fluences and availabilities have emphasized the nuclear testing aspects. MFTF-α+T, on the other hand, is expected to be a vehicle for the demonstration of subsystem technology and for the examination of the behavior of high-Q plasmas, as well as for nuclear testing. It is important that the test classifications reflect the differences in test objectives. The tests can be categorized in a number of ways. For example, the tests can be characterized by the duration of the tests, by when they are performed during the operating lifetime, by component, by discipline, or by plasma fuel type (H only, DD, DT). For the purpose of this evaluation, the major classifications of tests are preoperational checkout tests, demonstration and design verification tests, planned tests and experiments, and nuclear systems tests.

The preoperational tests consist of subsystem checkouts and calibration with all hardware in place. The types of tests that are considered to be in this category are the verifications of the performance of the magnet system, the vacuum systems, and the maintenance system. If deficiencies in performance are found at this stage, modifications can be implemented without having to contend with neutron-activated materials that would result from DD or DT plasma operation. Also, the information obtained from these tests would provide a significant addition to the engineering data base, since these major systems represent the state-of-the-art in fusion technology.

Demonstration and design verification tests center on the performance of the reactor subsystems during plasma operation. Included in the demonstration tests are performance evaluations of:

1. The central-cell neutral beams.
2. The end-cell ECRH, ICRH, and neutral beams.
3. The tritium recovery system.
4. The instrumentation and control equipment.

In addition, the response of several reactor systems to the plasma would be evaluated. Items in this category are:

1. Neutron flux profile measurements in both the central cell and end cells.
2. Thermal and particle flux profiles on the first wall, beam dumps, and end-cell walls.
3. Radiation field measurements outside of the reactor to verify shield performance.

Finally, when repairs are needed from time to time, the maintenance operations will be tested under actual field conditions. All these tests, being the first of their kind, would provide significant advances in the understanding of mirror devices.

2.1.3.7 Siting and Safety. Siting of the MFTF-α+T on project at the Lawrence Livermore National Laboratory appears to be feasible from a safety point of view. While the LLNL site, in common with much of the western part of the U.S.A., is subject to earth motions induced by earthquakes, extensive earthquake-fault mapping and analysis indicates that the maximum credible accelerations can be accommodated by careful design of the facility. Severe tropical storms and hurricanes are unknown in the area, as are tornados. The site is 400 ft above mean sea level, has good local water drainage, has no water reservoirs up-slope, and is more than 50 miles from the ocean.

Special hazards connected with the use of tritium in the facility have been surveyed, and there is a high degree of confidence that proper design will allow adequate containment. Neutron and gamma radiation present during and after typical operating scenarios for the MFTF-α+T are projected to fall within acceptable limits. Calculations of neutron-induced activation are proceeding, but the results obtained to date indicate that the facility can be designed and constructed to operate within existing guidelines and can be decommissioned after its useful life.

While DOE has placed requirements on construction of plutonium buildings (DOE 6430, Part 2), it has no comparable document setting forth requirements for tritium. However, the intent is that new tritium facilities also need to consider a "design basis accident" when designing the facilities. Environmental Safety and Health (ES&H) is preparing to write such a document. As far as legal requirements are concerned, the site boundary is our fence line, and the requirements are that a person presumed to be residing there continuously not receive more than 0.5 rem/yr. Normal operations should be designed to limit this dose to 170 mrem/yr. To put this into context, the present LLNL tritium facility has a design capability such that release of a mega-Curie of HTO (104 g of tritium) will give rise to 3 rem/yr at the fence line in a worst case situation.

The Tritium Systems Test Assembly is wrestling with the question of accountability, which is set at ± 100 Ci. For a tritium inventory of 400 g expected in the MFTF-Upgrades, this requires an accuracy of 25 ppm. This is considered unachievable due to various losses, e.g., permeation into the structure and into the water coolant. In addition, personnel at TSTA have not yet found equipment or methods adequate to deal with this question. It is one of the areas to be investigated in their program.

Material activation under the operating scenario seems to be acceptable. Nitrogen, where it occurs, is in a relatively low neutron flux region and should not activate appreciably. The copper insert coil will activate and will present problems both in handling and in waste disposal. Calculations are continuing on the levels of activation relevant to hands on maintenance. Early results indicate that components which see neutron fluxes equivalent to "first wall" will have to be handled remotely right from the beginning of the experimental program. Other areas may have low enough fluxes that some contact maintenance will be possible, at least initially.

In keeping with the contact maintenance requirements, the 24-hr shutdown dose rate on the inside surface of the vault wall should not exceed 0.5 mrem/hr. Vault wall activation for a few days after shutdown will be dominated by 15-hr ^{24}Na, which emits hard gammas of 2.75- and 1.37-MeV energies. Calculations for TDF showed that if the machine itself is properly shielded, the activation dose rate on the inside vault wall could be as high as 20 mrem/hr 24 hr after shutdown, depending on the sodium content of the concrete. If sodium activity poses a problem, there are at least three potential solutions:

1. Add shielding around the machine to decrease the neutron flux in the vault shield blocks.
2. Line the inside surface of the vault with a layer of lead or steel.
3. Delay access to 48 or 72 hr.

Because of the operating neutron flux in the vault (1×10^6 to 1×10^8 n/cm^2-s), argon activation will be significant; however, its half-life is only 1.8 hr. Thus, the principal concern for gaseous radionuclides in the vault will be the accidental release of tritium. With the A-41 present, the ionization chambers used to detect atmospheric tritium will not function and alternate methods must be devised.

The vault and its roof are presently being modified for use of DD in the MFTF-B. The following points about the facility should be noted:

- The vault is designed to operate at a positive pressure now; we will need to go to negative pressure because of the tritium.
- The "smoke clear" ventilation mode presently used in the event of a fire is two times the air flow. This clears out smoke and allows fire fighters to exit. For tritium operation, this system will need to be replaced by a remote fire suppression system, such as halon.
- After DT operation begins, the MFTF-α+T vessel will be contaminated with tritium, so any in-vessel maintenance will need supplied-air for the workers.
- Designs for new facilities will probably be required to comply with DOE guidelines for radiation workers of 0.5 mrem/hr. In addition, LLNL has dropped this another factor of 2 to 0.25 mrem/hr (i.e., a radiation worker should be treated the same as the general population). The special reportable level (to DOE) is still 5 rem/yr and 3 rem/qtr. Short-term exposures for special cases fall under these criteria.
- At 3000 sec, MFTF-B operation per 80-hr week, the time-averaged dose rate on the roof is 50 to 100 mrem/hr (peak rate during a shot, typically 30 sec, is 4 to 8 rem/hr for an integrated dose of 50 to 100 mrem).
- Sky shine back down to a ground level location 10 m outside of the wall is <1 mrem/hr.
- Local shielding may be required for sensitive access areas.
- The entire building is presently scheduled to be an exclusion area during the shots.

Operation with DT will markedly increase the flux of 14-MeV neutrons, and hence the shielding requirements, perhaps by a factor of 1000. The roof of the building will not support the additional shielding this would require. This means that more shielding will have to be incorporated into the machine structure itself, perhaps in the nature of additional shielding over and around the "hotter" central section of the α+T.

Calculations of radionuclide inventory are underway. The important time regimes for central cell activities are:

1. Immediately after shutdown, when afterheat levels will be greatest.
2. At 24 hr after shutdown, when some of the activities will be a consideration for the shutdown rate inside the vault.
3. Months after shutdown, when major replacements might be undertaken.
4. Years after shutdown, during decommissioning.
5. Decades after shutdown, for waste storage considerations.

The relatively high wall loading for MFTF-α+T (2 MW/m^2) is ameliorated by the rather low load factor (1.4%). Hence, for activation products with half-lives of several months or more, this scenario is equivalent to steady-state operation at 0.028-MW/m^2 wall loading.

Afterheat in the first wall steel right after shutdown will be about half that of Starfire, or about 0.4 W/cm^3, but will decay much more rapidly than in Starfire.

Choke coil activity will be dominated by the 5.3-yr Co-60, produced by the (n,a) reactor in Cu-63, and will determine the shielding and handling techniques needed to replace this coil.

Longer-term activation is thought to be more of a problem for decommissioning rather than waste storage. The total operating time of the central cell (about 0.14 MW-yr/m^2) is not likely to produce large inventories of very long-lived nuclides; furthermore, we are not addressing a whole series of machines, but one isolated test reactor. Decommissioning, if it occurs 5 to 10 yr after shutdown, is likely to be heavily influenced by Co-60 activity, just as in light water reactors. This Co-60 originates from Cu-63, Co-59, and Ni-60 and, being a hard gamma emitter, it will probably dictate the shielding needed during decommissioning.

Liquid nitrogen is used in the superinsulation for several magnets, such as the transition and yin-yang coils. We calculated the C-14 production in liquid nitrogen at the yin-yang coils, assuming a 14-MeV neutron source

strength of 5×10^{13} n/cm-s at this location and no additional shielding on the coils. The result was a C-14 production rate of 0.3 μC/ℓ/yr. To determine whether such a production rate is a problem, one would have to integrate over the entire nitrogen system and also make some assumptions about the N leak rate to the environment. The N-13 resulting from activation of the liquid nitrogen may be a hazard in the event of a massive leak under accident conditions.

The seismic criteria applicable to this type of facility depend on how the facility is classified. If it is a "low hazard" facility, at LLNL it must be built to 0.25-g horizontal acceleration (at zero period). If it is a "high hazard" facility, as the α+T almost certainly is, it must be designed to 0.5-g. It should be understood that the g-loads will amplify as a function of frequency (perhaps as much as a factor of 3 to 5 at periods of 1/2 to 1 sec). Calculation of damping due to ground interaction indicates that the amplification will be reduced, perhaps by 25 to 40%. The present design criteria are:

- No loss of life at 0.5 g.
- No collapse of building at 0.5 g.
- No major loss at 0.5 g.

Decommissioning will involve all the techniques developed for dealing with fission reactors. In particular, it will require a custodial period for the MFTF-α+T facility to allow the induced radioactivity to decay to levels that will allow disassembly and disposal. This period has been estimated at between 5 and 10 yr. During this time, maintenance must be performed on the facility to protect it against deterioriation and accidents.

Once actual decommissioning begins, the larger radioactive components must be disassembled to allow packaging for disposal. This may involve the use of a plasma torch, pools, and all the other techniques developed for fission systems. If the levels are low enough, near-surface burial may be possible; if not, the waste must be packaged as high-level waste. In any case, decommissioning of this system, as any other DT fusion devices, will provide a major challenge.

2.2 THE MFTF-B+T UPGRADE

2.2.1 Introduction

In this upgrade the 4-m DT axicell described for MFTF-α+T is inserted in the central cell of MFTF-B and the MFTF-B axicells are removed. The 6-T coil from the MFTF-B axicell is used in the transition region to enhance the pumping efficiency by the 40-kV beams in the transition. Figure 2-19 shows the magnet set and field profiles. Anchor sloshing beams and the high energy axial pump beams from MFTF-B are used, as is the ECRH system.

With this configuration the axicell insert can be operated in much the same way as in the α+T upgrade. However, the end plugs will not support the same β value in the insert so the density and fusion power are lower. Also lower is the wall flux, at 1.3 MW/m^2.

There are two modes of operation possible in this upgrade, the design mode and the TDF mode. As reflected in the parameter listing in Table 1-3, they differ in the amount of current injected into the insert section with neutral beams and pellets, and therefore the confining potential and electron temperatures differ. In the design mode the beam injection current is 150 A (trapped) while the TDF mode needs 279 A of beam and 720 A of pellets. The electron temperatures are 6.2 and 2.3 keV, respectively, while the confining potentials are 11 and 2 kV, respectively. Since the TDF mode has parameters not far different from those expected from TMX-U, we believe that success there will guarantee the 1-MW/m^2 performance in the insert needed to carry out the nuclear systems role for this upgrade.

This upgrade is not as expensive as the α+T upgrade because the end plug magnets are not replaced. However, there is not much difference in the tritium system, facilities, and other expensive items, so the differential is not large.

Because this insert option is a part of the α+T option described earlier, the physics and engineering descriptions that follow will center on features that are different in the two applications.

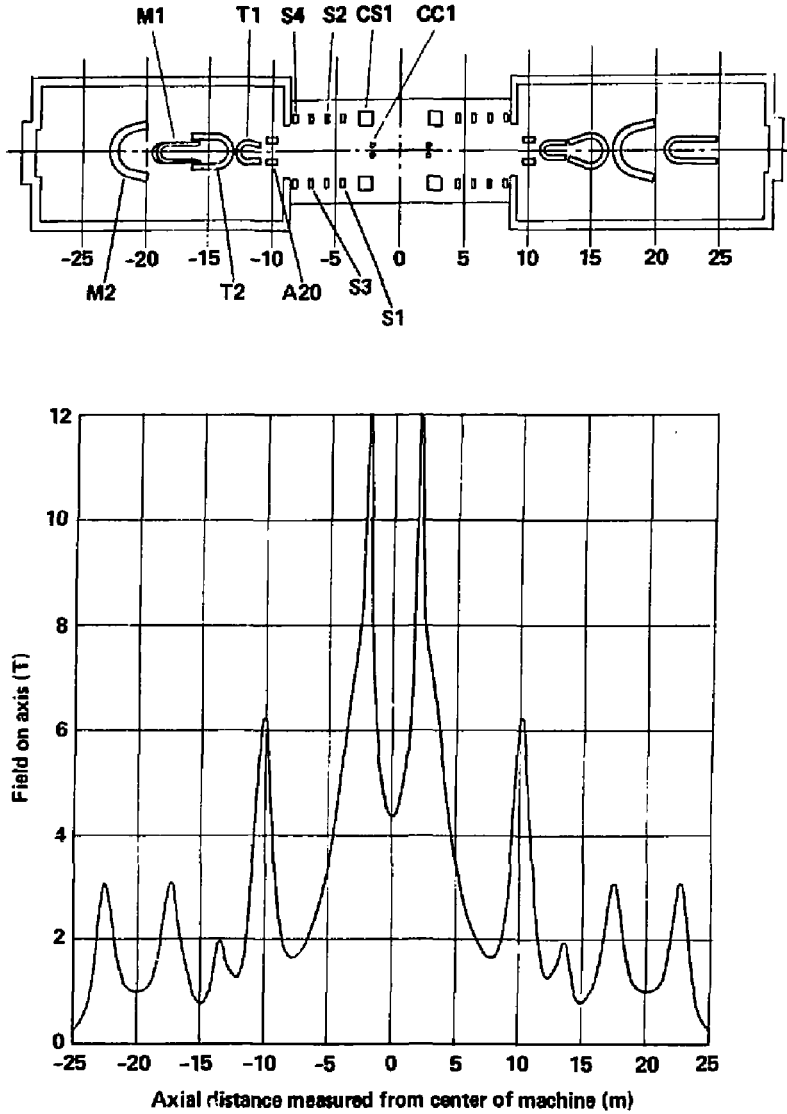

Fig. 2-19. MFTF-B+T magnet configuration, field on axis.

2.2.2 Physics Description

Profiles of magnetic field, potential, and density for the design mode of MFTF-B+T upgrade are shown in Fig. 2-20. In the axicell the density, electron energy, and warm ion energy are lower than they are in the MFTF-α+T operating mode, a situation traceable to the lower β-limit. With a lower warm ion energy the plugging potential is reduced to 11 keV (compared to 22 kV in α+T). A parameter set is given in Table 2-10.

With four neutral beams, the 150 A (trapped) needed to fuel and heat the axicell is provided. The trapped power is 9 MW and 7.3 MW of fusion power is produced, so that Q_c = 0.81. This power gives a neutron wall flux of 1.3 MW/m^2 at r_w = 25 cm.

By eliminating the axicells in MFTF-B and putting the 4-m insert in the central cell, the transition region now extends all the way to the 12-T choke coils. Pump beam currents would increase above their values in MFTF-B for these longer transitions were it not for the introduction of the 6-T coil into the transition. At that local peak in magnetic field the plasma is more dense and nearly circular, increasing the trapping efficiency. In MFTF-B the pump beam is poorly trapped because geometric constraints require that the pump beam pass through the narrow dimension of the elliptical fan.

In the plugs the power requirements are similar to those in MFTF-B. The sloshing current is 7 A (with 80-kV beams) and there is some increase in ECRH power to 950 kW per end. This ECRH requirement is comparable to the 1 MW required in the high Γ mode of MFTF-α+T.

Turning now to the TDF mode at operation in MFTF-B+T we have derived this scenario by searching for the lowest potential in MFTF-B+T that will give a wall loading in excess of 1 MW/m^2. In the following we describe the TDF mode of operation having a 2-kV confining potential. Such a mode allows for the possibility that impurities or instabilities might limit thermal barrier potentials well below ϕ_c = 30 kV. So, we have determined the minimum Q_c, T_{ec}, τ_{DT}, and ϕ_c needed to achieve a neutron flux of Γ_n = 1 MW/m^2. We find that, with a modest increase in axicell beams (eight instead of six), in present MFTF-B pumping beams (eight instead of four), and in ECRH power (≈1.6x), such a neutron flux can be achieved using the present MFTF-B end plugs with a Q_c = 0.3, T_{ec} = 2.3 keV, τ_{DT} ≈ 6.5 ms (including the pellet fueled population), and ϕ_c = 2 kV. The Q_c and T_{ec} required for this most conservative

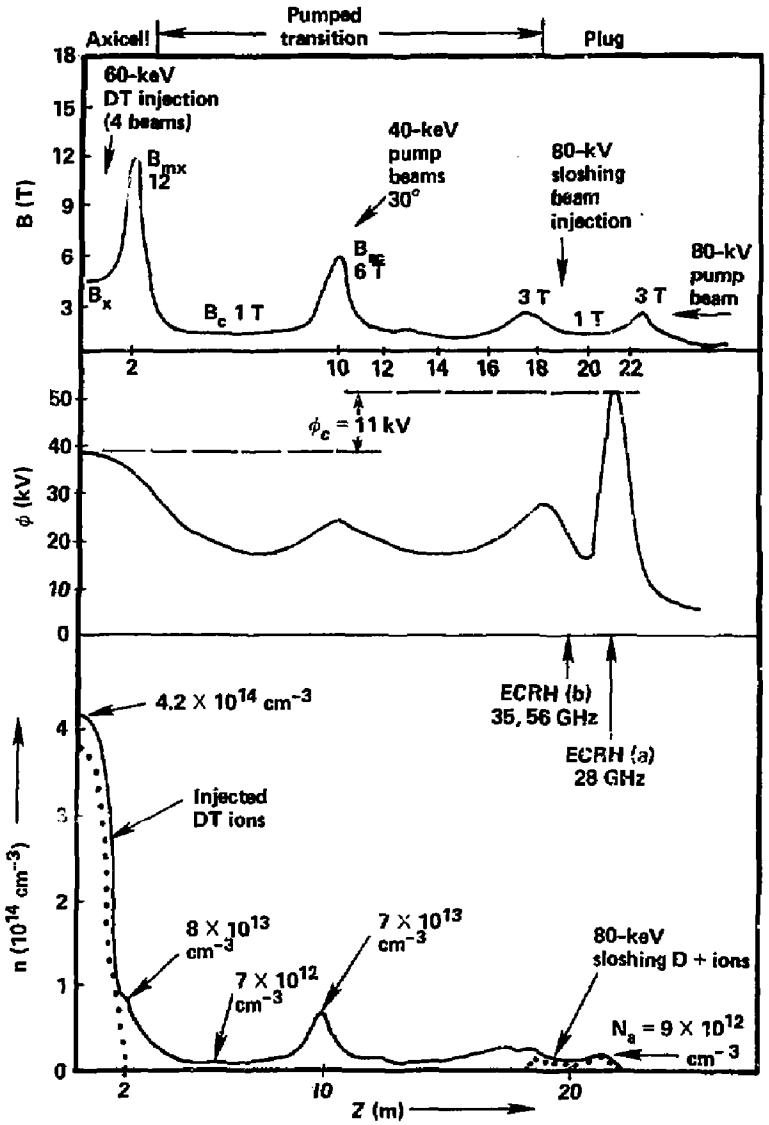

Fig. 2-20. MFTF-B+T axial pofiles of field, potential, and density, in the design mode.

Table 2-10. Physics parameters for the MFTF-B+T Upgrade.

Parameter	Value
Central cell	
Plasma length (m)	4
Plasma radius (m)	0.15
Solenoid field (T)	4.5
Peak β	0.4
Electron temperature (keV)	6.2
Hot-ion average energy (keV)	49
Hot-ion lifetime (ms)	42
Hot-ion density (cm^{-3})	3.8×10^{14}
Warm-ion temperature (keV)	9
Warm-ion density (cm^{-3})	3.8×10^{13}
Beam voltage (kV)	80
Trapped beam power (MW)	9 (150 A/60 keV)
Fusion power (MW)	7.3
Neutron wall flux (MW/m^2) at R = 0.25 m	1.33
Potential, ϕ_e (kV)	37
Choke/transition region	
Field at choke, B_{max} (T)	12
Plasma length (m)	14.6
Field at midplane (T)	1
Pumping beam current (each end)	50 A @ 40 kV
Injection angle, θ	$\sim 30^0$
Potential, ϕ_T (kV)	~27
Anchors	
Plasma length (m)	5.2
Plasma radius (m)	0.32
Plasma density (cm^{-3})	$\sim 10^{13}$
Field at mirror (T)	3
Field at midplane (T)	1
Potential, ϕ_A (kV)	~18
Sloshing neutral beams (each end)	7 A @ 80 kV
Trapping fraction, F_T	0.34
ECRH (each end)	~350 kW @ 35 GHz ~600 kW @ 28, 56 GHz
Hot electron energy (keV)	~200
Electron temperature (warm), T_e (keV)	22
Potential, ϕ_c (kV)	11
Pumping/beam current (each end)	5 A @ 60 kV

case are similar to those of the TDF,[2] and are about one-third of those required of the high Γ mode MFTF-Upgrade case and about one-sixth of the high Q mode. The low Q case requires a confinement time and potential well ϕ_c for the ions about an order of magnitude smaller than in the high Γ mode of the MFTF-Upgrade.

The layout of the machine is the same as for MFTF-B+T, but there are additional central cell and pump beams, and 720 A of gas is fed to the center with pellet injections. The axicell beam lines are designed to accommodate six beams + two spares, although only six beams would be used with the high Γ mode of the preferred MFTF-Upgrade. Thus, procurement of the axicell and its beam lines does not depend on the decision to upgrade the end plugs (which depends on MFTF-B data), and therefore can be committed earlier. The superconducting Nb_3Sn 12-T inserts in the choke coils at z = ±10 m of MFTF-B are removed in this design to permit access for more 40-keV pump neutral beams, which are needed to pump out the central solenoid region as well as the existing transition regions of MFTF-B. The need to pump out the entire region between the 12-T choke coils of the axicell and the potential peaks in the plugs, as was the case in the earlier B+T design, results from the limited MHD stability available with the present MFTF-B magnet set, which requires keeping the pressure low in all the bad curvature regions of the central cell as well as in the transitions in order to support the minimum $\langle\beta_x\rangle = 0.15$ required for $\Gamma_n = 1$ MW/m^2 in the axicell.

Figure 2-21 shows the resulting axial profiles of magnetic field, potential, and density along the axis of the low Q case. Table 2-11 lists plasma parameters in the axicell, central cell/transitions, and in the plugs for this case, Table 2-12 lists heating systems parameters, and Table 2-13 summarizes confinement parameters. Note in Fig. 2-22 the low density in the central cell, comparable to the density in the transitions, which gives a β of passing + trapped warm ions of only 1% ($\beta_\perp$), 4% ($\beta_\parallel$). Were the central cell region not pumped, the local β at 1 T would reach $\beta_\perp = \beta_\parallel = 24\%$, contributing enough additional bad MHD drive that the axicell β (and Γ_n) would have to be reduced significantly. Although bounce-resonance drift pumping could certainly be used to accomplish the pumping in this low Q case as in the preferred upgrade case, we avoided new, developmental hardware in the MFTF-B plugs to be conservative and to hold down costs. The total collisional

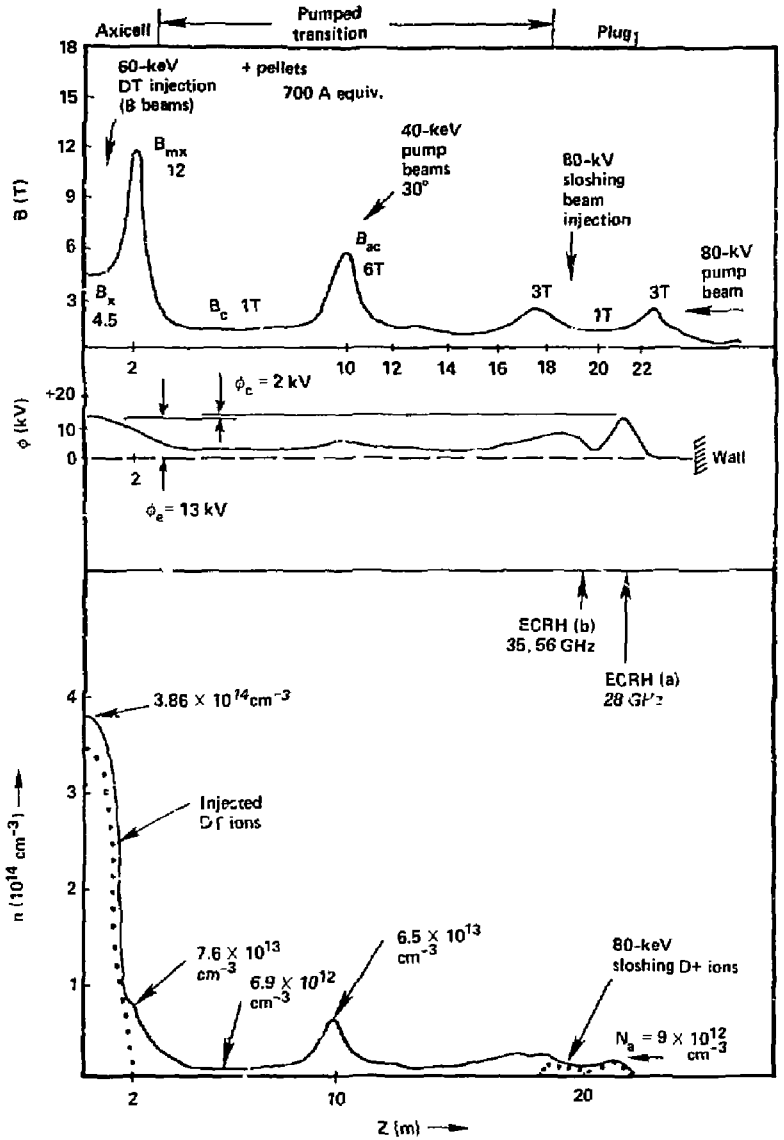

Fig. 2-21. Profiles of field, density, and potential in the TOF mode of MFTF-8+T.

Table 2-11. MFTF-B Upgrade (B+T, TDF mode).

Plasma parameter	Value
DT axicell	
B_x	4.5 T
B_{mx}	12 T
E_i	33 keV
T_{ec}	2.3 keV
n_x	3.86×10^{14} cm^{-3}
$\hat{\beta}_x$	0.22 (quartic)
$\langle\beta_x\rangle$	0.15 (profile)
ϕ_e	13 kV
ϕ_i	2 kV
$(n\tau)_{\text{local mirror}}$	9×10^{12} cm^{-3} sec
$\langle\sigma v\rangle_{DT}$	5.0×10^{-16} cm^3/sec
P_{fusion} (axicell)	5.53 MW
r_x	15 cm
r_{wall}	25 cm
$L_{axicell}$	4.0 m
L_{eff}	2.8 m
Γ_n (at r = 25 cm)	1.0 MW/m^2
Central cell + transition	
I_{trap}	86 A
I_{neo}	10 A
T_{ec}	2.3 keV
T_{ipass}	5.5 keV
n_{pass} (IT)	2.5×10^{12}
g_b	2.75
$\hat{\beta}_t$	0.01 ($\beta_\perp$) 0.04 ($\beta_\parallel$)

Table 2-11. (Continued.)

Plasma parameter	Value
Plug	
n_{pass} (point b)	1.37×10^{12} cm^{-3}
n_b	6.5×10^{12} cm^{-3}
g_b	2.75
G_b	4.75
n_a	9×10^{12}
B_a	1.34 T
$B_{a'}$ (injection point)	1.51 T
$\bar{E}_{eh}$	200 kV
T_{ew}	13 kV
β_p	0.55 (quartic)
$\langle\beta_p\rangle$	0.37 (profile)
$\delta\phi_{a' \to a}$	9 kV
$\delta\phi_a$	13 kV
$n_{slosh}/n_s(b)$	3.3

Table 2-12. MFTF-B Upgrade heating systems (B+T, TDF mode).

System	Trapped power current	Incident power current	Frequency (voltage)
Axicell beams	18.4 Mw 279 A	21.6 360 A	$\bar{E}_{inj}$ = 60 keV $\theta_{inj} \geq 75^{o}$
Axicell pellet injector	720 A	1000 A	100 Hz
Transition pump beams	3.3 MW 82 A (each end)	4.0 MW 100 A (each end)	$\bar{E}_{inj}$ = 40 keV (high molecular 80 kV accel) $\theta_{inj} \simeq 30^{o}$
Plug ECRH	500 kW each plug (b) 345 kW each plug (b) 100 kW each plug (a)	600 kW 414 kW 120 kW	28 GHz 35 GHz 56 GHz
Plug sloshing beam	56 kW each plug 0.7 A each plug	225 kW each plug 2.8 A (each plug)	80 keV

Table 2-13. MFTF-B Upgrade (B+T, TDF mode).

Confinement parameters

$(n\tau)_{DT} = 9 \times 10^{12}\ cm^{-3}\ sec$

$(n\tau)_{hot + pellet} = 2.5 \times 10^{12}\ cm^{-3}\ sec$

$\tau_{DT} = 0.023\ sec$

$\tau_{particle\ beam + pellet} = 0.0065\ sec$

$$Q_c \quad \frac{P_{fusion}\ (axicell)}{axicell\ energy\ losses} = 0.30$$

$$Q_{ceff} \quad \frac{P_{fusion}\ (axicell)}{energy\ losses - alpha\ heating} = 0.32$$

$$Global\ Q = \frac{P_{fusion}\ (axicell)}{total\ axicell + plug\ injected\ power} = 0.21$$

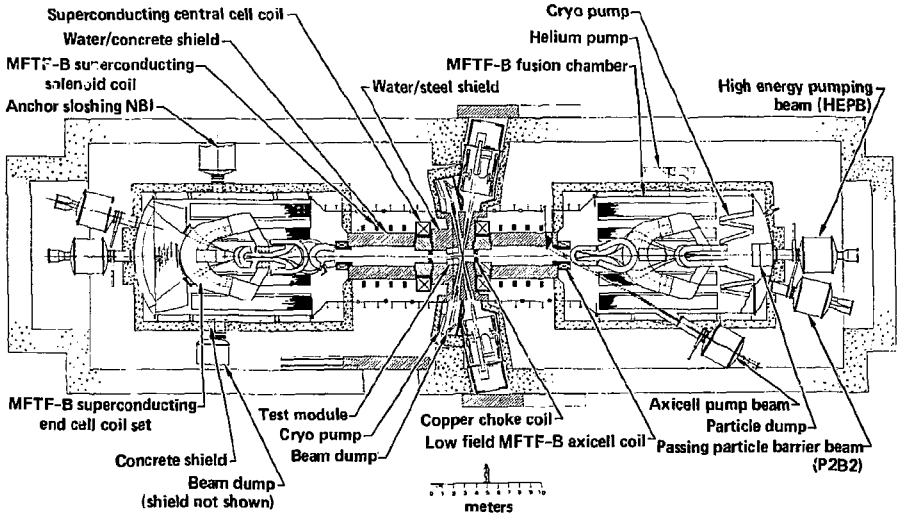

Fig. 2-22. Layout of the MFTF-B+T Upgrade in the vault.

trapping current in this low Q case, I_{trap} = 86 A (both ends), is much larger than the 2 A trapped in MFTF-B, partly because of the low temperature of the passing warm ions (5.5 keV vs 15 keV in MFTF-B), partly because of the higher density (n_{throat} = 7.6 x 10^{13} cm^{-3} vs 3 x 10^{13} cm^{-3} in MFTF-B), and partly because of the longer region to be pumped (19 m each end vs 10 for MFTF-B). Thus, more 40-kV pump neutral beams are required, but most importantly, the trapping efficiency of those beams must be greatly increased to manage the 86-A pumping requirement. This is accomplished by "compressing" up the passing ion density in a local 4- to 6-T mirror through which the pump beams pass, using a pair of the NbTi axicell backing coils of MFTF-B. The pump beam footprint should pump between 3 T and the mirror peak as it passes through. Because of the high local density ($\sim$6 x 10^{13} cm^{-3}), circular plasma cross section, and shallow beam angle ($\theta_{inj} \sim 30^{o}$), the total beam attenuation is estimated at 85%, and the pumping requirement is therefore satisfied with 4- to 25-A incident 40-kV pump beams at each end.

Based on Fokker-Planck studies of the axicell ion distribution function in TDF[1] (nearly the same local T_{ec}, mirror ratio, and low potential well ϕ_c as in this low Q case), a source of gas or pellets of roughly twice the injected beam current is required to keep the mirror loss-cone region of the distribution sufficiently filled to prevent loss cone microinstabilities. Such a low energy neutral D^{o} source is needed only when the potential well ϕ_c is small compared to the mean ion energy in the axicell, as in this case and in TDF. Due to the high axicell density, a pellet injector similar to the one envisioned for TDF is needed for this low Q case. Besides filling the axicell distribution loss cone, the extra-warm ion-end losses resulting from the pellet injection will help damp any sloshing ion microinstabilities as did stream in 2XIIB and TMX. The pellet injection raises the gas pumping requirements in the end tanks substantially, but the low Q mode should tolerate higher end tank pressures than is normal for MFTF-B.

2.2.3 Engineering Description

The MFTF-B+T Upgrade device is shown in Fig. 2-22 in the vault. The DT axicell used in α+T is shown at the midpoint of the MFTF-B machine. The MFTF plugs and end cells are used with suitable modifications to allow steady-state operation.

The axicell is identical to that of MFTF-α+T, but with an additional neutral beam injector in each beamline to provide the appropriate neutral particle injection. In the central cell, the two inner axicell coils of MFTF have been removed and the remaining 5-m-dia solenoids relocated to provide the confining field to the outer axicell coil, which has been reconfigured to generate 6 T at its midpoint. The remainder of the MFTF-B magnets are maintained in their original configuration. Pump beams are added that intersect the plasma at the center of the 6-T coil.

Shielding is provided throughout the interior of the coil set to protect the superconducting coils from excessive neutron heating (neutron damage is not a consideration in this design). The central cell region requires less shielding than it would in α+T, because of the much lower reaction rate in B+T.

The vacuum pumping is replaced with cyclable pumps in the same manner as α+T. Careful design is required to provide adequate pumping speed for the relatively high gas load in the limited space available in the end cell.

Shielding is placed outside the end vacuum cells to keep the after-shutdown radiation dose rate low enough to allow contact maintenance in the vault.

The remaining systems are al. similar to their equivalents in α+T with minor differences to match the details of the MFTF-B+T requirements.

2.3 THE MFTF-α UPGRADE

2.3.1 Introduction

One option for the future use of the MFTF facility is to improve the physics performance with the end plug upgrade that was part of the MFTF-α+T option. Although this option would use DT fuel to achieve Q ∿ 2, the pulse length would be set by physics consideration to 1000 sec. It differs only by the absence of the central axicell and the use of ICRH bulk heating, rather than neutral beams, for the central cell. One would produce 6.5 MW of fusion power in the central cell, but at too low a flux for blanket testing.

The tritium inventory is substantially lower here than in the previous options, and that, along with the absence of the DT axicell, reduces the cost of this option significantly. A further large reduction in cost would accrue if one were to operate with deuterium gas.

2.3.2 Physics Description

This option is nearly identical to the high Q mode of operation in MFTF-α+T. A 62-kV confining potential is produced by the 200-kV negative ion beam, here needing only 2.2 A per plug rather than 4.1 A (incident current). The ECRH power is also lower (the higher requirements on current and ECRH were associated with the high T mode) than for MFTF-α+T. All requirements should be taken from the list for the high Q mode, with the exception of the central cell beam power.

For the proper mix of particles and energy in the central cell, a combination of pellet injection and ICRH heating replaces the 30-A beam in the MFTF-α+T Upgrade. This simplifies the heating technology and reduces the tritium throughput.

Profiles of field, density and potential for MFTF-α are shown in Fig. 2-23. These should be very similar to the high Q mode of MFTF-α+T but may differ somewhat because the scenario was calculated earlier with slight modelling differences. Table 2-14 gives a more complete summary of plasma parameters for this upgrade.

2.3.3 Engineering Description

The MFTF-α Upgrade is shown in Fig. 2-24. Though similar in appearance to MFTF-α+T except for the central cell beamline, there are some important differences. Bulk heating in the central cell is produced by 4 MW of ICRH, while DT fuel pellets provide particles. The tritium throughput is much lower than with beams (that are only ∿ 30% gas efficient) and the total inventory is lower. The 1000-sec pulse also contributes to a lower inventory.

Shielding requirements could be ameliorated depending on the duty cycle for these shorter pulses. Also, with 1000-sec pulses, ordinary cryopanels could be used rather than recyclable cryopanels.

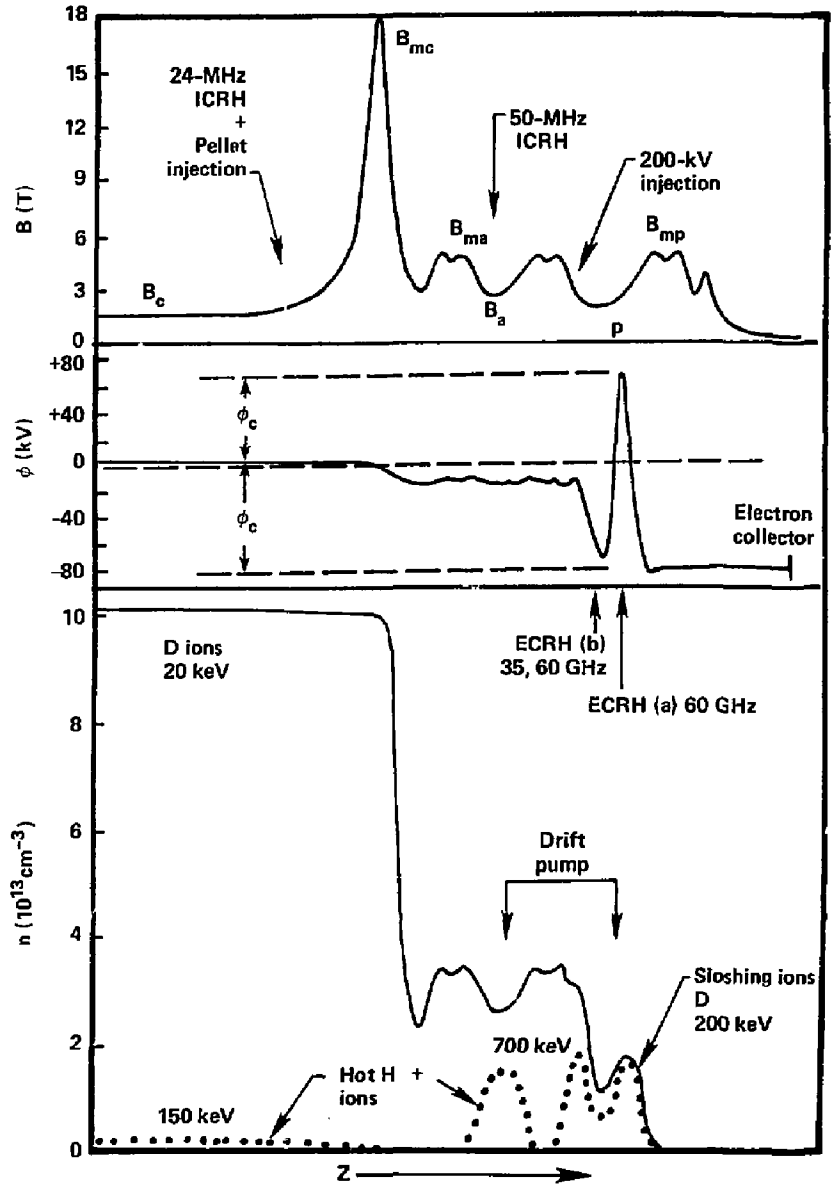

Fig. 2-23. Field, potential, and density profiles for MFTF-α.

Table 2-14. MFTF-α end plug upgrade plasma parameters.

Parameter	Value	
	Central cell	
T_{iwc}	20 keV	
T_{ec}	12 keV	
n_{iwc}	10^{14} cm^{-3} D^+	
n_{iHc}	5×10^{12} cm^{-3} H^+	
E_{iHc}	150 keV	
B_c	1.6 T	
$\hat{\beta}_c$	0.6	
$\langle\beta_c\rangle_{ave}$	0.4 (quartic profile)	
ϕ_c	68 kV	
ϕ_e	79 kV	
$(n\tau)_{Pastukhov}$	5.5×10^{14} cm^{-3} sec	Particle $n\tau$
$(n\tau)_{radial}$	1.27×10^{14} cm^{-3} sec	Particle $n\tau$
$(n\tau)_{tot}$	1.0×10^{14} cm^{-3} sec	Particle $n\tau$
$(n\tau)_{cE}$	5.8×10^{13} cm^{-3} sec	Energy $n\tau$
Q_c	2.1	Effective, including 1.3 MW α heating
Q_{tot}	1.8	Effective, including 1.3 MW α heating
L_c(eff)	16.5 m	
r_c	0.28 m	
P_{fusion}	6.5 MW	

Table 2-14. (Continued.)

Parameter	Value
Anchor	
$n_{pass}(B_A)$	5×10^{12} cm^{-3}
$n_H(B_A)$	1.4×10^{13} cm^{-3}
$\bar{E}_H$	700 keV (H^+)
B_A	2.6 T (vac)
B_{res}	3.3 T (with plasma)
R_{vac}	1.85
$\hat{\beta}_A$	0.6
$\langle\beta_A\rangle_{ave}$	0.4
τ_H	1.8 sec (particle)
I_{trap} (passing D^+ ion loss)	10.5 A (each end)
I_H (trapped H^+ ion loss)	0.2 A (each end)

Table 2-14. (Continued.)

Parameter	Value
Plug	
n_{pass} (point b)	2×10^{12} cm^{-3}
n_b (point b)	1×10^{13} cm^{-3}
n_a (point a)	1.65×10^{13} cm^{-3}
$n_{a'}$ (point a')	3.8×10^{13} cm^{-3}
$B_{a'}$ (point a')	3.1 T, 3.0 T β depressed
B_p (point b)	2 T vac, 1.25 T β depressed
B_a (point a)	2.2 T vac, 1.65 T β depressed
$\bar{E}_{eh}$	700 keV
T_{ew}	110 keV
$\hat{\beta}_p$	0.6
$\langle\beta_p\rangle$	0.4
$\delta\phi_{a'\to a}$	78
$\delta\phi_a$	135
n_{slosh}/n_s(b)	2.7
g_b	2
G_b	5

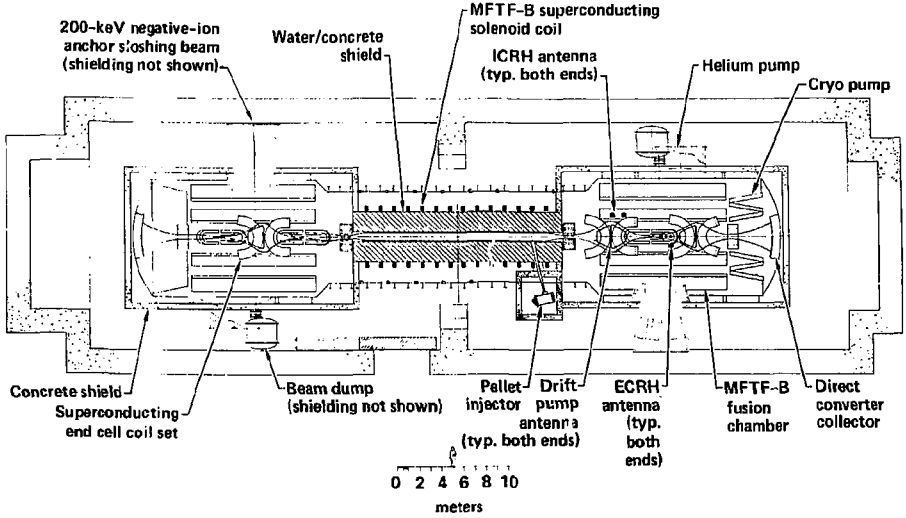

Fig. 2-24. Layout of the MFTF-α Upgrade.

REFERENCES

1. D. E. Baldwin and R H. Bulmer, Lawrence Livermore National Laboratory, Livermore, CA, UCID-19562 (1982).
2. K. I. Thomassen and J. N. Doggett, "A Technology Demonstration Facility," J. of Fusion Energy (to be published).
3. F. H. Coensgen, J. F. Clauser, D. L. Correll, W. F. Cummins, C. Gormezano, B. G. Logan, A. W. Molvik, W. E. Nexsen, T. C. Simonen, B. W. Stallard, and W. C. Turner, "2XIIB Plasma Confinement Experiments," in Proc. 6th Inter, Conf. Plasma Physics and Controlled Nuclear Fusion Research, Berchtesgaden, Fed. Rep. of Germany, 1976 (IAEA, in preparation), Paper CN-35/C1; also Lawrence Livermore Laboratory Rept. UCRL-78121, Rev. 1.
4. D. D. Ryutov and G. V. Stupakov, Pisma Zh. Eksp. Teor. Fiz. 26, 186 (1977) [JETP Lett. 26, 174 (1977)]; Fiz. Plazmyu 4, 501 (1978) [Sov. J. Plasma Phys. 4, 278 (1978)]; Dokl. Akad. Nauk. SSSR 240, 1036 (1978) [Sov. Phys. Dokl. 23, 412 (1978)]. See also R. H. Cohen, Nucl. Fusion 19, 1579 (1979), and Comments Plasma Phys. 4, 157 (1979).
5. T. H. Batzer and W. R. Call, A Continuous Cryopump for Steady-State Mirror Fusion Reactors, Lawrence Livermore National Laboratory, Livermore, CA, UCRL-87732 (1982). (Also given at the 29th National Vacuum Symposium, Baltimore, MD, Nov. 16-19, 1982.)

3. ROLE OF THE UPGRADE

3.1 OBJECTIVES FOR MFTF-B UPGRADE

Our objectives for the MFTF-B Upgrade are to advance a number of mirror technologies, improve our physics experimental data base, and gain important nuclear engineering experience in the operation of the power and fuel cycles in fusion blankets. Through the construction and operation of this upgrade we would gain experience in the following:

- Steady-state physics performance with significant alpha heating, including impurity control and operation in a vacuum equilibrium.
- Steady-state operation of plasma heating and particle control systems.
- Steady-state vacuum system operation.
- Integration of plasma production technologies and operation in a high level neutron environment.
- Tritium fuel-cycle operation, including blanket recovery and air/water cleanup systems.
- Equilibrium power-cycle operation with fusion blankets.
- Operation, maintenance, and safety requirements in an activated fusion device with a substantial tritium inventory.
- Verification of thermal-mechanical and tritium-breeding features in a variety of fusion blankets.

Of this list, those objectives dealing with nuclear systems issues are among the more important for upgrading the facility. Nonetheless, the remaining items on the list encompass a variety of activities that will significantly reduce the risks inherent in proceeding with construction of a full scale engineering test reactor, whether it be a tokamak or tandem mirror.

3.1.1 Power and Fuel Cycle Technology

One purpose of the upgrade is to provide a fusion environment for blanket technology tests. After examining the types of tests required, we found that they fall in three classes: tests for initial point failures, tests for early failure modes, and design qualification tests. The first of these are tests to confirm that the blanket operates, on initial turn-on, as designed. The second class of tests searches for early failure modes that limit the life to

about 10% or less of the design operating life. The last test is a lifetime test to qualify a design for a demonstration power plant.
Table 3-1 summarizes these tests and their purpose.

These three classes of tests should all be carried out at a wall flux of 1 to 2 MW/m^2 to be of reactor interest. At that flux level there are nominal test times for each class. To confirm a given design and to demonstrate survival at the initial turn-on, thermal-hydraulic and tritium breeding and recovery tests should be performed. Characteristic times are set by temperature equilibration in the blanket and heat exchanger loop for thermal/hydraulic effects, and by the tritium equilibration time for breeding and recovery tests. Fluence is not important in these tests, but one should plan for a series of test runs for times longer than these characteristic times.

Early-life failures might occur after 1000 to 10,000 hrs of running time, and could result from a variety of things. For example, materials incompatibility could lead to problems like the mass transport of activated corrosion products in $Li_{17}Pb_{83}$ blankets. Ceramic breeding materials might sinter, holding up tritium in the blankets. Welds might prematurely fail from thermal stressing or other causes. Ceramic-to-metal brazes (e.g., from SiC blanket tubes) might fail under thermal loading. The list of possibilities is probably quite long, and the failures are those not anticipated in the design. Any proper design would avoid known problems.

Design qualification requires an integrated test time of ~ 5 $mW\text{-}yr/m^2$ of neutron fluence, and is beyond the scope of MFTF-Upgrades. Qualification tests are left for ETRs, which in the mirror program is the second phase of our FPD device.

In MFTF-Upgrade we can perform tests to confirm blanket designs and show survival against initial failure modes. To discover early failure modes probably requires a minimum of 100 test runs of 10 hr each, which is at the limit of what we believe we can be do in this facility. Since this testing capability is very important, we intend to examine further the limiting availability of the machine.

In summary, the upgrades will be used primarily for thermal/hydraulic and tritium breeding and recovery tests. The characteristic thermal lines are $\sim$1/10 hr for liquid metal blankets, and $\sim$ 1/2 hr for blankets with ceramic breeding materials. Tritium concentrations reach an equilibrium in $\sim$1/10 hr

Table 3-1. Characteristic times for fuel/power cycle tests[a] on blankets and auxiliary equipment.

Purpose of test	Uninterrupted test time and subject	Total test time needed	Issues being addressed
Thermal/ hydraulic behavior	∿1/10 hr (liquid metal blankets) ∿1/2 hr (ceramic breeding blankets)	Tens of well-instrumented tests	Design confirmation--or: heat transfer/removal, structural effects, MHD pressure drops, off-normal (LOCF, LOCA) response.
Tritium breeding/ recovery	∿1/10 hr (lead lithium) ∿10 hr (pure lithium) ∿100 hr (ceramic breeders)	Tens of well-instrumented tests	Design confirmation--or. production/recovery rates, tritium accountability, permeation rates.
Early failure modes	1 to 100 hr	1,000 to 10,000 hr	Corrosion, sintering, mass transport, materials compatibility, weld performance, safety systems, any problems that lead to early system failures.
End of life	∿100 hr	10,000 to 100,000 hr	Lifetime demonstration--or: radiation damage to structures, fatigue, embrittlement, swelling, all issues in the design which limit the design-life to ∿10 MW/yr/m^2.

[a]Flux level at least 1 MW/m^2.

for lithium-lead blankets, ~10 hr for pure lithium blankets, and ~100 hr for ceramic breeders. The last of these time constants calls for a longer run period than now envisioned, and our ability to extend the run is being examined. In these tests we will determine heat transfer and removal rates, MHD pressure drops (liquid metal) structural behavior, off normal responses (magnet quenches, loss of coolant, loss of coolant flow, etc.), tritium production rates, recovery rates, and permeation of tritium into dumps, heat exchangers, etc.

3.1.2 Systems Integration

To construct a large facility like MFTF, a great deal of attention is given to systems integration. The components in MFTF-B are quite complex, and when they are present in large numbers and combined with other complex systems, the availability of the facility could be quite low when all systems are integrated together, if such matters are not carefully planned. A proper plan for reasonable availability affects component reliability, maintenance, and spare parts inventories. The target availability will depend on the required run time and duty cycle, and for the MFTF-Upgrades we are venturing into new territory with 10-hr run times.

The introduction of tritium and production of neutrons adds complexity to the systems integration task, since component and system designs must accommodate this new environment. Maintenance considerations complicate the designs and impact the mean-time-to-repair, therefore they directly impact the availability. The MFTF-Upgrades provide a focus for solving problems that limit machine availability, and also give us an early opportunity to gain experience with the types of systems in DT mirror devices. During the lifetime of the machine we would expect to increase the availability from the initial 1% to as high a value as is possible.

3.1.3 Operations, Maintenance, and Safety

There is a major difference in operations between MFTF-B and any upgrade that uses a tritium inventory of hundreds of grams and which produces 10 to 20 MW of fusion power for hours at a time. We have already noted that this difference affects availability, and there are other impacts on operations.

Operational procedures must be developed for many new subsystems, procedures that reflect a greater responsibility for safety from the additional hazards of tritium handling and activation. Additional instrumentation for radiation monitoring, tritium accountability, safety interlocks, and other such systems needs to be developed. Off-normal operations need to be considered, including the operation of emergency air and water cleanup systems, protective operations during loss of coolant or coolant flow in test blankets, and other emergency operations.

Maintenance procedures and equipment must be developed for the upgrades, and actual maintenance experience at this level can be very valuable. Systems studies of fusion reactors show that maintenance costs, including facilities for maintenance, are a sizeable fraction of the reactor cost. Furthermore, the estimates suffer from lack of detail. Real maintenance experience is needed before requirements and specifications necessary for costing can be set.

As we have learned from systems studies, the ability to efficiently maintain a machine requires that components and subsystems be designed with this requirement in mind. By adopting this general design philosophy for the new components and subsystems, we will gain detailed knowledge of the impact on the machine and determine the critical problems to be addressed in future devices.

Safety will be an important issue in the design and operation of the upgrade. We will learn what new systems are necessary and hopefully demonstrate through safe operations that fusion devices pose no undue hazards. The tritium and activation levels in the upgrade are sufficient to make this a meaningful demonstration.

3.2 *BENEFITS TO THE MIRROR PROGRAM*

The upgrade can be viewed in the context of its place in a mirror programmatic sequence, and we do that in Sec. 4. Here, we consider the benefit in a "roll-forward" sense from our base of physics and technology as it will be developed by MFTF-B and other mirror devices in the program.

3.2.1 Physics Improvements

New end plugs in MFTF-B, patterned after the recent MARS design, would lead to substantial improvements in tandem mirror physics. By increasing the magnetic field level and the sloshing beam energy, the plugging potential could be doubled, leading to a particle confinement time given by $n\tau = 10^{14}$ (including radial loss). Correspondingly, one could operate at $Q \sim 2$ rather than $Q \sim 0.2$-0.4, as now envisioned in MFTF-B. With the more optimum MHD design of the new plugs the central cell β is doubled (average $\beta \sim 40\%$) and when operating at 1.6 T in the central cell, $\beta_c B_c^2$ increases five-fold.

In this upgrade the conditions in the plasma are more relevant to the reactor. End plugging is good enough that radial losses dominate (MARS regime), the central cell heating and power losses dominate over the plug power, the central cell population is more nearly isotropic, and α-heating is significant.

Two new and improved physics concepts are incorporated in the end plugs. Drift pumping replaces beam charge-exchange pumping, with an attendant improvement in Q. Drift pumping also removes impurities, an essential ingredient for long pulse or steady-state operation. Another feature is the addition of a region of good MHD curvature in the transition. This region becomes the MHD anchor and adds to the MHD damping of the plug region--the other good curvature region with large plasma pressure. MFTF-B, with its "double-fan" transition region, also has this additional good curvature region, but its axial extent and mirror ratio are too small to be used. In the upgrade, as in MARS, this region was emphasized in the design to very good effect.

3.2.2 New Technologies

Just as MFTF-B served to focus and push needed development for mirrors, the upgrade would serve the same function. Negative ion beams and high field choke coils are purposefully introduced in the upgrade to drive the development of those technologies.

In the end plug upgrade the 200-kV, 5-A beam is the only new ion beam of any significance required in the machine. (Central cell beams like those used

here are being developed for MFTF-B.) A negative ion beam with these parameters could be developed on the requisite time scale if this goal is set. Similarly, the 18-T choke coil requires a vigorous development effort, but there does not appear to be any obstacle to achieving this goal.

Finally, with radial loss predominating, the biased end collector is a simple plate to capture electrons. (Ions go out radially to the edge, then axially to the end of the machine. An equal current of electrons escapes through the core to the end plate). This is perhaps the most elegant and simple form of direct converter yet envisioned. This technology would be tested at reactor-relevant scale in the upgrade.

3.2.3 Relation to FPD

If MFTF-B performs as expected, generating a 30-kV confining potential and holding plasma particles for nearly 1 sec against radial and axial loss, the basis for proceeding to Phase I of the Fusion Power Demonstration (FPD) will have been established. In Phase I the end plug performance required for a tandem reactor will be demonstrated. This will be a DT physics test in a long enough machine for the center to ignite. In Phase II the central cell will acquire blankets for power and tritium production to demonstrate power breakeven and tritium self-sufficiency.

In an aggressive program, the main purpose of the MFTF-B Upgrade would be to permit the boldest possible step in FPD by reducing the risk. It would do this by providing earlier operating experience on a facility having all the elements of FPD but on a more modest scale. On the other hand, if FPD were delayed, the MFTF-α+T would greatly advance the tandem mirror data base and thereby strengthen the case for FPD when the funding picture improves.

3.3 BENEFITS TO THE FUSION PROGRAM

The scientific feasibility demonstrations expected in Tokamaks and mirrors reflect a maturity of understanding in plasma physics and signal the urgency to further pursue fusion technology. This technology has progressed remarkably in order to produce, heat, and contain plasmas in the breakeven experiments now in hand, but the nuclear technologies needed for power breakeven devices are in their infancy. There are two advantages to the

fusion community in building MFTF-B Upgrade: First, the machine is an affordable, early step toward a program to demonstrate engineering feasibility, and, as such, will serve to focus issues and develop the programs to address them. Second, the experience gained in building and operating the device and in testing blanket modules should reduce risk in ETR and perhaps allow an early start on that device.

3.3.1 Steps Toward Engineering Feasibility

Engineering feasibility has been defined as the readiness to build a fusion demonstration plant (DEMO), and to some that means successfully building and operating an ETR that reaches power breakeven and supplies its own tritium fuel. This is an ambitious goal and one that cannot be bridged directly from TFTR and MFTF-B. In the Tokamak program a fusion core demonstration is thought to be required, while the mirror program would do Phase I of FPD before Phase II, the ETR equivalent. The value of an early start on such an enterprise is very high.

An early start provides focus and accelerates the development of the requisite nuclear technologies. A good example is the impact that the facility would have on the blanket and shield program. Ideas for fusion blankets abound, and there are proponents for various concepts using different structural materials, coolants, and breeding media. By setting a date to test certain designs, a process of selection and development would be set in motion, leading to the fabrication of a few chosen blanket designs.

Issues relating to siting and safety, to design standards, to operations and maintenance, to radioactive waste disposal, and to decommissioning would all have to be addressed at a much earlier stage than for ETR. To do so should have enormous benefit to the program.

Finally, there is a feeling among the engineering community that it is very important to proceed as quickly as possible to build a device with a burning plasma for engineering purposes. Such a demonstration would be a hallmark to some that fusion is of age.

3.3.2 Contribution to ETR

Many consider the ETR undertaking to be too risky at this stage, and although opinions may differ on the reasons, a major factor is the engineering complexity beyond that of present experiments. One risk is the failure to gather the engineering data base from ETR needed to undertake a DEMO plant. This failure could result from low availability, or because the facility is prematurely closed for reasons of safety or inability to repair the device (at reasonable cost) after an accident.

By the construction and operation of MFTF-B Upgrade, engineering data and experience will be gathered on systems of a comparable complexity to those in ETR. Thus, on a system where only a 1% availability is demanded, we can make a confident projection of the availability goals of ETR, which will likely be in the 25 to 50% range. The common subsystems with ETR are superconducting magnets, ICRH and ECRH systems, tritium facilities, instrumentation and control, maintenance systems and facilities, waste disposal and decommissioning, and many operational and safety aspects of the facility.

4. RELATION TO THE MIRROR PROGRAM PLAN

4.1 INTRODUCTION

The physics and technology database needed to design a thermal-barrier tandem-mirror fusion reactor will be largely provided from operation of four machines (TMX-U, TARA, GAMMA 10, and MFTF-B) during the 1980's. Construction and operating periods of these machines and the proposed schedule for a fusion power demonstration (FPD) are shown in Fig. 1-3.

The basic physics design of the thermal-barrier tandem-mirror reactor concept will be substantially verified in the TMX-U, TARA, and GAMMA 10 experiments. Experiments in the MFTF-B facility that will become operational in 1986 will demonstrate scaling to plasma conditions near those of a full scale reactor, will provide definitive information for long-time scale processes, will provide transport information at reduced collisionality in the central cell plasma, and will advance development of technologies that must be demonstrated in the presence of confined plasma to near reactor energy and power levels. In the scheduled 4-yr period of MFTF-B operation, the initial configuration of this machine will be fully exploited to resolve those issues critical to a tandem mirror reactor.

4.2 THE EXPERIMENTAL PROGRAM PLAN

4.2.1 Physics Issues to be Addressed

The demonstrations listed below include a set of physics issues and a set of technology issues critical to development of a mirror reactor. The physics issues are categorized under the broad headings identified in the report of the US/Japan Bilateral Discussions (Q9, see Appendix A). The first five topics correspond to the following critical issues for the mirror program listed in Table 2-5 of the MFAC Panel I Report on Tandem Mirrors and Tokamaks:

- Microstability,
- Low-frequency stability,
- Thermal barriers and potential enhancement,
- Axial confinement,
- Radial confinement,

- RF heating,
- Startup.

Each of these categories encompasses a set of questions fundamental to operation of any tandem mirror in the thermal-barrier mode, as well as a set that becomes important only as the parameter regime of reactors is approached. The current experiments (TMX-U, TARA, GAMMA 10) will provide information on the first set of these issues, with MFTF-B providing the confirmation of scaling to near-reactor parameters. The second set of the issues can be uniquely addressed only by MFTF-B because of field configuration and accessible parameter regime.

The more important issues to be resolved in each of the above categories are summarized below; further detail can be extracted from the tables of Appendix A.

The microstability of both electrons and ion modes is of special concern in open systems because of the non-Maxwellian nature of one or more species' distribution function. For ions, both loss-cone and anisotropy-driven modes have been observed in past experiments. In thermal barriers, the appropriate ion distribution can also be susceptible to streaming-type modes. For hot electrons in thermal barriers, both loss-cone and anisotropy-driven modes can occur and have been observed in selected nonbarrier experiments. In theory, high performance machines can be designed to be either stable to all of these modes, or have fluctuation levels less than the corresponding classical rates. Verifying and augmenting this body of theory will be an important mission of each new generation of experiments.

Equilibrium and low-frequency stability requirements most directly impact magnetic field design. Both depend on the details of the magnetic line curvature, and both are affected by radial electric fields. For equilibria, the principal issue is minimization of flux-tube distortion in the central cell as a result of currents parallel to B-generated in the end regions For stability, the issue is to maintain a configuration with separated regions of favorable and unfavorable magnetic curvature, compounded by added destabilization due to rotation of the central cell driven by radial electric fields. Stability will be limited to the extent that perturbations can be localized to unstable regions. This localization can occur either by magnetic line bending, as in MHD balloon modes, or by the electrostatic ballooning caused by trapped particles. Ultimately, MHD and electrostatic ballooning

place the limits on the plasma pressure (for both modes) and communicating density (for the trapped particle modes) that an unstable region can hold stably. They are strong functions of the magnetic and configuration design, and the theoretical tools for this design must be calibrated.

A special aspect of the question of low frequency stability concerns the behavior of the hot electrons in the thermal barrier, where they contribute a majority of the local pressure. As demonstrated in EBT, their kinetic effects can dramatically alter their low frequency behavior. The question for tandem mirrors vary from how to correctly describe the hot electrons to how to actively capitalize on their increased stability.

Thermal barriers and potential enhancement introduce entirely new physics issues. Most simply, they entail generating their potential profiles by controlling the electron distribution at the same time as the ion distribution. The added means is selective electron heating, initially via ECRH but possibly otherwise in some applications, raising issues of wave penetration and deposition, avoidance of runaways, and instability. Ion distributions will initially be controlled by charge-exchange on injected neutral beams. However, assessments of this technique in reactor conditions point out the need for alternative means, such as the use of rf fields, particularly to prevent accumulative impurities and alpha particles in the thermal barrier.

Reactors require ion confinement times 50 to 100 times their 90^{o} scatter time, in turn requiring a net confining potential of about 2.5 T_i. Various related means for developing the required plugging potential include thermal barriers, potential enhancement, and negative operation. Each requires different types and amounts of applied power and thus implies different performance parameters, such as the system's overall nuclear power gain Q. These issues, in addition to those of stability and technology requirements, will ultimately dictate the detailed operating mode of a tandem mirror reactor.

Radial ion and electron heat confinement must at least be comparable to axial confinement. The radial ion step size is controlled by the average geodesic curvature as seen by an ion transiting the end cells. Therefore, it depends on magnet design and alignment. However, ion drifts also play an important role in affecting this average so that ion transport is a sensitive function of the radial electric field in the transition region. Electron heat

diffusivity in a reactor must be < 800 cm^2/sec. This value is less than present-day Tokamaks and would have been masked by axial electron power flow in current machines.

The dependence of equilibrium, low frequency stability, and ion radial transport upon details of the radial electric field strongly indicate that some form of radial potential control may be called for. Techniques for this include segmentation of end wall potentials, such as those employed in the rotating plasmas in Novosibirsk, as well as radial variation of power and particle deposition in the plasma.

Radio frequency heating may play an increasing role in tandem mirror confinement. For ion heating, it can supplement or replace neutral beams. Its role in electric potential manipulation has been mentioned above, and at low frequency it may prove a useful means for preventing ion accumulation in thermal barriers, i.e., "pumping."

Startup of a thermal barrier requires initiation of a low-collisionality plasma that satisfies conditions of micro- and MHD-stability. Their establishment centers around formation of plasma in the central cell that is allowed to flow out axially. Dump tanks reduce thermal contact with end walls to allow high electron temperature. Gas control, which is discussed in Sec. 4.2.2, is critical during startup when neutral beam coupling is weak and microwave coupling is poor.

4.2.2 Plasma Technology Development

Development of the following technologies requires successful demonstrations in plasma containment experiments:

- Impurity control,
- Fueling,
- Gas control,
- Alternative ion pumps,
- Direct conversion,
- Active feedback control.

Impurity concentrations in energetic plasmas must be kept to low levels to limit radiation cooling. Furthermore, in thermal barrier regions, impurities also enhance the trapping rate of passing particles, which then increases the required ion pumping and lowers Q. Effective impurity control

requires very low impurity content in the neutral beams as well as effectively preventing radial inward diffusion of impurities.

The central cell plasmas in TMX-U, TARA, and GAMMA 10 are fueled by gas penetration in the radially thin fan regions. It is unlikely that this method will be satisfactory for large, denser, more energetic reactor plasmas. Injection of solid pellets (which has been demonstrated in Tokamaks) may be required in future machines. However, as plasma containment in linear systems differs from that in Tokamaks, it is necessary to demonstrate pellet fueling in an operating device.

Neutral gas incident on the plasma leads to energy and particle losses and hence must be kept to suitably low density. This requirement is met by reducing all gas sources to minimum, high speed pumping by actively gettered panels or cryopanels, reduction of streaming gas from neutral beams and reduction of desorption and recycling from plasma chamber walls. Pellet fueling may reduce unwanted gas associated with plasma fueling.

Both the anchor and transition regions of a tandem mirror system require that the cool trapped ions be removed. Neutral beams injected at small angles to magnetic field lines are used for this purpose in TMX-U, TARA, GAMMA 10, and MFTF-B. However, this method is ineffective for removing impurities. Alternative pumping methods have been proposed that do remove both the impurities and the cool ions. These methods may also improve power efficiency.

Direct conversion of the energy carried by loss of plasma from the ends of a linear system is a standard feature of all mirror reactors. Although successful small-scale tests have verified the basic concept, there is a need for full scale integration at high power levels in an actual containment experiment. Direct conversion may indeed be the preferable energy removal option in future facilities.

We anticipate that active feedback control will be needed to maintain the operating-point parameters in long-pulsed and continuously operating reactors.

4.2.3 Alternative Geometries

The tandem mirror with thermal barriers can be realized in several alternative forms by varying the axial magnetic field geometry and/or by changing the axial electrostatic potential distribution. These alternatives could result in improved performance and the following three specific variations are part of the present experimental plan.

4.2.3.1 TARA, Alternative Magnetic Geometry. The TARA experiment at MIT is a largely axisymmetric machine stabilized by relatively low-field minimum-B cells located outboard at each end. A high-field axisymmetric cell at each end of the central cell contains both the thermal barrier and confining potential peak. The advantage of this geometry comes from the reduced anchor fields and the lower anchor density required to provide MHD stability. However, with reduced flow of central cell ions to the minimum-B anchor regions, the details of electrostatic-ballooning (trapped particle) modes become more important for achieving stable operation. In addition to testing the viability of this alternative geometry, the TARA experiment will address many of the physics and technology issues relevant to thermal-barrier reactor concepts in general. Projected contributions from FY 83 to 86 are listed in Appendix A.

4.2.3.2 GAMMA 10, Alternate Magnet Geometry. GAMMA 10 is an intermediate, thermal-barrier tandem mirror experiment located in the university at Tsukuba, Japan. In contrast to other thermal barrier facilities, the plasma has unrestricted access to the MHD anchors. This is accomplished by forming the positive confining potentials in circular-mirror-cells at each end of the machine. Resonant radial transport should be minimized because the magnetic fields are completely axisymmetric at ion turning points.

4.2.3.3 The Negative Tandem, Alternative Potential Geometry. In contrast to the normal mode of tandem operation, the negative tandem uses a negative central cell potential to confine central cell ions. Without changing the magnetic geometry, the electrostatic field profile is depressed relative to the (ground) end wall by magnetically confined hot electrons in the plug region. The advantages are produced by the elimination of sloshing-ion beams, with the attendant questions of ion microstability, and lead to the possibility of an rf-driven reactor. Variations of the negative tandem place the central cell potential at various levels, thus controlling the radial E-field and, hence, the rotational drive for MHD instability. Neoclassical particle transport is also minimized.

Initial tests of the negative tandem mode in TMX-U are scheduled for late FY 83, with an assessment of the results due in the second half of FY 84.

4.2.4 Experimental Program Plan

The anticipated schedule for acquisition of data from the four thermal barrier tandem-mirror facilities is shown in Table 4-1. We obtained data for GAMMA 10 from the report of the Q9 workshop; we obtained TARA data both from the Q9 workshop report and DOE milestones; we obtained TMX-U and MFTF-B data from the experimental teams working on these experiments. These data include, but are more extensive than, published milestones.

We have subdivided the anticipated experimental results into the following four categories:

1. Initial results (Δ)--This category means that a particular issue has been identified and investigated in the machine. The outcome of the investigation could be that the issue does not appear to be a problem or that it will require some means of control.
2. Substantial verification (□)--This category is used to indicate that a means of control over a particular issue has been demonstrated in a given machine. The control method does not necessarily extrapolate to a reactor, but does demonstrate a detailed understanding of the issue.
3. Scaling (⬡)--This category is used to indicate when a control method scalable to a reactor has been demonstrated.
4. Reactor application (○)--This category is used to indicate when the technology of a control method has been demonstrated for plasmas that approach reactor conditions. These conditions include such things as thermal loading, plasma collisionality, size, magnetic fields, power, etc.

The machine on which data will be obtained is identified by a letter inside the category symbol The key is:

A - MFTF

B - TMX-U

C - TARA

D - GAMMA 10.

Progress indicated in Table 4-1 for each issue is briefly discussed below. As shown in Table 4-1, all critical physics issues will have been verified, resolved, or controlled before the MFTF-Upgrade decision in FY 84. The scaling demonstration for all identified issues will be complete before the FY 88 decision point on FPD and on the MFTF end plug upgrade.

Table 4-1. Mirror program data acquisition schedule.

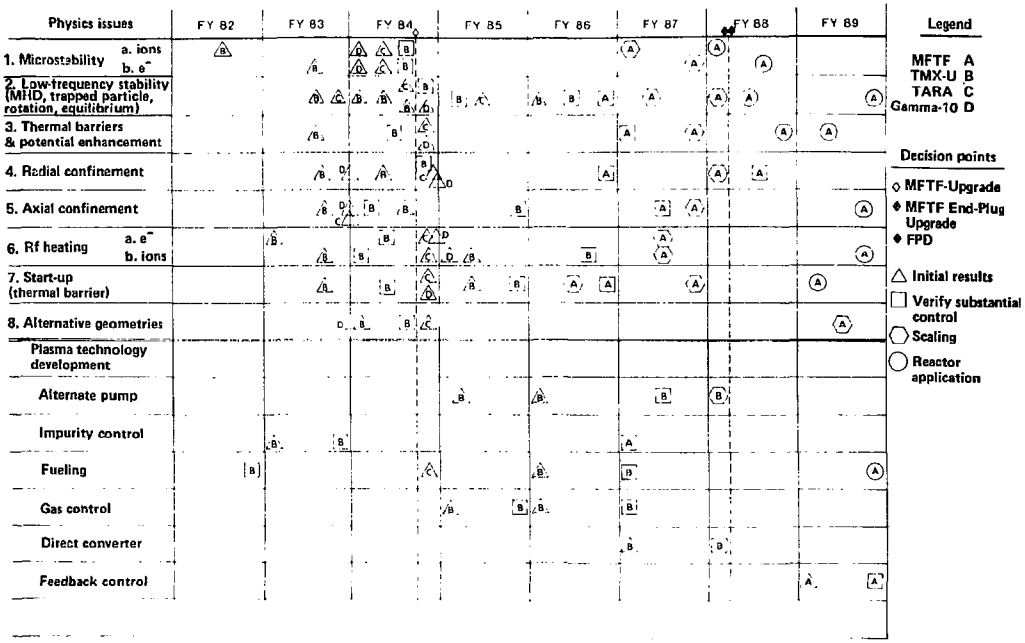

Microstability issues concern both electrons and ions. In FY 82 TMX-U experiments showed that a sloshing ion distribution in the plug greatly reduced the rf noise associated with ion microstability. Further studies of the various modes for both electrons and ions, and then control, will be carried out on TMX-U, TARA, PHAEDRUS, and GAMMA-10 in late FY 83 and 84. Scaling to reactor conditions will be demonstrated on MFTF-B in FY 87 to FY 88.

Low-frequency stability issues include MHD problems such as ballooning and interchange modes, equilibrium, trapped particle modes, and rotationally driven instabilities. Experiments in late FY 83 and early FY 84 on TMX-U and TARA will clarify the relative importance of various modes to tandem operation as densities and temperatures increase. Successful control of MHD instabilities will be shown in late FY 84; control of trapped particle instabilities in FY 85. Experiments on TMX-U in FY 84 and TARA in FY 85 will investigate the importance of rotational instabilities. Control by means of controlling $\phi(r)$ will be first demonstrated in FY 84 and more fully explored in FY 86. TMX-U and TARA will also study the effects of parallel currents in FY 85 to FY 86. Evaluation of trapped-particle modes will be extended to a low-collisionality regime in MFTF in FY 87. The controllable axicell potential in MFTF will also affect these modes through modification of the passing density. Radial potential control at high central-cell potentials more nearly typical of reactors will be addressed in MFTF in FY 88.

Thermal barriers and potential enhancement address the problem of establishing the barrier and plug potential profiles, in particular the maintenance of separated electron populations. The erection of a thermal barrier will be shown on TMX-U in FY 83, as well as on TARA and GAMMA-10 in FY 84. Detailed studies in FY 84 will clarify the means required to get the desired potentials. Control of the electron energy distribution will be performed on MFTF-B in FY 87. Issues of particular importance in the MFTF-B parameter regime include testing of new methods of electron runaway control and control of the spatial shifts in the microwave absorption zones due to β effects, relativity, and doppler shifts. Demonstration of a reactor-level barrier and potential profile in FY 87 and FY 88 will follow.

When the central cell plasma is well-confined axially by the plug potential, the dominant loss channel becomes radial transport. Radial transport can be reduced by, for example, reducing the fraction of central cell ions that traverse quadrupole regions and by reducing the radial

potential gradient. TMX-U will begin by measuring radial transport under conditions of good axial confinement in late FY 83. In FY 84 TMX-U and GAMMA-10 will investigate reducing the radial transport by decreasing the radial potential gradient. Installation of throttle coils on TMX-U in FY 84 will demonstrate the effect of increasing the central cell confining mirror ratio, with azimuthal symmetry. The trim coils in MFTF-B will be used in late FY 86 to investigate the effect of varying radial step size. MFTF will verify radial transport scaling at low collisionality and will demonstrate control by varying the passing-density with the axicell potential. The effects of radial potential control on radial transport will be extended to near-reactor levels in FY 88.

All of the present generation of tandem machines will begin studying axial confinement in FY 83. TMX-U will complete this phase with power balance measurements by the end of FY 84. When the throttle coil is installed on TMX-U, axial confinement of high energy ions will be affected directly, and the decrease of passing ions should allow the plug and barrier to be operated more efficiently and/or at higher potentials. Characterization of the operation with throttle coils will be completed with power balance measurements by the end of FY 35.

The availability of the axicell beams and pump beams for fueling the central cell gives MFTF-B the ability to vary $f_i(E)$ in the central cell more directly. The resulting effect on axial confinement and the scaling to reactor conditions of all the parameters involved in axial confinement will be accomplished in FY 87. Relevant technologies for reactor application, including pellet fueling and ICRH in the central cell, will be demonstrated in FY 89.

The rf heating is required for a number of reasons: to magnetically trap electrons to establish the thermal barrier, to heat electrons to enhance the plug potential, to heat ions in the central cell during low density startup, and to maintain the central cell ion temperatures in steady-state operation when cold ions are a significant portion of the feedstock. TMX-U obtained a magnetically confined hot electron population in early FY 83, and will demonstrate both the use of ICRH during startup and the use of ECRH to establish a thermal barrier in FY 84. TARA and GAMMA-10 will also begin investigating both ICRH and ECRH in this same period. Use of rf heating of electrons and ions at reactor conditions will be demonstrated on MFTF-B in

FY 87, while full qualification for reactor application will be accomplished by the FY 89 experiments involving the fueling mentioned above.

Thermal barrier startup is perhaps the most difficult part of tandem mirror operation, as power requirements are at their peak, losses highest, and stability most precarious. TMX-U is currently developing the procedures required to obtain startup, which should be complete in FY 83. TARA and GAMMA-10 will also begin similar investigations in FY 83. Longer microwave power durations will extend the range of startup studies in FY 85 and FY 86. Beginning in FY 86, MFTF-B will apply the startup techniques already developed, as well as pursue techniques peculiar to its own configuration. Scaling to reactor conditions will be accomplished by the end of FY 87, and verification of all the technolgies required will be done in FY 89.

Identification of impurity content in TMX-U began in early FY 83 and will continue during thermal barrier experiments. The first tests of the control of oxygen impurities from the beam will occur with arc-box gettering later in FY 83, and the results will be summarized and reported in FY 84. Beyond this expected order-of-magnitude improvement, a further reduction of impurities from the beam will occur in MFTF experiments in FY 87 using magnetically separated beams.

Gas-box fueling tests have already been accomplished in TMX-U. Because gas-box fueling is expected to be ineffective for large-radius, high-density plasmas, we plan to investigate alternative fueling techniques. Pellet injection tests would start in TMX-U in FY 86, with control demonstrated by FY 87. Pellet fueling with reactor-like parameters will be done in MFTF-B in FY 89.

Gas control techniques become more important as the thermal barrier permits operation with low density in the anchor. Techniques for controlling gas streaming from neutral beams will be tested in TMX-U in FY 85, with substantial verification to be accomplished later that year. Halo drive tests to improve gas attenuation will commence in FY 86 and continue into FY 87. These tests will include halo rf stoppering to improve gas and power efficiency.

Proposed alternative ion pumps will be tested in the TMX-U facility in FY 85 and FY 86. Any successful designs will subsequently be scaled to reactor plasmas.

Direct converter tests based on the radial separation of ions and electrons arising from radial transport will be started in TMX-U in FY 87, with control demonstrated in FY 88.

Anticipating a need for automatic maintenance of operating-point parameters in a steady-state reactor, tests of feedback control will begin in FY 89 in MFTF-B. Control techniques applicable to reactor operation will be demonstrated by late FY 89.

4.3 TECHNOLOGY DEVELOPMENT FOR MIRRORS

4.3.1 Needs

The technology development needs of tandem mirror reactors are shown in Table 4-2, extracted from the National Mirror Fusion Program Plan.[1] Developments needed for MFTF-B Upgrade are, in most cases, in between the present state of the art and those needed for a reactor.

4.3.2 Plan for Development

The general plan for technology development is described in two documents, the National Mirror Fusion Program Plan (Plan)[1] and the Fusion Technology Development Plan (FTDP).[2] The Plan is specific to mirror needs while the FTDP discusses all planned technology development sponsored by the Development and Technology (D&T) division of the Office of Fusion Energy (OFE), including nuclear technology. The following is a brief outline of the present plans and with an indication of how they would fit the needs of MFTF-B Upgrade.

A. High-field magnets.

Tandem mirror reactor performance depends strongly on the fields obtainable in the barrier coils. The MARS reactor design uses 24-T coils. Because these coils are relatively small and circular, fields up to 24 T are feasible using a combination of superconducting coils and a copper insert. This will require development of both copper inserts and superconducting coils to as high a field as practical. At these field levels, mechanical stress is a critical issue. Because the copper coil acts as a neutron shield for the superconducting coil, radiation damage to the insert and its insulation is a major concern.

Table 4-2. Technology development needs of tandem mirror reactors.

		TMX-U	TARA	MFTF-B	MFTF-B Upgrade		FPD	MARS
Neutral beams	Accel.potential(kV)	17	20	30, 80	80	200	475[a]	475[a]
	Current/module (A)	50	60	30, 50	70	5	10	10
	Duration	75 ms	30 ms	30 sec	Cont.	Cont.	Cont.	Cont.
	Ion base	Positive	Positive	Positive	Neg.	Neg.	Neg.	Neg.
Magnets	Conductor	Cu	Cu	Nb_3Sn,NbTi	NbTi,Nb_3Sn,Cu		Cu,Nb_3Sn	Cu,Nb_3Sn
	B_{max}(T)	2	3	12	18		20[a]	24[a]
Electron-cyclotron resonant heating	Frequency (GHz)	28	28	28,35,56	35,56		84[a]	84[a]
	Power (kW)	200	200	200,200,200	200,200		1000	1000
	Duration	75 ms	30 ms	30 sec	Cont.		Cont.	Cont.
Direct converters		Test	No	Test	Yes		Yes	Yes
Tritium handling		No	No	No	Yes		Yes	Yes
Vacuum technology		Gettering LN_2 panels	Gettering Plasma pump LN_2 panels	Gettering LHe panels	LHe panels (cont.)		LHe panels (cont.)	LHe panels (cont.)
Materials and radiation damage	Neutron dose	None	None	Moderate	Reactor environment (low fluence)		Reactor environment	Reactor environment
	Energy	NA	NA	2.5 MeV	14MeV		14 MeV	14 MeV
	Radiation damage	None	None	Minimal	Moderate		All materials subject to damage	All materials subject to damage

[a]Preliminary values.

The magnet development program presently planned stresses high-field conductor development with a goal of demonstrating feasibility of up to 16-T coils by FY 86 through 88. With development effort on copper inserts, the 18-T needed by MFTF-B Upgrade should be available. There is also interest in an international collaboration involving the Kernforschungszentrum (KfK) in Karlsruhe, Federal Replublic of Germany, to develop 18-T coils that would be compatible with a subsequent installation into MFTF-B Upgrade.

B. High energy neutral beams.
With the successful demonstration of the 30-sec 80-keV beams for MFTF-B and the 120-keV TFTR beams, work on positive-ion-based neutral beams will diminish. The neutral beam plan concentrates on negative-ion-based beams with a demonstration of a 200-keV, 5-A system in FY 84 or 85. These beams will be suitable for the upgrade in the planned program, and will meet our requirements in a timely way. Continued development should improve the performance of these beams.

C. Microwave power sources.
The present gyrotron development program will meet upgrade needs in the near future with 60-GHz continuously operating gyrotron tubes. The larger-unit-size (1-MW) higher-frequency devices planned are necessary for FDP and a MARS-type reactor.

D. Particle control.
Particle control is a broad term including vacuum maintenance, fueling, and dealing with the plasma flowing out the ends of a tandem mirror. MFTF-B Upgrade will be significantly different from MFTF-B in two areas: (a) the continuous operation (hours) will bring the reflux from the walls into equilibrium; (b) the presence of T_2 will limit the amount of gas that can be trapped and held. Both of these factors will impact the design and require some kind of continuous pur ing, e.g., cyclically degassed cryopumps. Gettering will probably not be feasible.

The current development and technology program is very weak in this whole area with the possible exception of pellet fueling technology. A substantial upgrading of the program would be necessary to accommodate the upgrade's needs. Substantial amounts of information could also be obtained on TMX-U and MFTF-B.

E. Nuclear technology.

Tritium handling technology developed by the design and operation of TSTA will be sufficient for MFTF-B Upgrade operation. Development of the remaining nuclear technology is not a critical issue for the upgrade, but its availability would lead to substantial changes in the program because availability of this capability was not anticipated when the FEDP and Mirror Plan were written.

REFERENCES

1. R. R. Borchers, C. M. Van Atta, Editors, The National Mirror Fusion Program Plan, Lawrence Livermore National Laboratory, Livermore, CA 94550, UCAR-10042-82 (1982).
2. Fusion Technology Development Plan, Office of Fusion Energy, Department of Energy, Washington, D.C. (1982).

5. COST AND SCHEDULE

The three options described in Sec. 2 are costed here, and a discussion of the schedule is given. The projects are described by a work breakdown structure for purposes of definition and costing. All costs given in this section are mid-1983 dollars and include all direct, indirect, and contingency costs for the projects.

5.1 THE LLNL PREFERRED OPTION (α + T)

5.1.1 Work Breakdown Structure (WBS)

The work breakdown structure follows the recommendations of a Battelle Laboratory study of WBS accounts for fusion. Table 5-1 lists these accounts at level 4, although costs were estimated at a lower level.

5.1.2 Unescalated Cost

In arriving at the cost for this option, we used equipment and facilities from MFTF-B, either as-is or modified to the fullest extent. The costs presented here represent the added cost for modifications and new equipment to construct the upgrade. Credits for facilities, cryogenics, vessels, electrical gear, utilities, control systems, and diagnostics are significant. The total value of this contribution is estimated to be $270M in mid-1983 dollars.

In Table 5-2 the estimated cost is given for the WBS accounts. Account 22.01 for Reactor Equipment is summarized at level 3, while all other accounts are at level 2. These costs include all but project management, systems engineering, and contingency, estimated at 5%, 4%, and 25%, respectively, of all sub-element totals, which are added separately. Each sub-element includes component engineering, fabrication, installation, and checkout. Project management covers QA and safety, financial and technical management, scheduling, planning, and documentation. Systems engineering includes overall configuration design and systems integration. We have also looked at the possibility of placing the upgrade on a different location at LLNL adjacent to the existing facility but still taking advantage of the MFTF hardware. This

Table 5-1. Work breakdown structure accounts--MFTF-α+T.

Account	Description
21.00.	Structures and facilities
0.01	Reactor vault upgrade
0.02	Hot cell building
0.03	Tritium building
0.04	Ventilation stack
22.01	Reactor equipment
22.01.01	Vacuum vessel upgrade
0.01	DT axicell
0.02	Solenoid cell upgrade
0.03	End cell upgrade
22.01.02	Shield and first wall
0.01	DT axicell shield
0.02	Central cell shield
0.03	End cell shield
0.04	DT axicell first wall
0.05	Central cell first wall
22.01.03	Magnets
0.01	New DT axicell background coils
0.02	New DT axicell choke coils
0.03	New end choke coils (east and west)
0.04	New transition coils
0.05	New plug coils
0.06	New dc coils
0.07	Remove existing coils
22.01.04	Heating and fueling
0.01	Central cell beams and beamlines
0.02	Particle fueling
0.03	Anchor cell ICRH upgrade
0.04	ECRH relocation
0.05	Negative ion sloshing beam
0.06	New anchor ICRH
0.07	Drift pumps

Table 5-1. (Continued.)

Account	Description
22.01.05	Support structures
0.01	End cell supports
0.02	New fueling injector supports
0.03	New end cell neutral beam supports
0.04	New end cell shield supports
0.05	Central cell support upgrade
0.06	New central cell beam support
0.07	New beam dump support
22.01.06	Vacuum system
0.01	End dump
0.02	DT axicell beam dump
0.03	Plug sloshing beam dump
0.04	End cell cryopanels
22.01.07	Power supplies
0.01	Large S/C solenoid power supply
0.02	Copper coil power supply
0.03	NBI power supply upgrade
0.04	Low frequency RF power supply upgrade
0.05	ICRH power supply upgrade
0.06	ECRH power supply upgrade
0.07	200 kV neg. ion beam power supply
0.08	End cell coil power supplies
22.01.08	Direct converter
0.01	Insulator
0.02	Cables
0.03	Load resistors
0.04	Regulators
0.05	Controls
0.06	Miscellaneous
22.02	Heat transport systems
0.01	Reactor heat removal upgrade
0.02	Heat rejection upgrade
22.04	Radwaste system

Table 5-1. (Continued.)

Account	Description
22.05	Fuel processing system
0.01	Fuel purification and preparation
0.02	Water cleanup system
0.03	Atmospheric detritiation system
0.04	Other tritium processing systems
0.05	Data acquisition system
22.06	Maintenance system
22.07	Instrumentation and controls upgrade
0.01	Superconducting coil I & C
0.02	Copper resistive coils I & C
0.03	Data acquisition instrumentation
0.04	Supervisory controls
0.05	Test cell diagnostics I & C
24.00	Electrical system
0.01	Pulsed power substation upgrade
0.02	Facility power upgrade
0.03	Tritium facility power
25.00	Balance of plant
0.01	Bulk materials and supplies

Table 5-2. MFTF-α+T costs--mid-1983 K$.

Account	System	alpha + T
21.00	Structures and facilities	23750
22.01.01	Vacuum vessel	7380
22.01.02	Shield and first wall	14425
22.01.03	Magnets	58228
22.01.04	Heating and fueling	43037
22.01.05	Support structures	2120
22.01.06	Vacuum system	18100
22.01.07	Power supplies	9766
22.01.08	Direct converter	3000
22.02	Heat transport	6250
22.04	Radiation safety	515
22.05	Fuel process	40375
22.06	Maintenance	35125
22.07	Instrumentation and control	6518
24.00	ac electrical power	13025
25.00	Balance of plant	13000
	Total direct cost	294,614
	System engineering (4%)	11800
	Management (5%)	14730
	Sub-Total	321,144
	Contingency (25%)	80286
	Total cost	401,430

approach would provide a more optimum facility for housing the upgrade and might have some scheduling advantage because of greater decoupling from the MFTF-B experimental program. By our estimate this scheme would add about $200M to the overall cost while not appreciably shortening the schedule and is therefore not considered an advantage to the program.

5.1.3 Schedule and Cost Profile

Figure 5-1 contains schedule of activities to show how the upgrade could be constructed. We imposed two constraints on scheduling: a cost profile based on limited funding during the years of MFTF-B operations, and a physics checkpoint in the first quarter of FY 88 to confirm the projected performance of the end plugs. Until that time no activities specifically pertaining to the end plugs are planned except for design and systems integration. The early years of the project are devoted to design, central cell construction, and facility modifications that will be required even if the end plugs are unchanged.

Although this forces the funding level to peak late in the project, such a funding profile is workable. Table 5-3 gives the construction funding profile used for scheduling. Completion in mid FY 92 is projected.

Table 5-3. Construction budget schedule for the preferred option (α + T).

								Total
Fiscal year	86	87	88	89	90	91	92	
Construction budget ($M)	15	20	50	60	100	100	56	401

5.1.4. Impact of Delayed Start

A delay in starting the MFTF-α+T Upgrade until MFTF-B has operated and yielded data that could trigger a decision on the upgrade would result in a 3-yr slip in the completion date. We assume construction would not begin, at the earliest, until FY 89 if FY 88 data were needed. Operation of MFTF-B could continue until the end of FY 90 and the upgrade would not be completed until mid FY 95.

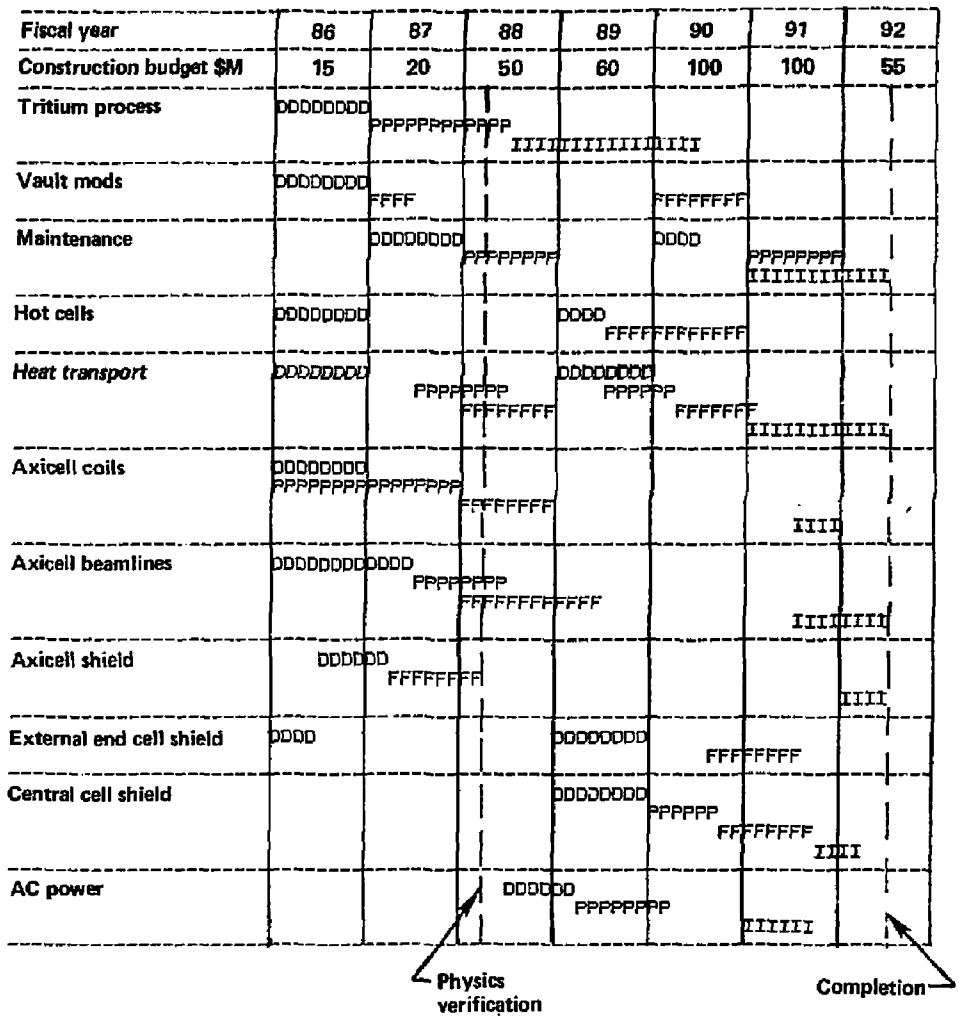

Comments on the schedule:

1. Overall system conceptual design and central cell requirements are completed in FY 85.
2. Some noninterfering modifications and additions to the MFTF-B facility are scheduled to occur during the operational period of FY 86 through FY 89.
3. MFTF-B is assumed to shut down at the end of FY 89 and the facility made fully available for modification.

Fig. 5-1. MFTF-α+T construction schedule.

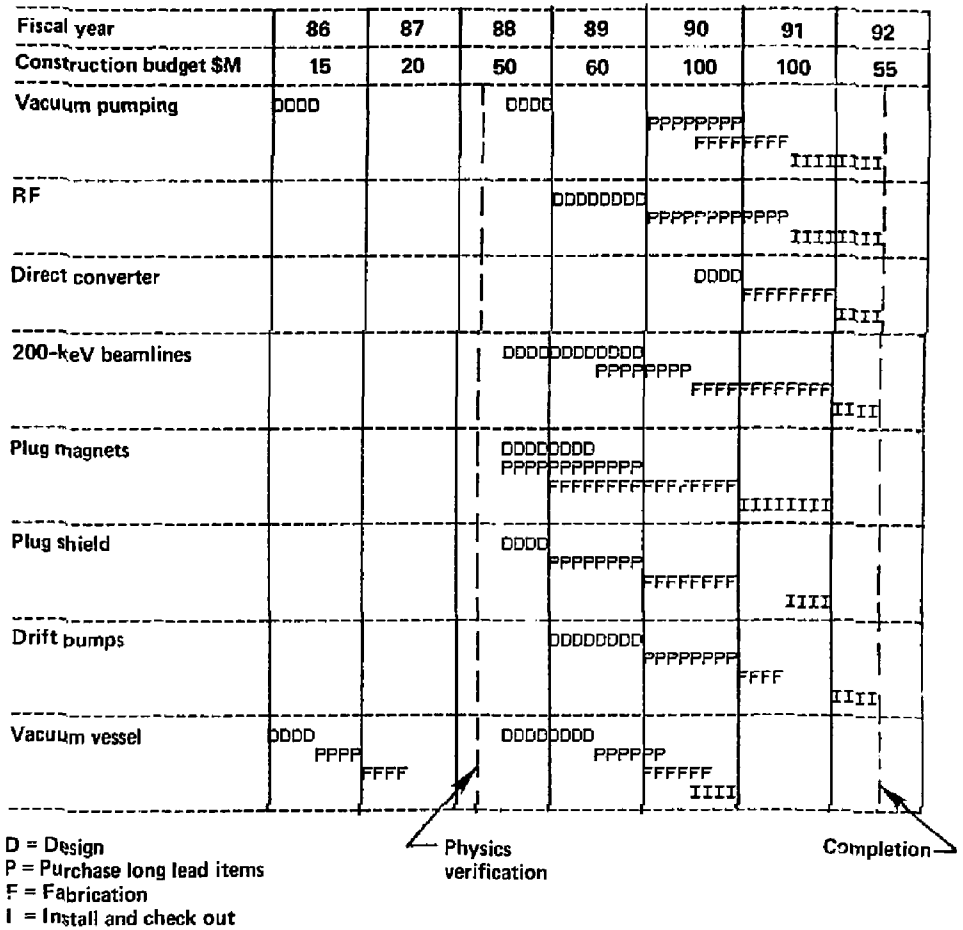

4. High field choke coil and 200-keV negative ion beam development are assumed to be provided by the D&T program.
5. Drift pump design data are to be provided by the TMX-U and MFTF-B experimental program.
6. Detail design of the end plug upgrade or central cell only upgrade will be triggered by data available in the first quarter of FY 88.

Fig. 5-1. (Continued.)

5.2. THE MFTF-B+T UPGRADE

5.2.1 Work Breakdown Structure

The work breakdown structure for the central cell (Table 5-4) upgrade is a duplicate of the preferred option with the ommission of unneeded systems.

5.2.2 Unescalated Cost

The costing for the central cell upgrade option (B+T) as shown in Table 5-5 is extracted from the unit costs for MFTF-α+T. The total cost is less because the new plugs of α + T are not incorporated in this design. The principal cost differences result from the savings accrued by not incorporating new plug coils and 200-keV negative ion beams. Some cost increases result from the additional 80-keV beams and added gas load required for this option.

5.2.3 Schedule and Cost Profile

The overall schedule will be the same as for MFTF-α+T. The principal difference is in the emphisis and scope of work that would occur after the physics are confirmed in the first quarter of FY 88. The work on the end plugs would consist of modifications such as adding shielding to the existing end plugs. The other systems are essentially identical to their counterparts in MFTF-α+T with slight changes to accommodate the different parameters.

The early cost profile of course is the same as that of MFTF-α+T. Beginning in FY 89 the funding required is reduced to match the lower total cost of this option. The overall cost profile is shown in Table 5-6.

5.3. THE MFTF-α UPGRADE

5.3.1 Work Breakdown Structure

The work breakdown structure for this option is shown in Table 5-7. It extracts the necessary subsystems from the WBS structure of the MFTF-α+T upgrade.

Table 5-4. Work breakdown structure accounts--MFTF-B+T.

Account	Description
21.00.	Structures and facilities
0.01	Reactor vault upgrade
0.02	Hot cell building
0.03	Tritium building
0.04	Ventilation stack
22.01	Reactor equipment
22.01.01	Vacuum vessel upgrade
0.01	DT axicell
0.02	Solenoid cell upgrade
0.03	End cell upgrade
22.01.02	Shield and first wall
0.01	DT axicell shield
0.02	Central cell shield
0.03	End cell shield
0.04	DT axicell first wall
0.05	Central cell first wall
22.01.03	Magnets
0.01	New DT axicell background coils
0.02	New DT axicell choke coils
0.03	Remove existing coils
22.01.04	Heating and fueling
0.01	Central cell beams and beamlines
0.02	Anchor cell ICRH upgrade
0.03	Added pump beams

Table 5-4. (Contin ed.)

Account	Description
22.01.05	Support structures
0.01	End cell supports
0.02	New fueling injector supports
0.03	New end cell neutral beam supports
0.04	New end cell shield supports
0.05	Central cell support upgrade
0.06	New central cell beam support
0.07	New beam dump support
22.01.06	Vacuum system
0.01	End dump
0.02	DT axicell beam dump
0.03	Plug sloshing beam dump
0.04	End cell cryopanels
22.01.07	Power supplies
0.01	Large S/C solenoid power supply
0.02	Copper coil power supply
0.03	NBI power supply upgrade
0.04	Low frequency RF power supply upgrade
0.05	ICRH power supply upgrade
0.06	ECRH power supply upgrade
0.07	200-kV neg. ion beam power supply
0.08	End cell coil power supplies
22.01.08	Direct converter
0.01	Insulator
0.02	Cables
0.03	Load resistors
0.04	Regulators
0.05	Controls
0.06	Miscellaneous
22.02	Heat transport systems
0.01	Reactor heat removal upgrade
0.02	Heat rejection upgrade
22.04	Radwaste system

Table 5-4. (Continued.)

Account	Description
22.05	Fuel processing system
0.01	Fuel purification and preparation
0.02	Water cleanup system
0.03	Atmospheric detritiation system
0.04	Other tritium processing systems
0.05	Data acquisition system
22.06	Maintenance system
22.07	Instrumentation and controls upgrae
0.01	Superconducting coil I & C
0.02	Copper resistive coils I & C
0.03	Data acquisition instrumentation
0.04	Supervisory controls
0.05	Test cell diagnostics I & C
24.00	Electrical system
0.01	Pulsed power substation upgrade
0.02	Facility power upgrade
0.03	Tritium facility power
25.00	Balance of plant
0.01	Bulk materials and supplies

Table 5-5. MFTF-B+T costs--mid 1983 K$.

Account	System	B + T
21.00	Structures and facilities	23750
22.01.01	Vacuum vessel	7380
22.01.02	Shield and first wall	11000
22.01.03	Magnets	18329
22.01.04	Heating and fueling	46000
22.01.05	Support structures	1500
22.01.06	Vacuum system	18000
22.01.07	Power supplies	6766
22.01.08	Direct converter	1000
22.02	Heat transport	7000
22.04	Radiation safety	515
22.05	Fuel process	40375
22.06	Maintenance	35125
22.07	Instrumentation and control	6518
24.00	ac electrical power	11025
25.00	Balance of Plant	11000
	Total direct cost	245283
	System engineering (4%)	9811
	Management (5%)	12264
	Sub-Total	267358
	Contingency (25%)	66840
	Total cost	334198

Table 5-6. Construction budget schedule for the MFTF-B+T.

								Total
Fiscal year	86	87	88	89	90	91	92	
Construction budget ($M)	15	20	30	40	80	90	59	334

Table 5-7. Work breakdown structure accounts--MFTF-α.

Account	Description
21.00.	Structures and facilities
0.01	Reactor vault upgrade
0.02	Hot cell building
0.03	Tritium building
0.04	Ventilation stack
22.01	Reactor equipment
22.01.01	Vacuum vessel upgrade
0.01	End cell upgrade
22.01.02	Shield and first wall
0.01	Central cell shield
0.02	End cell shield
0.03	Central cell first wall
22.01.03	Magnets
0.01	New end choke coils (east & west)
0.02	New transition coils
0.03	New plug coils
0.04	New dc coils
0.05	Remove existing coils
22.01.04	Heating and fueling
0.01	Pellet fueling
0.02	Anchor cell ICRH upgrade
0.03	ECRH relocation
0.04	Negative ion sloshing beam
0.05	New anchor ICRH
0.06	Drift pumps
0.03	Added pump beams

Table 5-7. (Continued.)

Account	Description
22.01.05	Support structures
0.01	End cell supports
0.02	New fueling injector supports
0.03	New end cell neutral beam supports
0.04	New end cell shield supports
0.05	Central cell support upgrade
22.01.06	Vacuum system
0.01	End dump
0.02	Plug sloshing beam dump
0.03	End cell cryopanels
22.01.07	Power supplies
0.01	Copper coil power supply
0.02	Low frequency RF power supply upgrade
0.03	ICRH power supply upgrade
0.04	ECRH power supply upgrade
0.05	200-kV neg. ion beam power supply
0.06	End cell coil power supplies
22.01.08	Direct converter
0.01	Insulator
0.02	Cables
0.03	Load resistors
0.04	Regulators
0.05	Controls
0.06	Miscellaneous
22.02	Heat transport systems
0.01	Reactor heat removal upgrade
0.02	Heat rejection upgrade
22.04	Radwaste system

Table 5-7. (Continued.)

Account	Description
22.05	Fuel processing system
0.01	Fuel purification and preparation
0.02	Water cleanup system
0.03	Atmospheric detritiation system
0.04	Other tritium processing systems
0.05	Data acquisition system
22.06	Maintenance system
22.07	Instrumentation and controls upgrade
0.01	Superconducting coil I & C
0.02	Copper resistive coils I & C
0.03	Data acquisition instrumentation
0.04	Supervisory controls
0.05	Test cell diagnostics I & C
24.00	Electrical system
0.01	Pulsed power substation upgrade
0.02	Facility power upgrade
0.03	Tritium facility power
25.00	Balance of plant
0.01	Bulk materials and supplies

5.3.2 Unescalated Cost

This option was costed from estimate of subsystems in MFTF-α+T. In Table 5-8 these costs are listed according to the WBS categories given above, but summarized at level 2 in mid-FY 83 dollars. The total cost is $267M.

5.3.3 Schedule and Cost Profile

Unlike the other two options, MFTF-α would have a project start date of FY 89 because there is no rationale for an early start as with the nuclear insert. We would construct this option in about 5 yr and require a $20M/yr increment to the mirror base budget starting in FY 89.

5.4 OVERALL PROGRAM BUDGET REQUIREMENTS

5.4.1 Program Elements

During the 1980's the mirror base program will be funding TMX-U, TARA, and MFTF-B as its major facilities as well as supporting devices like Phaedrus, STM, and other smaller machines. TARA is expected to operate into the 1990's, while TMX-U might phase out in the late 1980's. In the upgrade planning we assume MFTF-B operates through FY 89 before shutting down to incorporate modifications.

5.4.2 MFAC Budget Guidance

The overall mirror program funding requirements were listed in the MFAC panel report on tandem mirrors and Tokamaks, so this section ties the upgrade funding requirements to these envisioned earlier. Tables 3-10 and 3-11 from the panel report give the relevant information, and they are repeated here as Tables 5-9 and 5-10. These tables show projected funding for the Mirror Base program, the Support Base in APP and D&T, and the increment needed for the so-called "Program-Driven" Case.

Section 1 of this report gave the cost profile for MFTF-α+T and compared it to the Mirror Base profile of $108M/yr beginning in FY 85. Note that the yearly increment (FY 85 through 87) of $15 to 20 M needed to build

Table 5-8. MFTF-α costs.

Account	System	
21.00	Structures and facilities	20000
22.01.01	Vacuum vessel	5000
22.01.02	Shield and first wall	10000
22.01.03	Magnets	40700
22.01.04	Heating and fueling	25000
22.01.05	Support structures	1500
22.01.06	Vacuum system	5000
22.01.07	Power supplies	5000
22.01.08	Direct converter	3000
22.02	Heat transport	5000
22.04	Radiation safety	515
22.05	Fuel process	29000
22.06	Maintenance	24000
22.07	Instrumentation and control	6518
24.00	ac electrical power	8000
25.00	Balance of plant	8000
	Total direct cost	196233
	System engineering (4%)	7849
	Management (5%)	9811
	Sub total	213893
	Contingency (25%)	53473
	Total cost	267367

Table 5-9. Tandem mirror budget (in $M's, constant $>84). (MFAC Table 3-10, Ref. 1, Sect. 1).

	Fiscal year							
	82	83	84	85	86	87	88	89
Mirror base								
MFTF	48.7	46.0[a]	61.0	61.0	61.0	61.0	61.0	61.0
Other LLNL	20.7	23.5	30.6	30.0	30.0	30.0	30.0	30.0
Non-LLNL	8.1	12.0	15.0	17.0	17.0	17.0	17.0	17.0
	77.5	81.5	106.6	108.0	108.0	108.0	108.0	108.0
Support base								
APP	4.9	4.9	5.5	6.2	7.0	8.0	9.0	10.0
D&T	7.0	10.8	14.5	18.0	19.5	22.0	19.0	19.0
	11.9	15.7	20.0	24.2	26.5	30.0	28.0	29.0
Increment for program-driven case								
To maintain MFTF schedule[b]			19.0	9.0	5.0			
MFTF-Upgrade				11.0	15.0	20.0	20.0	20.0
Confinement			6.0	10.0	10.0	10.0	10.0	10.0
FPD/ETR				2.0	7.0	12.0	150.0	250.0
Mirror D&T			4.0	7.0	11.0	14.5	15.0	15.0
Other D&T (includes TDF)			21.0	110.0	165.0	170.0	175.0	140.0
			50.0	149.0	213.0	226.5	370.0	435.0

[a]Needs $15 M in FY 83 to maintain schedule at given FY 84 level; see Table 3-14.

[b]Assumes 46.0 only in FY 83; see Table 3-14.

Table 5-10. Tandem mirror confinement program (in $M's, constant $>84). (MFAC Table 3-11, Ref. 1, Sect. 1).

	Fiscal year							
	82	83	84	85	86	87	88	89
LLNL programs[a]								
TMX-U/S	18.7	21.9	29.0	29.0	29.0	29.0	29.0	29.0
Advanced systems	0.5	0.6	0.7	0.3	1.0	1.0	1.0	1.0
HVTS	1.5	1.0	0.9	0.7				
	20.7	23.5	30.6	30.0	30.0	30.0	30.0	30.0
Other programs								
TARA, MIT	5.1	8.5	11.0	11.0	11.0	11.0	11.0	11.0
Phaedrus, U. of Wisconsin	1.2	1.4	1.4					
STM, TRW	1.2	1.5	1.5					
				4.0	4.0	4.0	4.0	4.0
MMX, UCB	0.35	0.5	0.5					
LAMEX, UCLA	0.1	0.1	0.1					
Other	0.45	0.4	0.5	2.0	2.0	2.0	2.0	2.0
	8.1	12.0	15.0	17.0	17.0	17.0	17.0	17.0

[a]Excluding MFTF.

the upgrade is consistent with the MFAC projections (in FY 85, a $6 M increment to maintain the MFTF+B schedule is listed in Table 7-4 of Sec. 7 as a base program cost and in the MFAC table as an increment). Beginning in FY 88 the increment increases to $40M/yr to complete the upgrade by mid-FY 92.

6. INDUSTRIAL ROLE IN MFTF-UPGRADE

Since the Mirror Fusion Test Facility (MFTF) construction project was started in October 1977 at LLNL, we have had a policy of doing as much work as practical using industrial capabilities. A large fraction of the construction project money was placed with industry, primarily in the form of performance contracts, including design, construction, and testing of major components. Nearly $200M in contracts each over $1M was spent in industry, with 20 contracts in the $1 to 5 M range, 7 in the $5 to 20 M range, and 3 over $20M.

LLNL is currently taking an additional step with industry for a cost-sharing participation in plasma heating and diagnostics systems for MFTF. The efforts also allow an opportunity for the company to gain direct experience in operational aspects of fusion by performing the integration and test operations of the components provided, leading to an expanded industrial capability.

In the future, the MFTF-Upgrade will proceed in a similar manner with evolution towards greater industrial responsibility. Larger system fabrications and system integration functions will be encouraged. This method could evolve to an industrial participation in the next large mirror machine, Fusion Power Demonstration/Mirror Engineering Test Reactor (FPD/METR), similar to that previously envisioned for the Center for Fusion Engineering. While this would be a mirror-specific endeavor, it would accomplish many of the objectives sought by the Engineering Act of 1980.

We can imagine that the MFTF-Upgrade at LLNL could lay the basis for a FPD/METR at a new site evolving from a lead laboratory and a strong industrial team. This transition from a program based on scientific research and development to one that includes major engineering objectives has been endorsed by the scientific community, the Congress, and the Department of Energy. Indeed, the fusion program is now turning from research--characterized by a step-by-step evolution--to engineering development, which is characterized by definite goals and complex and highly integrated programs. Such a program requires a strong central management organization capable of technically understanding and directing the program.

The final organization could take many forms. It could remain affiliated with the host laboratory or it could become an independent single-purpose national laboratory, either with its own independent board of directors or under a parent company, university, or consortium. A governing principle

should be that the organizational transition take place with a minimal disruption of the functioning of existing technical teams and technical work. Strong involvement of industry would be a major goal, which offers opportunities for continuing involvement that will help prepare industry for the commercial development of fusion.

APPENDIX A

Report of the US-Japan Bilateral Discussions (Q9)
on the Coordination of Experimental Plans
(GAMMA-10, TMX, TARA, Phaedrus),
November 7 to 10, 1982

The experimental data base that is required for the design of a thermal barrier tandem mirror (TBTM) reactor can be broken into several distinct areas. Each of these requires demonstration under present laboratory conditions and requires a supporting, validated theoretical base that permits scaling to reactor conditions. By the late 1980's, this scaling should have been verified by the performance of MFTF-B or other high performance machines that become operational.

Beyond these issues associated with the basic thermal barrier tandem mirror, there are several avenues for improved performance of the same configuration or for alternate modes of tandem mirror operations. Again, each of these ideas needs to be tested in present-day machines and theoretically analyzed and evaluated.

The issues for the TBTM reactor are given below in summary form, and more detail is given in Tables 1 through 7.

Microstability

The TBTM requires maintenance of the anisotropic and loss-cone ion and electron distributions with fluctuation levels having induced scatter rates not significantly increased over their classical values.

Low Frequency Stability

The TBTM requires maintenance of a magnetic geometry that is stable to curvature- and rotation-driven modes at β-values compatible with reactor parameters.

Thermal Barriers and Potential Enhancement

A tandem mirror reactor with economically attractive recirculating power requires production of the plugging potentials at reduced plug densities by means of selective particle control in the end cells. The thermal barrier with charge-exchange pumping is the best developed technique, although alternative techniques are currently being pursued with the aim of reducing complexity and power requirements.

Axial Confinement

The TBTM requires an axial confinement $n\tau$-value of 50 to 100 times the $n\tau$-value for ion-ion scatter in the central cell with good electron thermal isolation from material end walls maintained. This must be demonstrated at parameters such as density and temperature that are relevant to reactor operation.

Radial Confinement

The TBTM requires a particle radial confinement time against all transport processes which is comparable to or greater than the above axial confinement time. Such a level of particle transport is sufficient for removal of α-particle ash. Similarly, electron thermal transport to cold edge plasma cannot exceed the power associated with end loss.

RF Heating

RF heating of ions and electrons is of increasing importance in several areas of tandem mirror development. The control of velocity distributions by selective deposition of RF power to both electrons and ions is required for potential control, startup, and pressure in the MHD anchor.

Startup

Startup of a thermal barrier require initiation of a low collisionality plasma that satisfies conditions of micro- and MHD-stability.

Tables 1 through 7 contain a breakdown of these general statements to more detailed, specific issues. Also given is the likely method of plasma control, the present day machines and dates in which the issue can be investigated and, underlined, the first such machine which is expected to have significant results. The category labels I, II, III, and IV identify these issues according to the following definitions:

I - Basic or essential for present-day experiments

II - Necessary to design a MARS-type TBTM reactor

III - Would lead to a fundamentally improved reactor concept

IV - Would lead to an improvement of the MARS-type reactor.

For completeness, we have included Japanese and U.S. machines outside those in the official exchange title, such as RFC-XX, STM, and MMX.

Table 1. Microstability issues.

	Mode	Means of control	Machine	Date	Category
Ion	DCLC & AIC	Sloshing ions + tipped potential; hot electrons rf plugging	TMX-U	1983	I, II
			GAMMA 10	1983-84	
			TARA	1984	
			RFC-XX	1983	
	AIC	Sloshing ions	TMX-U	1982 done	I, II
			GAMMA 10	1983-84	
			TARA	1984	
			PHAEDRUS	1984	
	Two-stream in barrier	Number of trapped ions hot electron fraction	TMX-U	1983	II
			GAMMA 10	1983-84	
			TARA	1984	
Electron	Whistler	Limit anisotropy	TMX-U	1983	II
			GAMMA 10	1983-84	
			TARA	1984	
			STM	1983	
	Upper-hybrid loss-cone	Control ratio of densities	TMX-U	1983	II
			GAMMA 10	1983-84	
			TARA	1984	
			STM	1983	

Table 2. Low frequency stability issues.

Issue	Means of control	Machine	Date	Category
Trapped particle modes	Passing fraction ratio collisionality	TARA	1984	II
		TMX-U	1984	
		PHAEDRUS	1983	
		MMX	Now	
		GAMMA 10	1984	
Rotational instabilities	Electric field control	TARA	1985	II
		TMX-U	1984	
		PHAEDRUS	1983	
		GAMMA 10	1984	
Parallel current	Magnet design of geodesic curvature	TARA	1985	II
		TMX-U	1984	
		GAMMA 10	1984	
Ballooning β limits in central cell	Magnetic field design	TARA	1985	II
		TMX-U	1984	
		PHAEDRUS	1983	
		MMX	Now	
		GAMMA 10	1984	
	Stabilization in axisymmetric mirrors and cusps	UCI	Now	III
		PHAEDRUS	1983	
		STM-I	1983	
		RFC-XX	1983	
Hot electron anchor in quadrupole	Ion pressure	TMX-U	1983	II
		PHAEDRUS	1983	
		TARA	1983	
		GAMMA-10	1984	

Table 3. Thermal barrier and potential enhancement issues.

Issue	Means of control	Machine	Date	Category
Vacuum	(a) Improved walls	TMX-U (c)	1983	I, II
	(b) Improved beamlines	TARA (b)	1984-85	
	(c) Improved halo	GAMMA 10 (a,c)	1984-85	
		PHAEDRUS (b,c)	1983-84	
Impurity accumulation	(a) Radial pumping	TMX-U (a,b)	1984-85	II
	(b) Improved neutral beams	TARA (b)	1985	
	(c) Improved walls	GAMMA 10 (c)	1984-85	
Radial fueling and control	(a) Gas feed/halo	TMX-U (a)	1983	I, II
	(b) Low energy beams	TARA (a,c)	1984-85	
	(c) Pellets	GAMMA 10 (a,d)	1983	
	(d) Cross field plasma injection	PHAEDRUS (a,b)	1983	
Hot electron fraction, goal $n_{eh}/n_e > 0.8$	(a) Vary gas/plasma feed	TMX-U (a,b)	1983	II
	(b) Vary heating profile	TARA (b)	1984	
		STM	1983	
		GAMMA 10 (a,b)	1984	
		PHAEDRUS (b)		
Prevent hot electron run-away	(a) Control of heating profile	TMX-U	1983	II
		GAMMA 10	1984	
Limits on ϕ_{max} due To cold-electron deposition; overlap of hot/warm electron populations	(a) Axial heating profile	TMX-U (a,b,c)	1983	II
	(b) Gas control and variation	TARA	1984	
	(c) Scaling of ϕ_{max} with ECH	GAMMA 10 (a,b,c)	1984	
Non-linear processes associated with ECRH	(a) Observation of fluctuations (e.g., by forward microwave scattering)	TMX-U (a,b)	1983	IV,II
		TARA (a,b)	1985	
		GAMMA 10 (a,b)	1983-84	
	(b) Plasma scaling with ECRH power	PHAEDRUS (a,b)	1983-84	
Prevent enhanced barrier filling: breakdown of quasineutrality (sheathes)	(a) Scaling of $n_{trapped}$ with pumping	TMX-U (a,b,c)	1983	II
	(b) Observe oscillations	GAMMA 10 (a,b)	1983-84	
	(c) Observe possible relaxation oscillation in ϕ, n			
Negative tandem operation	(a) Strong ECRH in plug to choke electron flow	TMX-U	1984	III
		TARA	1986	
		PHAEDRUS	1984	
		CONSTANCE	1984	
Concept improvement	(a) Parallel heating of electrons	TARA (a)	1984	III
		PHAEDRUS (a)	1984	
	(b) e⁻beam heating	GAMMA 10 (b)	1984	III,IV
		CONSTANCE (b)	1983	

Table 4. Radial transport.

Issue	Means of Control	Machine	Date	Category
Radial step size	Control of geodesic curvature by coil design; mirror ratio in axicell	TMX-U	1984	II
		TARA	1984	
		GAMMA 10	1984	
		MFTF-B	1987	
Control of radial electric field	Segmented rings on ends, rf enhanced electron loss	PHAEDRUS	1984	II
		TMX-U	1983	
		GAMMA 10	1983	
		TARA	1985	
		MFTF-B	1986	
Alternative barrier pumping and ash removal	Geodesic curvature plus rf phase decorrelation	MFTF-B	1988	IV
		TMX-U	1984-85	
		GAMMA 10	1985	

Table 5. Axial transport.

Issue	Means of control	Machine	Date	Category
$n\tau_{axial}/(n\tau)_{ii} \sim 50\text{-}100$	Tandem configuration	All	1983	II
Isolate electron energy from walls		All	1983	II
Achieve these conditions at reactor-relevant parameters		MFTF-B	1988	II

Table 6. Radio frequency heating issues.

Issue	Species	Machine	Date	Category
Control of energy deposition $(z,r,v_\perp,v_\parallel)$ and T_{hot} vs T_{warm}	Electrons	TMX-U	1982	II
		STM	1982	
		GAMMA 10	1984	
	TARA	1984		
	Ions	TMX-U	1983	II
		PHAEDRUS	1982	
		STM	1983	
		TARA	1984	
		GAMMA 10	1984	
Fueling by rf trapping	Electrons	TMX-U	1983	II
	Ions	PHAEDRUS	1982	IV
		STM	1984	
	TARA	1984		

Table 7. Startup scenarios.

Startup scenarios encompass the broad range of issues outlined in Tables 1 through 6. In this table we outline the similarities and differences in startup methods being employed on thermal barrier tandem mirror devices.

Startup scenarios to establish potential barriers center around formation of plasma in the central cell which is allowed to flow out axially. Dump tanks reduce thermal contact with end walls to allow higher T_e. Central cell ICRH is planned to increase the temperature of target ions in the thermal barrier to decrease ion collisional filling of thermal barriers. MHD and microstability is maintained during the startup.

A. Magnetic configuration	
a. Combined plug/anchor	TMX-U, MFTF-B
b. Inside thermal barrier	TARA
c. Outside thermal barrier	GAMMA 10
B. Anchor startup	
a. High electron β	
cw ECRH, pulsed ICRH	TARA
pulsed ECRH, pulsed NB	TMX-U
cw ECRH, pulsed NB	MFTF-B
b. High ion β by N.B.I, E-beam and R.F. assisted	GAMMA 10
C. Barrier target formation	
a. Cross-field central cell injection and ICRF trapping and heating in anchor	GAMMA 10
b. Anchor hot electrons, ICRF, central cell gas feed, and cw ECRH	TARA
c. Gas and ICRH in central cell feed anchor hot electrons	TMX-U, MFTF-B
D. Electron heating of mirror-confined electrons in barrier	
a. Pulsed ECRH	TMX-U, GAMMA 10
b. cw ECRH	MFTF-B
c. E-beam	GAMMA 10
E. Pumping configuration	
a. Into sloshing distribution	TARA, GAMMA 10
b. Into loss cone	TMX-U
c. Into central cell	MFTF-B

MD/rp/kt/mm

DISCLAIMER

Printed in the United States of America
Available from
National Technical Information Service
U.S. Department of Commerce
5285 Port Royal Road
Springfield, VA 22161
Price: Printed Copy $; Microfiche $4.50

Page Range	Domestic Price	Page Range	Domestic Price
001-025	$ 7.00	326-350	$ 26.50
026-050	8.50	351-375	28.00
051-075	10.00	376-400	29.50
076-100	11.50	401-426	31.00
101-125	13.00	427-450	32.50
126-150	14.50	451-475	34.00
151-175	16.00	476-500	35.50
176-200	17.50	501-525	37.00
201-225	19.00	526-550	38.50
226-250	20.50	551-575	40.00
251-275	22.00	576-600	41.50
276-300	23.50	601-up[1]	
301-325	25.00		

[1]Add 1.50 for each additional 25 page increment, or portion thereof from 601 pages up.